Crystallization, Mechanical, Rheological and Degradation Behavior of Polytrimethylene terephthalate, Polybutylene terephthalate and Polycarbonate blend.

Thesis submitted for the degree of

DOCTOR OF PHILOSOPHY

By

LAFI M. AL-OMAIRI

SCHOOL OF CIVIL, ENVIRONMENTAL AND CHEMICAL ENGINEERING

RMIT University

August, 2010

Acknowledgements

I wish to thank my supervisor Professor Sati Bhattacharya for his advice, assistance, time and patient during the course of this project. I would like to thank my co-supervisor Professor Robert A. Shanks for his assistance during the duration of this project. I would like to thank Dr Johnson Mathew for his technical, emotional support and his continuous belief in me but most of all his friendship. I would also like to thank him for his patience during the entire course of the work. I would like to thank Dr Adam Al-Mulla for all his advices.

Summary:

Blends of polycarbonate (PC), polytrimethylene terephthalate (PTT) and poly butylene terephthalate (PBT) are an important class of commercial blends with numerous applications providing good chemical resistance, impact resistance even at low temperatures, and improved flow characteristics compared to the neat polymers. Polycarbonate/polyester blends are known to react during thermal processing causing the formation of copolymers to have new mechanical and thermal properties.

The aim of this project was to study the crystallization, mechanical, rheological and degradation behavior of blends of PC, PTT and PBT and explain these behaviors in terms of transesterification and other plausible mechanisms.

PC, PTT and PBT (50:25:25 wt/wt ratio) were melt-blended in a single screw extruder and the extruded blends were pelletized. Non isothermal crystallization kinetics of the blend and neat polymers were investigated using a Perkin Elmer diamond DSC instrument having a fast response time. This thermoplastic blend was able to crystallize rapidly from the melt. Non isothermal crystallization kinetic parameters were analyzed using different numerical methods. The parameters of the blend lay between those of PTT and PBT. The cause of this behavior could be due to the nature of PC as an amorphous polymer.

Rheological properties of the blends were also studied at different temperatures. Rheological measurements were conducted to study the storage modulus, loss modulus, and viscosity values vis a vis the neat materials. Changes in complex viscosity (η^*) and shear viscosity (η) were attributed to transesterification. The study presented in this work showed two fundamental issues that have never been addressed in the literature: one is the synthesis of a novel tricomponent system and other is how transesterification during polymer processing might affect the degradation and rheological properties of the tricomponent blend.

Effect of blending on mechanical properties was carried out using tensile tests revealing a higher yield strength and elastic modulus of the blend. The morphology of the blend and neat polymers was studied using Scanning electron microscope (SEM), showing immiscibility of the blend components. X ray analysis was carried out to determine the crystalline nature of the blend vis a vis neat polymers. Existence of PTT and PBT peaks proved the immiscible nature of the system.

Polymer blends can undergo, during processing, degradation because of the presence of both temperature and mechanical stresses. Compared to neat polymers, degradation of polymer blends shows distinct features because of the interaction between the different chemical species. These interactions can give rise to degradation or to the formation of copolymers which act as stabilizing agents. This latter phenomenon is particularly important in the processing of condensation polymers.

The non isothermal degradation kinetics of the blend and neat polymers were studied using dynamic thermogravimetry. The thermal stability of the polymers in air was studied and compared to that in nitrogen. The kinetic parameters were analyzed using different numerical methods. The solid state degradation is found to occur by a phase boundary controlled reaction mechanism both for the neat polymers and the blend.

Polymers normally transesterify, above their melting points and interchange reactions commonly occur between polyester moieties or among polyester and polycarbonate entities. The transesterification occurring in the blend was analyzed with the help of Fourier Transform Infra- Red (FTIR) using spectral features based on changes of infra red bands. Solubility and infrared absorption studies indicate the occurrence of exchange reactions between PC, PTT and PBT leading to formation of possible transesterified products (PTTC and PBTC). In these products PC is soluble, whereas PTTC and PBTC remain insoluble.

Properties of a blend which are important for industrial application include thermal, mechanical and processing conditions. Areas of fundamental interest in polymer blends include the later

properties and physical properties like morphology, crystallization, chemical structure and of most compatibility. The morphology study using SEM indicates non compatibility between the polyester and PC. Melting point and crystallization behavior data are consistent with SEM conclusion and suggest that very little if any interchange reactions occur between the ester and carbonate groups during melt mixing. Wide angle x-ray scattering (WAXD) has been used to observe liquid –induced crystallization in PC/PTT/PBT blends. From studies of crystallization kinetics, it was concluded that transesterification to a little extent occurs in this blend. FTIR has also been used to analyze ester interchange in this blend and the results obtained support the occurrence of trans reaction. Due to reasonably good interfacial adhesion between PC and the polyester the blend is found to have better yield stress and modulus among the tensile properties. Thermogravimetric analysis indicates that the thermogravimetric stability of the tricomponent blend improved compared to the polyesters possibly due to trans reactions occurring at elevated temperatures. The blends developed using PC/PTT/PBT if blended with modifier like polyester/EPDM could find applications in the automotive industry. This blend can meet specific demands like dimensional stability under heat, rigidity, fuel resistance and of all easy processability. These blends can be used for automotive body applications.

The novelty of this work is the development of PC/PTT/PBT blend which achieves good modulus and thermal properties compared to the neat polyesters through the addition of a third thermoplastic ingredient i.e, PC.

TABLE OF CONTENTS

List of Figures

List of Tables

Glossary

A	Pre-exponential factor
ASE	Average sum of errors
ABA	p- acetoxybenzoic acid
ASA	Acrylonitrile Styrene Acrylate
ATR-FTIR	Attenuated total reflectance fourier transform infrared spectroscopy
BHBT	Bishydroxybutyl terephthalate
BPA	Bisphenol A
ΔHc	Enthalpy of crystallization
DDTG	Derivative thermogravimetry
DMT	Dimethyl terephthalate
DSC	Differential scanning calorimetry
DTG	Differential Thermogravimetry
Δt	Infinitesimal time interval
E	Activation energy (kJ/mole)
G	Ratio of the linear growth rate
G'	Storage modulus
G"	Loss modulus
GC/MS	Gas chromatograph/mass spectrometry
ΔHc	Overall enthalpy of crystallization
IR	Infrared spectroscopy
iPP	Isotactic polypropylene
k_A	Avrami crystallization rate constant
k_T	Tobin crystallization rate
KBr	Potassium bromide
m_{tr}	Torque (mPa-s)
MDPE	Medium-density polyethylene
MDSC	Modulated differential scanning calorimetry
n	Decomposition reaction order
n	Integer the order of diffraction

N	Nucleation rate
n_A	Avrami exponent of time
n_T	Tobin exponent
PBT	poly (butylene terephthalate)
PE	Polyethylene
PEN	Poly (ethylene naphthalate)
PET	Poly(ethylene terephthalate)
PES	Polyesters of (PET) and (PBT)
PC	polycarbonate
POM	Poly(oxymethylene)
PPO	Poly(propylene oxide)
PPS	Poly(phenylene sulfide)
PTT	poly (trimethylene terephthalate)
PBTC	Possible product of transesterification of PC and PBT
PTTC	Possible product of transesterification of PC and PTT
PU	Polyurethane
R	Gas constant (J K^{-1} $Mole^{-1}$)
r	Distance from the axis
r_c	Radius of the cone
SAXS	Small angle x-ray scattering
SEM	Scanning electron microscope
t	Crystallization time (minute)
T	Absolute temperature (°C)
T_c	Crystallization temperature (°C)
T_p	Temperature corresponding to inflection point (°C)
T_p	The peak temperature (°C)
Δt_c	Apparent total crystallization period (minute)
T_f	Fusion temperature (°C)
T_g	Glass-transition temperature (°C)
TG	Thermogravimetry
TGA	Thermogravimetric analysis

T_m	Apparent melting temperature (°C)
T_{max}	Temperatures of maximum degradation (°C)
T_o	Onset temperature (°C)
TVA	Thermal volatilization analysis
WAXD	Wide angle x-ray diffraction
WAXS	Wide-angle x ray scattering
V	Linear velocity
α	Fractional extent of reaction
α_a	Small angle
β	Rate of heating
$d\alpha / dt$	Weight-loss rate
λ	Wavelength
η	Viscosity
η^*	Complex viscosity
τ	Shear stress
ϕ	Cooling or heating rate
θ	Angle between the incident collimated x-ray beam and an atomic lattice plane
$\theta(t)$	Relative crystallinity as a function of time

CHAPTER 1 INTRODUCTION

1.1 Purpose and scope

Polymer blending was industrially started in the early 1866 by Alexander Parkes who mixed natural rubber with gutta percha to obtain materials suitable for water proofing cloth. From that day, onward polymer reaction and blends aroused interest around the globe. With today's advancement in polymer science, their significant technological importance arises from the fact that blending of materials with specific properties is cheaper than the new polymer produced by chemical synthesis. In addition, polymer blends have many other benefits that can be cited e.g. (i) providing material with full set of desired properties at the lowest price. (ii) extending the engineering resins' performance. (iii) improving specific properties, viz impact strength or solvent resistance. (iv) offering the means for industrial and/or municipal plastic waste recycling. Blending also benefits the manufacturer by offering (i) improved processability, product uniformity, and scarp reduction in processing temperatures. (ii) quick formulation changes, (iii) plant flexibility and high productivity. (iv) reduction of the number of grades that need to be manufactured and stored. (v) inherent recyclability, etc.

General Electric company found that by blending polystyrene with polyphenylene oxide, the polystyrene allows the viscous polyphenylene oxide to be melt-processable. In ternary blends, a third component is usually added to an immiscible pair to achieve miscibility in cases where the third component is miscible with each of the other two polymers as a result of hydrogen bonding or van der Waals physical forces [1]. Additionally, miscibility and

phase homogeneity in polymer blends are enhanced owing to chemical interactions in the ternary blends. Ternary blends consisting of [PC/PBT]/LCP in the ratio [60/40]/10 wt% has been synthesized by Tjong *et al.,* [2]. Here a solid epoxy resin (Bisphenol type –A) has been used as a compatibilizer for the composites. In this research work, PC/PBT blend is incorporated into a liquid crystal polymer to improve the fibrillation of the LCP in the matrix and also improve adhesion between matrix and LCP. Thus, the modulii of the ternary PC/PBT/LCP composites are higher than those of PC/LCP blends. This blend can be used to make a myriad of products, including CDs and CD-ROMs and also be used for large exterior parts in automotive industry.

It is well known that the physical and mechanical properties of semicrystalline polymers depend to a great extent on the degree of crystallization, which in turn was affected by the crystallization conditions. The crystal structure and morphology are established during the solidification process that takes place through the nucleation and spherulite development. Isothermal crystallization measurements are usually used to study the crystallization behavior of polymers while non isothermal crystallization approaches simulate closely the industrial conditions of polymer processing such as extrusion molding and melt-spinning of synthetic fibers. To control the rate of crystallization and the degree of crystallinity and to obtain materials with better physical properties, a great deal of effort has been devoted into studying the crystallization kinetics and determining the change in material properties [3, 4].

Zhu *et al*., [5] studied the morphological properties of microbially synthesized poly(3-hydroxybutyrate-co-4-hydroxybutyrate)s, P(3HB-co-4HB)s, with different molecular weights and 4HB compositions. Oscillatory shear measurements have been carried out to

characterize the flow behavior of these biopolyesters as a function of temperature at different flow conditions. The rheological characteristics of these samples show that the 4HB content does not appear to strongly affect the critical molecular weight (M_e) for chain entanglement. Under low stresses during creep measurements, the shear viscosity of the sample with low 4HB content diverges abruptly in a narrow temperature range due to polymer crystallization. Apart from the creep measurements, the crystallization behavior of the semicrystalline sample has been further characterized using stress-controlled oscillatory shear measurements during a cooling-heating cycle at a constant rate of temperature ramping. The rapid increase and decrease of the dynamic viscosity and storage modulus are interpreted as corresponding to crystallization and melting, respectively, during the thermal cycle. It is established that the polymer with sufficiently high 4HB content is amorphous and obeys the time-temperature superposition. Capillary flow measurements of all the samples in their molten state have indicated that the variation in 4HB content does not significantly alter the value of M_e. Moreover, the viscosity of these samples appears to have nearly the same temperature dependence in their molten state, indicating that the frictional dynamics are essentially independent of the HB contents. Carrot *el at*., [6] has investigated the rheological behavior of high density polyethylene (HDPE) using isothermal crystallization from the melt using dynamic oscillatory experiments. During crystallization, the molten and crystallizing polymer provides a useful model for filled polymers, the crystalline phase being the filler and the liquid phase being the matrix. Owing to the amorphous phase linking liquid and crystallites, the adhesion between matrix and filler in the system is perfect. The rheological results have been compared to those obtained from differential scanning calorimetry (DSC) under identical

conditions. The relative sensitivity of various rheological parameters (storage and loss moduli, loss angle) to structural changes of the liquids has been studied.

It was found that during isothermal crystallization from the melt, the fraction of growing spherulites changes continuously with time and the adhesion with the matrix is found to be perfect. Plots of storage, loss and tan (δ) plots as function of time at a frequency of 1 rad/s indicates that these parameters are very susceptible to structural changes in the fluid. The decrease in tangent of the loss angle versus increasing filler content indicates a sensitivity of the storage modulus, from this point of view, it was concluded that the loss modulus governing the change of elastic parameter and viscosity parameters are different.

The rate of polymer crystallization depends on temperature, and shear rate. Dynamic rheology can give a more detailed understanding of the mechanism of crystal growth and orientation, and their effect on the ultimate properties of the product. The literature clearly shows the effect of thermo-mechanical history on the morphology and physical properties of semi-crystalline polymers [7, 8].

The systematic study of polymer degradation reactions, which has continued to the present time, only started about 1930 with the birth of the modern synthetic plastics industry. Processing polymers involve melting the material so that it is subjected to high temperatures and shear forces necessary to form usable parts. This condition often results in changes in polymer molecular weight, either through chain scission or transesterification. Consequently, properties of blend polymers are almost universally inferior to those of neat polymers. In addition, polymer blends generally undergo the same degradation reactions as the original polymers, but in most cases the rate of degradation

changes, depending on the nature of the polymer added, or on the degree of miscibility of the polymer pair or on the interaction of degradation products.

FTIR is a useful tool to study the conformations and conformation regularities of polymers, intra-and intermolecular interactions of polymer chains (e.g. by hydrogen bonds) and chemical reactions. Additionally, semicrystalline polymers show infrared bands which correlate to the crystallinity, as inferred by, for example, DSC or using an analytical tool like TGA. The existence of regular ordered sequences (conformation) promotes the crystallizability. With the FTIR method alone it is difficult to distinguish between the influences of conformation and crystallinity on IR bands. The melt blend of semicrystalline poly (butylene terephthalate) (PBT), poly (trimethylene terephthalate)(PTT) and amorphous polycarbonate (PC), a technologically interesting blend, is a system with many possible influences on the vibration behavior of its components by chemical reactions. Exchange reactions could take place between PC, PTT and PBT during thermal treatment. Transesterification is the process in which diesters undergo transformation with diols to form macromolecules. Devaux *et al.,* [9] have postulated transesterification to be the most important exchange reaction occurring between PBT and PC, resulting in a new chemical structure of copolymers with IR bands of the aromatic ester at 1740 and 1070 cm^{-1} and of the aromatic aliphatic carbonate at 1770 cm^{-1}. The IR band of the formed aliphatic-aliphatic carbonate at 1763 cm^{-1} was assigned according to Berti *et al*., [10].

Poly (butylene terephthalate)/bisphenol A polycarbonate blends are known to undergo transesterification reactions when they are heated to temperatures greater than 270^{o}C [9, 11, 12].

The transesterification pathways yield two main transesterification products, the aromatic ester (C=O stretch at 1740 cm^{-1} in IR) and the aliphatic-aromatic carbonate (C=O at 1770 cm^{-1} in IR). The aromatic ester also gives rise to a new band in the IR at 1070 cm^{-1}. These transesterification products have previously been indentified with IR but previous work at GE Plastics [13] was unable to show the presence of the aliphatic-aromatic carbonate in heated PBT/PC blends although evidence for the presence of the aromatic ester was found.

The aim of this study is to prepare poly (trimethylene terephthalate)(PTT) –poly butylene terephthalate)(PBT) – polycarbonate(PC) blends to provide a combination of toughness, strength, and environmental resistance, from these potentially compatible but immiscible polymers, and to interpret their morphology and properties by comparison with analogous polyesters and reference to polymer blend theory.

1.2 Aim and Objectives.

The aim of this project was to study the crystallization, mechanical, rheological and degradation behaviors of blend of PC, PTT and PBT and explain these behaviors in terms of miscibility, transesterification and other plausible mechanisms.

The objectives were:

A. To prepare PC, PTT, PBT blend in the ratio of (50:25:25 wt %) using a single screw extruder.

B. To study miscibility of the blends by measurement of variation in the glass transition temperatures of the component polymers and to determine whether PC will cause nucleation of PTT (or PBT) crystallization.

C. To extrude the samples and do injection molding to obtain test specimens by injection molding for the determination of tensile strength according to ASTM (D-638)

D. To interpret the crystal structure of neat materials and blend using X-ray analysis.

E. To investigate the phase morphology of the samples using a scanning electron microscope (SEM).

F. To study rheological properties of the blend and relate rheological properties to crystallization behavior under shear.

G. To measure the degradation of the blend and neat polymers in nitrogen and air. A plausible mechanism based on phase boundary controlled reaction will be explained for the solid state reaction occurring on degradation.

H. To study possible transesterification reactions which occur in the tricomponent blend using Fourier Transform Infrared Spectroscopy (FTIR).

The thesis is divided into five chapters; A thorough literature review is given in chapter 2. The review includes polymer crystallization (isothermal and non isothermal), morphology (SEM and WAXD), mechanical properties (tensile), rheological properties and non isothermal degradation. Materials and experimental techniques are described in chapter 3. This includes polycarbonate (PC), poly (trimethylene terephthalate), (PTT) and poly (butylene terephthalate), (PBT) as materials. The techniques used in the experiments are:

- Differential scanning calorimeter measurements for conducting experiments related to crystallization kinetics of neat polymers and the blend.
- Scanning electron microscope (SEM) measurements, X-ray measurements and Fourier transform infrared spectrometer (FTIR) measurements for conducting experiments related to morphology of the neat polymers and the blend.

- Tensile measurements for conducting experiments related to mechanical properties of the neat polymers and the blend.
- Cone and plate rheometer measurements for conducting experiments related to rheology of the neat polymers and the blends.
- Thermogravimetric analysis measurements for conducting experiments related to degradation of neat polymer and the blends.

Chapter 4 deals with the study of non isothermal and isothermal crystallization studies of neat polymers and blend. It also includes scanning electron microscopic (SEM) measurements, x-ray analysis, measurement of mechanical properties and rheology of the neat polymers and the blend. Fourier transform infra red analysis (FTIR) and non isothermal degradation study also form a part of this chapter. Chapter 5 deals with the general conclusion of each study discussed in the chapter 4.

CHAPTER 2 REVIEW OF RELEVANT LITERATURE

2.1 Polymer Crystallization.

Guijuan *et al*. [14], investigated the crystallization kinetics after reactive blending of a binary system consisting of poly(trimethylene terephthalate) (PTT)/poly(butylene terephthalate) (PBT). The blends of PTT/PBT were in the ratio: 10/90, 25/75, 40/60, 50/50, 60//40 and 75/25 (w/w%) respectively. The crystallization kinetics of the binary blends were studied using a Perkin-Elmer differential scanning calorimeter (DSC). All the runs were performed under nitrogen atmosphere to prevent extensive thermal degradation. The samples, sealed in aluminum pans, were heated from room temperature to 280°C at a heating rate of 20 °C/minute and the samples were kept at that temperature for 1 minute. The temperature was then reduced to 20°C at a cooling rate of 10°C/minute and kept at 30°C for 1 minute. The exothermic curve was recorded as a function of temperature. From the crystallization studies, it was found that there are two crystallization peaks when the ratio of PTT and PBT is 40:60 or 50:50; the double peaks were attributed to the two components crystallizing and melting independently in the crystalline regions. This phenomenon suggests that PTT/ PBT forms a nonhomogeneous phase system. In the amorphous part of the nonhomogeneous phase system, PTT and PBT molecular chains were miscible.

Xue *et al.,* [15], investigated the influence of Polycarbonate (PC) and compatibilizer Ethylene-propylene-diene copolymer graft glycidyl methacrylate (EPDM-g-GMA) and

epoxy resin, E-03 (609) on the crystallization behavior of PTT using DSC. Blends of (PC/PTT) in the ratio of: (100/0), (75/25), (50/50) , (25/75) and (0/100) (w/w%) were considered for the studies. He found that the crystallization behavior of PC/PTT blends were interfered by the presence of PC, the interference increasing with PC content. The EPDM-g-GMA had little effect on the nucleation and spherical growth mechanism, presence of an epoxy made a positive contribution to the PTT crystallization. Moreover, the influence of epoxy on the crystallization behavior of PC/PTT blends were correlated with percent of epoxy added.

Semicrystalline polymers can crystallize between their glass-transition temperature (T_g) and their apparent melting temperature (T_m). The bulk crystallization process can be classified into two categories, depending on the initial state from which the polymers are brought to crystallize. If the polymers are brought to crystallize from the molten state (i.e., from a temperature higher than (T_m)), it is called melt-crystallization. On the contrary, if the polymers are brought to crystallize from glassy state i.e., from a temperature lower than (T_g), it is called cold-crystallization. Both physical and mechanical properties of semi-crystalline polymers strongly depend on the extent of crystallization and the morphology developed during processing; studies related to crystallization kinetics provide key information for gaining an understanding of the relationship among the processing conditions, the developed structure, and the properties of the final products. Studies related to the kinetics of polymer crystallization are of great importance in polymer processing, due to the fact that the resulting physical properties are strongly dependent on the morphology formed and the extent of crystallization occurring during processing. It is therefore very important to understand the processing–structure–property interrelationships

of the studied materials, which, in this case, are PTT, PBT, and PC. The overall crystallization process in semicrystalline polymers can be divided into two main processes: primary crystallization and secondary crystallization. The primary crystallization process is a macroscopic development of crystallinity as a result of two consecutive microscopic mechanisms: primary nucleation and secondary nucleation (i.e., subsequent crystal growth). The secondary crystallization process is mainly concerned with the crystallization of interfibrillar melt, which was rejected and trapped between the fibrillar structure formed during the growth of crystalline aggregates (e.g., axialites, spherulites, etc.) [16-18].

If the crystallization time becomes very long, other types of secondary crystallization (i.e., crystal perfection and crystal thickening) may become significant enough to increase the ultimate absolute crystallinity. For the purpose of describing the evolution of crystallinity under isothermal conditions, a number of mathematical models [19-25] has been proposed, based primarily on the notion of primary nucleation and subsequent crystal growth microscopic mechanisms, The contributions from Kolmogoroff [19], Johnson *et al.,* [20], Avrami [21-23], and Evans [24] are essentially similar, it is the work of Avrami that has received the most attention. Based on different approaches, Tobin [25 -27] and Malkin *et al.,* [28] arrived at different mathematical models, which are also different from the Avrami model. Unlike the Avrami model, the use of the Tobin and Malkin models for the analysis of the isothermal crystallization data of semicrystalline polymers, is scarce. Critical descriptive comparisons between the Avrami and Tobin models were performed on the isothermal crystallization data of poly(ethylene terephthalate) (PET), poly(phenylene sulfide) (PPS) [29], medium-density polyethylene (MDPE), and poly(oxymethylene) (POM) [30]. Critical descriptive comparisons between the Avrami and Malkin models

were performed on isothermal crystallization data of polyethylene (PE), isotactic polypropylene (iPP), PET, poly(propylene oxide) (PPO), and polyurethane (PU) [28].

2.1.1 Isothermal crystallization

In the study of isothermal crystallization using differential scanning calorimetry DSC, the rate of evolution of the heat of crystallization as a function of time and the relative extent of crystallization θ(*t*) (or relative crystallinity) are related to one another according to the following equation:

$$\theta(t) = \frac{\int_{t_0}^{t} \left(\frac{dH_c}{dt} \right) dt}{\Delta H_c} \tag{2.1}$$

where *t* represents an arbitrary time during the course of isothermal crystallization process, *dHc* is the enthalpy of crystallization released during an infinitesimal time interval *dt*, and Δ*H*c is the overall enthalpy of crystallization for a specific crystallization temperature T_c. The overall crystallization kinetics of polymers is usually analyzed using the Avrami equation (21–23). In DSC study, it is assumed that the differential area under the crystallization curve with time corresponds to the dynamic changes in the conversion of mass from the melt phase to the solid phase. If χ^{∞} and χ^{t} are the maximum crystallinity obtained for particular crystallization condition and the dynamic crystallinity at arbitrary time *t* for the same crystallization condition, respectively, then the governing Avrami equation can be written as

$$\chi t / \chi\infty = \theta(t) = 1 - \exp[-(k_A t)^{nA}] \tag{2.2}$$

where θ(t) denotes the relative crystallinity as a function of time, k_A is the Avrami crystallization rate constant, and n_A is the Avrami exponent of time. Both k_A and n_A are constants typical of a given crystalline morphology and type of nucleation for a particular crystallization condition [31]. The data analysis based on the Avrami macrokinetic equation was carried out through the direct fitting of the experimental $\theta(t)$ function to equation (2.2). Aiming at improving the Avrami model, Tobin [25–27] proposed a different expression describing phase transformation kinetics with growth site impingement. The original theory was written in the form of:

$$\theta(t) = \frac{(k_T t)^{n_T}}{1 + (k_T t)^{n_T}} \tag{2.3}$$

where θ(t) is the relative crystallinity as a function of time, k_T is the Tobin crystallization rate constant, and n_T is the Tobin exponent. Based on this proposition, the Tobin exponent of time n_T need not be integral [26, 27], and it is governed directly by different types of nucleation and growth mechanisms. The data analysis based on the Tobin macrokinetic equation was carried out by the direct fitting of the experimental $\theta(t)$ functions to equation (2.3). Tobin kinetic parameters (i.e., k_T and n_T), along with the *ASE* values, were obtained from the best fits. Malkin *et al.,* [28] proposed a totally different form of a macrokinetic equation:

$$\theta(t) = 1 - \frac{(C_0 + 1)}{(C_0 + \exp(C_1 t)} \tag{2.4}$$

$$C_0 = 4^{n_M} - 4 \tag{2.5}$$

$$C_1 = \ln(4^{n_M} - 2)\left(\frac{k_M}{\ln(2)}\right)^{\frac{1}{n_M}} \tag{2.6}$$

where θ(t) is the relative crystallinity as a function of time. C_0 relates directly to the ratio of the linear growth rate G to the nucleation rate N (i.e., $C_0 \propto G/N$), and C_1 relates directly to the overall crystallization rate (i.e., $C_1 = a.N + b.G$, where a and b are specific constants). n_M represents Avrami exponent (n_A) in Malkin equation. Both C_0 and C_1 are temperature-dependent constants. The data analysis based on Malkin macrokinetic equation was carried out by the direct fitting of the experimental $\theta(t)$ function to equation (2.4). The Malkin kinetic parameters (i.e., k_M and n_M), along with the *ASE* values were obtained from the best fits.

Xue *et al.,* [15] studied the crystallization behavior of PTT of compatibilized and un compatibilized PTT/ Polycarbonate (PC) blends. DSC results in the study show that crystallization behavior of PTT/PC blend is sensitive to PC content. The Avrami exponent (n) has been found to decrease from 4.3 to 3.6 as the PC content increased, suggesting that nucleation mechanism exhibits the tendency of changing gradually from themal nucleation to a non thermal mode although the growth mechanism still remains three dimensional. These authors have not investigated the occurrence of transesterification.

2.1.2 Non isothermal crystallization

The energy released during non isothermal crystallization is a function of temperature. It is a function of time in case of isothermal crystallization. The relative crystallinity as a function of temperature, $\theta(T)$, is a modification of equation (2.1) and it can be written as follows:

$$\theta(T) = \frac{\int_{T_0}^{T} \left(\frac{dH_c}{dT} \right) dT}{\Delta H_c} \tag{2.7}$$

where T_o and T represent the onset temperature and an arbitrary temperature, respectively, dHc is the enthalpy of crystallization released during an infinitesimal temperature change (dT) and ΔH_c is the total enthalpy of crystallization for a specific cooling (i.e., for non isothermal melt-crystallization) or heating (i.e., for non isothermal cold crystallization) condition. Equation (2.1) is used with an assumption that each sample in a DSC cell experiences a similar thermal history. This could be realized when the lag between the temperatures of the samples and the furnace was minimal. If this assumption is valid, the relation between the crystallization time (t) and the sample temperature (T) can be written as follows:

$$t = \frac{T_0 - T}{\phi} \tag{2.8}$$

where T_0 is an arbitrary reference temperature and ϕ is the cooling or heating rate. According to equation (2.8), the horizontal temperature axis observed in a DSC thermogram for the non isothermal crystallization data can be transformed into the time domain.

The kinetics of non isothermal crystallization of three different types of linear aromatic polyesters PTT, PBT and PET was investigated by Supaphol *el at.,* [32] using (DSC). Analysis of the data was carried out based on the Avrami, Tobin and Ozawa, models. It was found that the Avrami model provided a more satisfactorily good fit to the experimental data for these polyesters than did the Tobin model. The Ozawa model was found to describe the experimental data fairly well. The Ziabicki's kinetic crystallizability

parameter, *G,* for these polyesters was found to be of the following order: PBT > PTT > PET. The effective energy barrier for non isothermal crystallization process of these polyesters, determined by the Friedman method, was found to increase as a function of the relative degree of crystallinity. These authors have not checked the occurrence of transesterification in this system. The rheology of this ternary system has not been investigated.

2.2 Rheology of blends

The properties of blends strongly depend on the structure and morphology of the system, and they are determined by their rheological characteristics. Dynamic rheology testing is thought to be a preferential method for investigating the structure/morphology of materials because the structure of materials exposed to the testing processes is not destroyed under small strain amplitude [33]. The rheology and morphology of multiphase polymer blends are strongly affected by interfacial characteristics. Several models have been proposed to describe the phase behavior of binary polymer blends, such as the time– temperature superposition principle [34-37], Han plots (log G'vs log G", where G' is the dynamic storage modulus and G" is the dynamic loss modulus). Polymer rheological properties help to formulate a polymer system in respect to its processing characteristics. These also give an insight into the physical properties and morphology of the system because there is an inter-play between the processing conditions, structures, and properties [38]. In an article by Varma *el at*., [38], the terpolymer ethylene-butyl acrylate-glycidyl methacrylate (EBAGMA) was used as the reactive compatibilizer to HDPE/PET blends, and melt rheological properties of the blends were studied by means of a capillary rheometer. Varma *et al*., [38] has discussed the morphology of the later blends and effects of the

compatibilizer content, shear rate, and temperature on melt viscosity of the blends. Wu *el at.,* [39] studied the rheological behavior of PBT/montmorillonite (MMT) nanocomposites prepared by melt intercalation using parallel plate rheometer. In the linear viscoelastic measurements, PBT/MMT displays a strain-sensitive linear behavior region much narrower than that of polymer matrix. The temperature independence of G'-G" for PBT/MMT suggests that the relaxation of the interaction between tactoids themselves is not sensitive to the experimental condition in the narrow region of linear viscoelasticity of the nanocomposites.

Xu *el at* [40] has studied the dynamic rheological behavior of ethylene-butene copolymers and their blends with low density polyethylene. Compared with the conventional ethylene copolymers, the metallocene-based copolymers exhibit the following dynamic rheological features: (1) lower viscoelastic moduli and viscosity at small frequencies, but larger viscoelastic moduli and viscosity at large frequencies, thus a small shear thinning effect; (2) larger values of flow activation energy; (3) a relatively fast relaxation rate. These features are the results of simultaneous absence of high molecular weight tails and low molecular weight tails in the metallocene-based copolymers. The dynamic rheological properties of blends of various ethylene–butene copolymers with LDPE were also investigated. It is found that the addition of LDPE can raise the viscosity at low frequencies but lower the viscosity and elasticity at higher frequencies, and retard the relaxation rate of the metallocene-based ethylene copolymers. However, the improvement in rheological properties by LDPE varies with the polymer samples and there is no improvement for the conventional copolymer.

Hong *el at.,* [41] studied the rheology and physical properties of ternary blends containing polyarylate (PAR) U-Polymer 100, a thermotropic liquid crystalline copolyester (LCP) Vectra A950 and a block copolyesterether Hytrel 7246. Addition of Hytrel to the PAR/LPC blend decreased both with dynamic viscosity and storage modulus over the normal processing temperature range.

2.2.1 Rheology and transesterification of PC/PTT/PBT blend.

Reaction between p-acetoxybenzoic acid (ABA) and poly ethylene terephthalate (PET) is primarily an acidolysis reaction [42]. Hamb [43] and the others had observed that acidolysis and esterolysis both occur readily when PET is heated at 275^{o}C with terephthalic acid and 4,4'-isoproplyidene diphenol diacetate with the formation of acetic acid. The effect of shear on the melt viscosities of these copolymers at 275^{o}C is dependent on the ABA content. As the ABA content increases, the polymer becomes shear sensitive at low shear rates. One of the most important properties of these copolymers is that the melt viscosities are shear rate dependent. As the shear rate increases melt viscosities are found to decrease possibly due to the formation of liquid crystalline structure found due to transesterification reactions. Berti *et al*., [44] studied different reactions that take place in melt blending of PC-PET in presence of titanium tetrabutoxide, $Ti(OBu)_4$, as catalyst that is effective in promoting ester/carbonate exchange reactions. They found that volatile cyclic ethylene carbonate introduced strong changes in the resulting chemical reaction. Wilkinson *et al*., [45] prepared PC-PBT blend with adding alkyl titanium as transesterification catalyst. As the degree of transesterification increased the blend changed from block copolymer to random copolymer. It is clear from the literature that extent of

transesterification reactions are strongly influenced by catalyst and reaction conditions. The effect of extend of reaction on blending PC/PTT/PBT has not received any attention. This thesis aims at studying the rheological behavior of melt blend containing PC/PTT/PBT. The polyesters used in this work have residual catalyst in them and could activate exchange reactions.

2.2.2 Rheometry

Rheology is the science of deformation and flow of matter. Deformation is the relative displacement of points of a body. It can be divided into two types: flow and elasticity. Flow is irreversible deformation; when the stress is removed, the material does not revert to its original form. This means that work is converted to heat. Elasticity is reversible deformation; the deformed body recovers its original shape, and the applied work is largely recoverable. Viscoelastic materials show both flow and elasticity. A good example is Silly Putty, which bounces like a rubber ball when dropped, but slowly flows when allowed to stand. Viscoelastic materials provide special challenges in terms of modeling behavior and devising measurement techniques.

In cone and plate viscometer, a low angle ($\leq 3°$) cone rotates against a flat plate with the fluid sample between them. The cone-plate instrument is a simple, straightforward device that is easy to use and extremely easy to clean. It is well suited to routine work because measurements are rapid and no tedious calculations are necessary. In most rotational viscometers the rate of shear varies with the distance from a wall or the axis of rotation. However, in a cone – plate viscometer the rate of shear across the conical gap is essentially constant because the linear velocity and the gap between the cone and the plate both

increase with increasing distance from the axis. The relevant equations for velocity, shear stress, and shear rate at small angle α of Newtonian fluids are equations (2.9), (2.10), and (2.11), respectively, where m_{tr} is the torque, r_c the radius of the cone, v the linear velocity, and r the distance from the axis.

$$\eta = 3\ \alpha\ m_{tr} / 2\ r_c^3 \tag{2.9}$$

$$\tau = 3\ m_{tr} / 2\pi\ r_c^3 \tag{2.10}$$

$$\gamma = dv / dr\ = \Omega / \alpha \tag{2.11}$$

Cone-plate geometry has several advantages over concentric cylinder geometry, including a smaller sample size, a homogenous shear rate, and easy conversion of data. Disadvantages are the need for precise adjustment of the gap, including resetting when the temperature is changed, also specimen drying, solvent evaporating, slinging of material from the gap, and the possibility of viscous heating, particularly at high shear rates.

2.3 Mechanical properties of blends

Anton *et al.,* [46] analyzed the mechanical properties of a binary blend of poly (ethylene terephthalate) (PET)/poly (butylene terephthalate) (PBT) (PES) and ternary blends of polypropylene (PP)/(PES) fibers containing 8 wt % of polyester as dispersed phase. He characterized the (PET/PBT) and PP/(PES) blends using an Instron (Type 1112). Fiber tensile strength was evaluated from 30 measurements. The impact of PET/PBT composition on tensile strength at break of the PP/PES blend fibers (8 wt % PES) indicate the contribution of higher compatibility of the PET/PBT blend with PP. Superior tensile strength of the fibers with higher content of PBT could be probably due to higher molecular

weight of PBT, higher adhesion bonds at interphase, and stiffening of PBT in presence of PET component. Remiror *et al.,* [47] studied the mechanical properties of poly(butylene terephthalate) (PBT)/bisphenol-A-polycarbonate (PC)/poly(hydroxyether of bisphenol-A) (phenoxy) ternary blends, with PBT contents varying from 0 to 30%. Tensile tests were conducted on specimens of (PBT)/PC/(phenoxy) using (ASTM D 638) [48]. The tests were carried out at 23 ± 2 °C in an Instron Tensile Chamber Tester at 10 mm/minute. Young's modulus, yield stress, tensile strength and deformation at break were obtained from the load-time plot. At least eight values were computed for each property. The average standard deviations of Young's modulus, yield stress, tensile strength and deformation at break were ±85MPa, ±1 MPa, ±2.9MPa and ±12% respectively. Kim *et al.,* [49] measured the tensile and flexural properties of PBT/ nylon 6 (PA6)/MAH-grafted EVA (EVA-g-MAH) ternary blends. A universal testing machine (Instron Tester, Model 3367) was operated at room temperature according to the ASTM D638 and ASTM D790 methods, respectively. A crosshead speed of 50 mm/minute and 5 mm/minute for tensile and flexural properties were used, respectively. Notched Izod impact tests were carried out using an Izod impact tester (Uheshima, IM-103) at room temperature. The impact strength of the PBT/PA6 blends increased with increasing EVA-g-MAH content regardless of PA6 content. The impact strength of PBT decreased with increasing PA6 content in general. The flexural strength of the PBT/PA6/EVA-g-MAH ternary blends was lower than those of PBT/EVA-g-MAH blends without PA6**.** A similar result was observed in the case of tensile strength. Although pure PBT showed much higher elongation at break because of its inherent ductile property in comparison to that of PBT/PA6 blends, the elongation at

break showed similar trends as that of the impact strength as a result of the toughening effect of the EVA-g-MAH.

Mechanical properties of plastics can be determined by short, single-point quality control tests, generally multipoint or multiple condition procedures that relate to fundamental polymer properties. Single-point tests include tensile, compressive, flexural, shear, and impact properties of plastics; creep, heat aging, creep rupture, and environmental stress-cracking tests usually result in multipoint curves or tables for comparison of the original response to post-exposure response.

Tensile properties are those of a plastic being pulled in an uniaxial direction until sufficient stress is applied to yield or break the material. Standard tests are ASTM D33 and ISO 527. For many materials, Hooke's law is valid for a portion of the stress-strain curve. If stress is relieved during this portion of the testing, any strain that has occurred is fully recovered. Elastomers generally do not show this linear response. Tensile curves can be used as an indication of polymer strength and toughness. The relationship normally observed is that high stress is necessary for yield or break with strength, whereas high elongation beyond yield is due to ductility (toughness). Similar curves can be generated for tests for comparison with flex, shear, and some form of impacts.

Mechanical properties are determined on solid polymers in arbitrary forms defined precisely by standard test method in ISO, ASTM, or other national standards organizations. Parts are formed by either injection molding, compression molding, or milling from extruded sheet or molded plaques. Viscoelasticity of polymers dictates that the technique used to make the parts must have a significant effect on the mechanical behavior of the

polymer. For valid comparison of materials, they should be prepared similarly and conditioned under the same environment. Viscoelastic effects are also the reason for the rate of strain effects on the modulus values of materials under tensile, flexural, and compressive testing.

2.4 Wide angle-x-ray diffraction

To observe the effect of mixing time (occurrence of transesterification reaction or not) on the PTT crystal structure developed in the blends, Chiu *et al.,* [50] have examined the WAXD patterns of PTT/PC-75/25 using wide-angle X-ray diffraction (WAXD). They used Siemens D5005 X-ray unit at room temperature. The X-ray used was CuKα radiation with a wavelength of 0.154 nm. The 2θ scan ranged from 101 to 351, and the scanning rate was set at 0.021/s with the X-ray generator operated at 40 kV and 30mA. The patterns show that the locations of the characteristic diffraction peaks for PTT crystals in the pure state and in the blends could be differentiated. They observed that as the mixing time increases, the peak intensity for PTT decreases, indicating reduction in crystallinity of PTT. The X-ray results indicate that the crystal structure of PTT is mainly independent of the incorporation of PC counterpart. Su *et al.,* [1] studied the WAXD patterns of poly(ethylene 2,6-naphthalate)/ poly(trimethylene terephthalate)/poly(ether imide) (PEN/PTT/PEI) blends. The experiments were performed with a Shimadzu XRD-6000 X-ray diffractometer with Cu Kα X-rays at a voltage of 40 kV and a 30 mA current in the 2h range of 5–35°C with a step scanning of 2°C/minute. He found that for PEN/PTT/PEI=33/33/33% (w/w%) blends, the scattering patterns contain features of both PEN and PTT when the peak positions of the two polymers were mixed. Peak position

shifting was not observed in blends crystallized at 280 °C. The arrangement of unit cells remained the same as in the original PEN and PTT sequences, and co-crystallization did not occur in the PEN/PTT/PEI blends.

A knowledge of the crystal structure of materials is essential in understanding its properties and how to identify them, their behavior under various conditions, and for the characterization of material at all stages of its preparation. The reproduction of materials with tightly controlled properties often requires x-ray analysis. Although single crystals are preferred for determining crystal structures of new materials, some materials are available only as small polycrystals. In recent years, there have been important advances in using powders for crystal structure determination and refinement. Many structures are already known and this information is used with the powder method in many types of studies that are essential for characterizing and analyzing materials. The importance of these techniques to materials science will be appreciated from the following list, all of which can be best performed by the x-ray powder method. The principal uses of the x-ray powder method are:

a) Identification of crystalline phases including qualitative and quantitative analysis of mixtures of phases;
b) Distinguishing between mixtures, various types of solid solutions and polymorphs;
c) Distinguishing between the amorphous and crystalline states;
d) Precision measurement of lattice parameters and thermal expansion;
e) Determination of the degree of preferred orientation and crystalline texture;

f) Measurement of certain physical characteristics, such as small crystallite sizes, strain, perfection, lattice disorder and damage;

g) Determination of phases and properties as a function of specimen environment either in situ or after treatment at temperatures from liquid helium to about 2000 ^{o}C, and pressures up to several hundred Kbar, in air, vacuum or selected gas.

Bragg's law defines the conditions for obtaining x-ray diffraction from a crystalline material, equation (2.12):

$$n\lambda = 2d \sin \theta \qquad (2.12)$$

where n is a small integer indicating the order of diffraction; λ is the wavelength of the characteristic line x-rays from the x-ray tube and is usually the CuKα double with = 1.540562 A; d is the distance (A) between a set of parallel lattice planes, and θ is the angel between the incident collimated x-ray beam and an atomic lattice plane in the crystal. The term reflection generally refers to the individual diffractions and should not be confused with the total reflection of x-rays as very small angle from highly polished surfaces.

Virtually all solid polymers contain fluctuations in electron density which scatter x-rays at small angle. Structures which can be studied by small angle x-ray scattering (SAXS), detected at scattering 2θ between 20^{o} and 2^{o}, have dimensions in the range 2-1000 nm; the features responsible for this scattering may be compositional fluctuations (block copolymers or blend), or density fluctuations associated with crystallite, voids or additives.

The principal application of wide-angle x ray scattering (WAXS) in the characterization of polymeric materials is the determination of crystallinity and information relating to crystallite size and perfection. In rheooptical studies, WAXS is used to determine the crystal orientation.

2.5 Transesterification analysis

Esters react with alcohol in an acid or base catalyzed transformation to achieve transesterification. It allows for direct conversion of one ester into another without proceeding through the free acids, equation (2.13).

(2.13)

In equation (2.13), R' and R" correspond to alkyl groups.

Acids can catalyse the reaction by donating a proton to the carbonyl group, thus making it more reactive, while bases can catalyse the reaction by removing a proton from the alcohol, thus making it more reactive. Transesterification is used in the synthesis of polyester, in which diesters undergo transesterification with diols to form macromolecules. For example, dimethyl terephthalate and ethylene glycol react to form polyethylene terephthalate and methanol, which is evaporated to drive the reaction forward. The reverse reaction (methanolysis) is also an example of transesterification, and has been used to recycle polyesters into individual monomers.

2.6 Determination of transesterification using FTIR

It is well established that in the absence of transesterification reactions between PC and PET such systems are normally immiscible [51-53]. It is understood that when transesterification reactions occur, the rate of conversion is greatest in the PC rich blends with the highest overall ratios occurring in a 50PET/50PC blend [54]. This route of achieving miscibility for such transesterification reactions are typically limited and generally absent, unless excess catalyst from the PET polymerization process is present or additional catalyst is introduced to promote copolymer formation/miscibility (via catalysis of the ester carbonate transesterification reaction) [53, 55]. The occurrence of exchange reaction between molten PC, PTT and PBT was indirectly established using solubility test coupled with infrared analysis. Soluble mixture of PC, PTT and the insoluble components containing exchange reaction products of PTT and PC (PTTC) and PBT and PC (PBTC) (polybutylene terephthalate) were analyzed at room temperature [55]. The reaction products were extracted with methyl chloride. In this solvent, PC is completely soluble, where as PTTP and PBTP remain practically insoluble. Structural changes corresponding to the soluble and insoluble components in methyl chloride were detected by infra-red spectroscopy.

When examining transesterification via IR spectroscopy, three distinct bands are of particular interest: (a) the 1775cm^{-1} band that corresponds to the carbonyl stretching of an amorphous aromatic carbonate (PC), (b) the 1720cm^{-1} band associated with the carbonyl stretching of an aliphatic ester PET), and (c) the 1740cm^{-1} band associated with the

stretching of a mixed aliphatic-aromatic carbonate, which is a product of the ester-carbonate transesterification reaction [51, 56, 57], Figure 2.1.

Transesterification in PC/PET was also monitored via ATR-FTIR, Figure 2.1. When copolymer formation occurs the PC peak (1780 cm^{-1}) decreases in intensity while the PET peak (1720 cm^{-1}) increases in intensity and a new peak develops at the 1740 cm^{-1} band associated with the stretching of a mixed aliphatic-aromatic carbonate, which is a product of the ester-carbonate transesterification reaction. Transesterification of PC/PET/ montmorillonite (mmt) nanocomposite blends were investigated by Mathew [58].

A commercially available organo-mmt, Cloisite 25A (C25A), with a CEC of 0.95 meq/g modified with dimethyl, hydrogenated-tallow, 2-ethylhexyl quaternary ammonium surfactant was used in this work. He observed significant enhancements in poly(ethylene terephthalate) nanocomposites material properties with respect to thermal stability, relative modulus, and crystallization behaviors, at low filler loadings, without observing, severe penalty in the composite ductility, especially when high thermal stability surfactant modification were applied to the layered silicate.

When comparing the carbonyl stretching of the aliphatic ester in the PET (1720 cm^{-1}) in the PET rich blend (75PET/25PC) to the corresponding nanocomposites, no significant intensity deviation was observed and no peak splitting was found to occur.

Polycarbonate Poly (ethylene terephthalate)

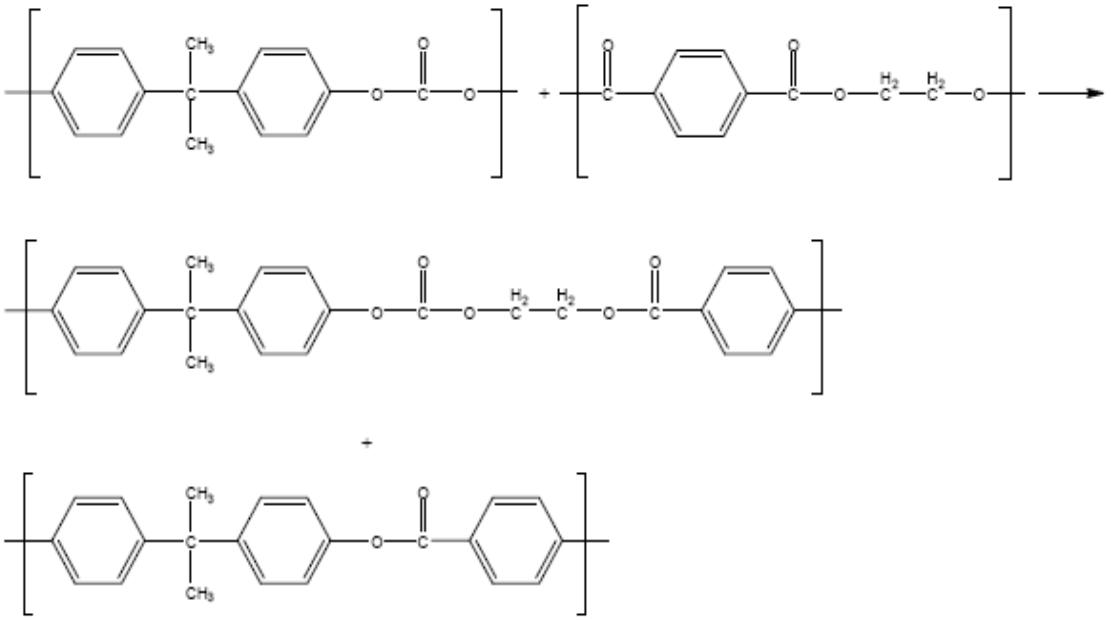

Figure 2.1: The products of the PC/PET ester-carbonate transesterification reaction leading to copolymer formation [54, 56].

If transesterification in the nanocomposites had occurred to a greater extent than in the unfilled blends, the intensity of the peak would have increased dramatically and would have shifted/split, with the new peak corresponding to the stretching of a mixed aliphatic-aromatic carbonate. Likewise, similar behaviors are found to occur in the equivalent blends (50PET/50PC) and the PC rich blends (25PET/75PC) in which no significant intensity deviations or peak splitting occurs. Thus, the result of the ATR-FTIR indicates that independent of blend concentration, phase morphology, or if the sample contains filler; no distinct differences in the transesterification behaviors are observed. Therefore, Mathew [58] concludes that any transesterification in the nanocomposite blends is no greater than

what occurs in the unfilled blends – and in general, any amount of transesterification that may be occurring is undetectable in the ATR-FTIR.

2.7 Degradation of polymers

The chemical reactions occurring during thermal processing of blends have been thoroughly examined [59]. In polycarbonate/polyester blends, transesterification reactions are known to start in the temperature range 250-300°C [56, 60]. Transesterification reactions could occur due to a variety of reasons like dipole-dipole forces, acid-base attraction, ion-ion interaction or hydrogen bonding [61, 62]. Transesterification in polyester blends depends strongly on the components' initial compatibility and on the blending conditions, including temperature, duration of mixing and preparation method [63]. As polyesters readily transesterify near and above their melting points, interchange reactions commonly occur between blend constituents [64, 65]. Blends of PC and PBT are slightly miscible since interchain reactions between the carbonate and ester are possible. More miscible systems can be obtained at temperatures greater than 270°C [12, 66]. Transesterification between PTT and PC have been reported by Yuvari *et al.,* [67]. DMA and DSC analysis for the transesterification between PTT and PC indicated two partially miscible phases in which the degree of crystallinity is reduced by increasing PC content. It was also concluded that annealing at 300°C causes the constituents to form a complex system of block copolymers with different block lengths [67]. Reports on PTT/PBT blends indicate that such systems are completely miscible and exhibit a single glass transition temperature dependent on the amount of PTT [68]. A ternary miscible blend system

comprising of PET, PTT and PBT was developed by Woo *et al.,* [69]. The ternary miscibility in this blend was essentially physical and no chemical transesterifications took place.

The study of degradation kinetics is important in understanding the mechanism of the degradation process. Both thermogravimetric analysis (TG) and differential thermal analysis (DTA) have been applied to determine the degradation kinetics of neat polyesters and polycarbonate [70, 71]. Generally, TG is the preferred technique for such determinations, since the relevant mass changes are easier to measure than the associated heat effects [72]. Few methods are cited in the literature for the study of solid thermal decomposition kinetics. These methods utilize mechanisms like Avrami-Erofeev and Prout-Tompkins. Most degradation studies describe such reactions with the n^{th} order reaction mechanism [73-75].

Some authors have described the decomposition of a solid as a heterogenous process [76, 77]. These studies have also established that thermogravimetric data of solid thermal decomposition reactions fit well with n^{th} order reaction mechanism. This is because thermogravimetric data under non isothermal conditions are analyzed with kinetic equations specific to heterogenous processes, which in turn fit well with those used to characterize n^{th} order reactions.

The degradation kinetics of this tricomponent blend has not yet been reported in the literature. The TG data obtained under nitrogen and air for the neat polymers and blend at several heating rates has been analyzed using Kissinger [78], Ozawa [79], Friedman [80] and Chang [81] models. Earlier studies [82] show that TG data follow Prout-Tompkins or

Avrami-Erofeev mechanisms, at a constant heating rate, and originate from first-order reaction. Other researchers [83, 84] evaluated experimental degradation data using reference theoretical curves called "master plot".

Kinetic information can be extracted from dynamic experiments by means of various methods like DSC and TG. All kinetic studies assume that the isothermal rate of conversion $d\alpha/dt$, is a linear function of the temperature-dependent rate constant, k(T), and a temperature-dependent function of the conversion, $f(\alpha)$, that is:

$$\frac{d\alpha}{dt} = k(T)f(\alpha) \tag{2.14}$$

α being the fractional extent of reaction. In equation (2.14), $f(\alpha)$ depends on the particular decomposition mechanism. According to Arrhenius equation:

$$k(T) = Ae^{-E/RT} \tag{2.15}$$

Where *A* is the pre-exponential factor, that is assumed to be independent of temperature, *E* is the activation energy, *T* the absolute temperature, and *R* is the gas constant. Combining equations (2.14) and (2.15) we have

$$\frac{d\alpha}{dt} = A\exp\left(-\frac{E}{RT}\right)f(\alpha) \tag{2.16}$$

If β is rate of heating then for non isothermal measurements at constant heating rate $\beta = dT/dt$, equation (2.16) transforms to

$$\beta \frac{d\alpha}{dT} = A \exp\left(-\frac{E}{RT}\right) f(\alpha) \tag{2.17}$$

Activation energy E can be calculated by various methods. The first one is based on Kissinger's method [78]. It is used in the literature in order to determine activation energy from plots of the logarithm of the heating rate versus the inverse of the temperature, in constant heating rate experiments.

The methods proposed by Kissinger [78] relies on experiments carried out at different heating rates, β, and is expressed by:

$$\ln\left(\frac{\beta}{T_p^2}\right) = -\frac{E}{RT_p} + \text{const} \tag{2.18}$$

Where β is heating rate, T_p is temperature corresponding to inflection point obtained from thermal differential degradation curve which correspond to maximum reaction rate, and R is the gas constant.

The thermal decomposition kinetics of copolymer can be also analyzed by the Ozawa method using the following kinetic equation (2.19):

$$\frac{d\alpha}{dt} = A \exp\left[\frac{-E}{RT}\right](1-\alpha)^n \tag{2.19}$$

where, α is weight loss of the polymer undergoing degradation at time t, $d\alpha/dt$ denotes weight-loss rate, A is the frequency factor, n represents decomposition reaction order, E stands for the activation energy of the thermal decomposition, R is gas constant, and T

symbolizes absolute temperature. For non isothermal thermogravimetry, if the heating rate is β i.e. dT/dt, equation. (2.14) can be modified as follows:

$$\frac{d\alpha}{dT} = \frac{A}{\beta}\exp\left[\frac{-E}{RT}\right](1-\alpha)^n \tag{2.20}$$

Ozawa technique [79] is a multiple heating-rate treatment method for TGA and DTG curves to obtain the kinetic parameters of thermal decomposition. The Ozawa equation can be represented as follows:

$$\log\beta = \log\frac{AE}{Rf(\alpha)} - 1.052\frac{E}{RT} \tag{2.21}$$

where $f(\alpha) = \int_0^{\alpha} \frac{d\alpha}{(1-\alpha)^n}$. Therefore, from a plot of log β against *1/T*, the value of *E* can be determined from the slope.

The third method is also an isoconventional one based on equation (2.14) and Arrhenius equation (2.15). Friedman [80] proposed to apply the logarithm of the conversion rate $d\alpha/dt$ as a function of the reciprocal temperature. He proposed an equation of the form:

$$\ln\left(\frac{d\alpha}{dT}\right) = \ln\left(\frac{A}{\beta}\right) + \ln(f(\alpha)) - \frac{E}{RT} \tag{2.22}$$

It is obvious from equation (2.15) that the function $(f(\alpha)) + \ln(A/\beta)$ is a constant. By plotting $\ln(d\alpha/dt)$ against *1/T*, the value of the *–E/R* for a given value of α can be

obtained. Using this equation, it is possible to obtain values for *E* over a wide range of conversions.

Chang technique is a single heating-rate treatment method for TG and DTG curves. It can be used to determine the kinetic parameters of thermal decomposition:

$$\mathrm{Ln}\left[\left(\mathrm{d}\alpha/\mathrm{dt}\right)/\left(1-\alpha\right)^{\mathrm{n}}\right]=\mathrm{Ln}\left(\mathrm{z}\right)-\mathrm{E}/\left(\mathrm{R.T}\right) \qquad (2.23)$$

According to Chang method [81], a plot of $\mathrm{Ln}\left[\left(\mathrm{d}\alpha/\mathrm{dt}\right)/\left(1-\alpha\right)^{\mathrm{n}}\right]$ against *1/T* yields a straight line if the decomposition order n is selected correctly. The slope and intercept of this line can provide the *–E/R* and *Ln (z)* values, respectively [85]. In this model, the value of n is assumed to be unity [85].

If the temperature of the sample undergoing thermal degradation increases at a constant rate, β, equation (2.16) can be integrated [38] into the following expression:

$$g(\alpha)=\frac{ART^2}{E\beta}\exp(-E/RT) \qquad (2.24)$$

From (2.16) and (2.24) we obtain:

$$g(\alpha)=\frac{RT^2}{E\beta}\frac{d\alpha}{dt}\frac{1}{f(\alpha)} \qquad (2.25)$$

for which, at α = 0.5 becomes:

$$g(0.5) = \frac{RT_{0.5}{}^2}{E\beta}\left(\frac{d\alpha}{dt}\right)_{0.5}\frac{1}{f(0.5)} \tag{2.26}$$

Where $T_{0.5}$ and $\left(\frac{d\alpha}{dt}\right)_{0.5}$ are the temperature and the rate when α = 0.5, respectively.

From equations (2.25) and (2.26), the following relationship is developed:

$$\left(\frac{T}{T_{0.5}}\right)^2 \frac{\left(d\alpha/dt\right)}{\left(d\alpha/dt\right)_{0.5}} = a\, f(\alpha)\, g(\alpha) \tag{2.27}$$

where $a = g(0.5).\frac{1}{f(0.5)}$ is a constant for a given mechanism.

2.8 Summary of the review on polymer blends

Polymer blending is an attractive alternative for producing new polymeric materials with desirable properties without having to synthesize a totally new material. Other advantages for polymer blends are versatility, simplicity, and inexpensiveness. Numerous published articles related to various aspects of binary blends of polyesters are available in the open literature. Some of these are, for example, blends of PET and PBT [86-89], PBT and an amorphous co-polyester of cyclohexane dimethanol, ethylene glycol, and terephthalic acid (PETG) [90], and PTT and poly(ether imide) (PEI) [91].

In PET/PBT blends, Escala *et al*., [92] reported that the blends showed a single and composition-dependent glass transition temperature at all compositions, suggesting that

PET and PBT were miscible in the amorphous state. Similar results were also reported by others [93, 94]. Based on various experimental techniques, Escala *et al*., [93] reported that, upon crystallization, PET and PBT did not co-crystallize. Avramova [94] confirmed such findings and added that, even though each component formed its own crystalline phase upon crystallization, both components could crystallize concurrently at all compositions of the blends and the presence of one crystalline phase did not deter or enhance the crystallization rates of the other.

Recently, Huang *et al*., [95] studied miscibility, melting, and crystallization behavior of PTT/PEI blends. They observed that the blends showed a single and composition dependent glass transition temperature over the entire compositional range studied, indicating that the blends were fully miscible in the amorphous state. They also reported that recrystallization of PTT during a heating scan in a differential scanning calorimeter (DSC) was either retarded or fully inhibited by the presence of PEI component, a direct result of decreased segmental diffusion of PTT molecules onto an existing growth face. Godard *et al.,* [96] have concluded that the most likely degradation mechanism to appear in poly (bisphenol A carbonate)/poly (butylene terephthalate) (PC-PBT) transesterification, in the molten state, is a reversible ester-ester exchange reaction, which produces a random four-component copolyester. Polycarbonate in a blend exhibits excellent mechanical properties like high and low temperature toughness. It also has limiting oxygen index (LOI) value of 27 and produces large fractions of char upon combustion [97]. These materials can meet the demanding chemical and electrical/ electronic needs of engineering thermoplastics.

The chemical reactions occurring in the thermal processing of blends have received continued attention in the literature [96, 98-101]. In the case of polycarbonate/polyester blends, reactions are known to start in the range of 250-300°C [60, 102], eventually causing the formation of copolymers to have new mechanical and thermal properties.

In order to obtain a better understanding of the degradation kinetics of polycarbonate/polyester blend and the nature of interaction between the components, a detailed study of the kinetics of thermal degradation of the novel blend PC/PTT/PBT (50:25:25 w/w%) has been carried out using the non isothermal TG approach. Also the applicability of such master plots in determining the reaction mechanism for the solid state decomposition of PC, PTT, PBT and the tricomponent blend will be discussed.

2.9 Objectives of the present work

A novel partially miscible ternary blend consisting of PC, PTT, PBT in the presence of possible trans reactions has been reported in this work. This is a novel work which synthesizes a partially immiscible ternary blend in which the constituents comprise of amorphous and semi crystalline polymers. Based on the literature review, the following objectives have been chosen for this work.

A. To develop blends of PC/PTT/PBT (50:25:25 wt/wt % ratio) using a single screw extruder.
B. To study miscibility of the blend by measuring variations (if any) in the glass transition temperatures of the component polymers.

C. To extrude the samples and conduct injection molding to obtain test specimens for tensile strength according to ASTM (D-638).

D. To determine the percentage crystallinity of the neat polymers and blend using X-ray analysis.

E. To study particle sizes for the dispersed phase in the polymer blends using scanning electron microscope (SEM),

F. To study rheological properties of the blend and relate rheological properties to crystallization behavior under shear.

G. To investigate the thermal decomposition kinetics of polyester polycarbonate blends and to establish its activation energy values through a dynamic thermogravimetric analysis in air and nitrogen atmosphere.

H. To study possible transesterification reactions which occur in the tricomponent blend using Fourier Transform Infrared Spectroscopy (FTIR).

Chapter 3 MATERIALS AND EXPERIMENTAL TECHNIQUES

3.1 Materials

3.1.1 Polycarbonate, (PC)

Polycarbonate (PC) used in this work was obtained from Century Enka Pvt Ltd., Pune, India. Average molecular weight of this resin provided by company was 28,000 g/mol. It is an unusual and extremely useful class of polymers. The vast majority of polycarbonate are based on bisphenol A (BPA) and sold under the trade names Lexan (GE), Makrolon (Bayer).

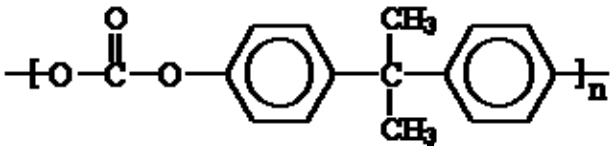

BPA polycarbonates, having glass-transition temperatures in range of 145-155 °C, are widely regarded for optical clarity and exceptional impact resistance and ductility at room temperature and below.

The T_g of polycarbonate is around 150°C, which is unusually high compared to other thermoplastics such as polystyrene (100°C), polyethylene terephthalate) (69°C), and nylon-6,6 (45°C). The high glass-transition temperature can be attributed to the bulky structure of the polymer, which restricts conformational changes, and to the fact that the

monomer has a higher molecular weight than the monomer of most polymers. The high T_g is important for the utility of polycarbonate in many applications, because, as the point which marks the onset of molecular mobility, it determines many of polymer's properties such as dimensional stability, resistance to creep, and ultimate use temperature. Polycarbonates of different structures have significantly higher or lower glass-transition temperatures. In addition, PC itself exhibits flame retardancy and produces a large fraction of char upon combustion [99]. Davis *et al.,* [103] assigned CO_2, phenol and bisphenol A as the main volatile products, together with a small amount of CO, alkyl phenols and diphenyl carbonate. They speculated that the carbonate group undergoes rearrangements, along with hydrolysis and alcholysis; they also proposed the formation of a xanthone unit during thermal degradation of PC [103-105]. McNeill *et al.,* [106, 108] investigated the thermal degradation mechanism of PC using thermal volatilization analysis (TVA) in nitrogen. They assigned some cyclic oligomers of bisphenol A carbonate and different phenol structures having masses less than 228 using gas chromatograph/mass spectrometry (GC/MS) and suggested a homolytic chain scission mechanism for the degradation of PC.

3.1.2 Poly (trimethylene terephthalate), (PTT)

Poly (trimethylene terephthalate) (PTT) was supplied in pellet form by Century Enka Pvt. Ltd., Pune, India. The weight-average and number-average molecular weight of this resin were provided by the company to be 78,000 and 34,700 g/mol, respectively. It had

a melting temperature (T_m) of 257 °C. It is a linear aromatic polyester and a member of the polyester family, with three methylene units in its chemical structure.

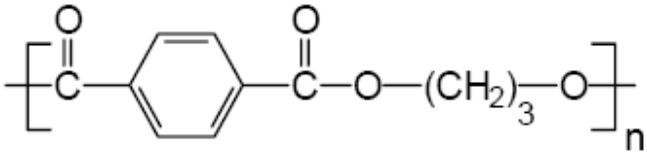

Uses for PTT are in areas such as fibers, films, and engineering thermoplastics. PTT has recently been introduced commercially by Shell Chemicals under the tradename Cortera. Numerous studies on crystal structure and mechanical properties of PTT have been reported [108-111]. Analysis of the crystalline structure of PTT shows that the aliphatic part of PTT takes a highly coiled structure of *gauche– gauche* conformation. PTT has a triclinic crystalline structure. Ward *et al.,* [109] performed a comparison study of three polyester fibers and found that PTT has a very good tensile elastic recovery property. It was ranked in the unexpected descending order of PTT, PBT and PET. Jakeways *et al.,* [108] studied the deformation of crystalline structure of PTT and PBT by drawing mono-filaments *in situ* in a wide-angle diffractometer, where changes in the fiber period *d* spacing along the *c*-axis were measured as a function of strain. They found that the deformation was reversible in both PBT and PTT below their critical strains, on the order of about several percent.

Poly (trimethylene terephthalate)(PTT), synthesized using 1,3-propandiol as a diol, is a high crystalline polymer. Its melting temperature is lower than that of PET by 20–30°C. Therefore, the processibility of PTT is superior to that of PET. Furthermore, the highly flexible PTT fibers are obtained as a result of its low initial modulus. The elasticity and dyeability of PTT are better than those of PET or poly(butylene terephthalate) (PBT), which makes it possible to use PTT as engineering plastics, films carpets, and clothing

materials. For these reasons, PTT is considered as the most promising candidate for a replacement of PET. It is well known that the number of methylene unit influences the physical properties of many polycondensation polymers such as polyamide and polyester, which is called the odd-even effect. PTT has a conformation with bonds of the –$O(CH2)_3O$– unit having the sequence of *trans*– *gauche*–*gauche trans,* leading to a concentration of the repeating unit. The opposite inclinations of successive phenylene groups along the chain force the molecular chains to take on an extended zigzag shape.

Investigations related to the chain conformation, crystal structure, and morphology of PTT have been carried out and reported in recent years [112, 113]. A few studies related to isothermal melt-crystallization kinetics of PTT include Avrami crystallization kinetics [114-116] and the kinetics of linear spherulitic growth rates [22, 23, 26].

The mechanical properties of PTT lie roughly between those of poly(ethylene terephthalate) (PET) and poly(butylene terephthalate) (PBT). PTT shows better tensile elastic recovery and lower modulus than PET and PBT [110]. These two properties are very desirable for making soft, stretchable fabrics with good toughness [117].

3.1.3 Poly (butylene terephthalate), (PBT)

Poly(butylene terephthalate) (PBT) used in this study was purchased from RTP Co. (United States). It had number- and weight-average molecular weights of 68,250 and 29,400 g/mol, respectively. It contained 0.063 equiv/kg of hydroxyl groups and 0.041 equiv/kg of carboxylic groups at chain ends. It had a melting temperature (T_m) 223 °C.

The thermoplastic (PBT) is prepared by polycondensation of 1,4-butanediol with dimethyl terephthalate.

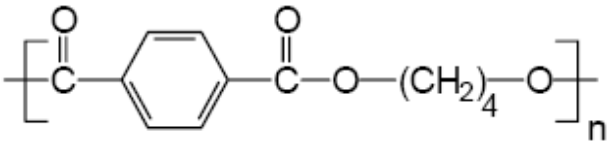

Because of its very easy processing and rapid crystallization, injection-moldable PBT compounds quickly became more popular than PET compounds. PBT (as well as PET) resins are high-performance materials that can be converted to various functional components and structural parts that used to be made of metal or thermosets. Property combinations such as high mechanical strength, high heat distortion temperature (up to 215°C for glass fiber-reinforced PBT), continuous use temperature of 140°C, dimensional and chemical stability and short cycle times in injection molding are primarily responsible for the success of this engineering plastic. The properties of PBT are strongly dependent on the crystalline portion and resulting morphology after processing. PBT is a prominent member of the engineering thermoplastics and is characterized by (i) high stiffness and strength, (ii) high toughness at low temperatures, (iii) high heat-deflection temperature, (iv) high stress-cracking resistance, (v) high resistance to fuels, oils, fats and many solvents, (vi) low coefficient of linear expansion, (viii) low water absorption. (viii) good friction and wear characteristics, and (ix) good processability. PBT is highly suitable for electrical applications, automotive, telecommunication, machine components, food and medical applications. PBT is polymerized in a two-stage process. In the first stage (the transesterification stage) bishydroxybutyl terephthalate (BHBT) is formed

through the transesterification of 4 dimethyl terephthalate (DMT) with 1,4-butanediol. In the second stage, the polycondesation, the BHBT is polycondensed into PBT with elimination of 1,4-butanediol. Solid-state polycondensation is used when a high molecular weight PBT is required. The properties of PBT can be modified in many ways to meet the requirements of specific fields of application, as is the case with most engineering plastics. Copolymerization, blending with other polymers (e.g., rubber, PC, ASA) and the addition of reinforcements, flame retardants, stabilizers, etc., during compounding are different ways to modify the properties of PBT. PBT is blended with amorphous polymers to reduce shrinkage and to increase dimensional stability.

3.2 Experimental approach for conducting experiments related to crystallization kinetics of neat polymers and the blend

3.2.1 Sample preparation

PTT, PBT and PC resins were dried in a vacuum oven at 110°C for 5 hours prior to use. PC/PTT/PBT (50:25:25 wt/wt %) pellets were placed in plastic zipper bags, mixed by vigorous shaking, and mechanically blended in a single-screw extruder at a screw speed of 100 rpm with extruder barrel temperature zones of 220, 250, 255, and 235 °C. The strands from the extruder were cooled in a water bath and pelletized. Pellets of PTT, PBT, PC and PC/PTT/PBT (50:25:25 wt/wt %) were crushed into fine powder by using a Retsch (ZM- 200) mill operating at a speed of 18000 rpm for X-ray, SEM and FTIR analysis.

3.2.2 Differential scanning calorimeter measurements

A Diamond DSC (Perkin–Elmer) was used to record non isothermal melting endotherms and the subsequent crystallization exotherms of these polymers. Calibration for the temperature scale was carried out using pure indium standard (having a melting temperature of 156.6^{o}C and enthalpy value of 28.5 Jg^{-1}) on every run to ensure accuracy and reliability of the data obtained. The temperature sensor is providing an indication of the specimen temperature to ± 0.01°C. Another calibration is a software correction routine where several materials, (indium, lead and zinc alloy) with melting temperature of 327 °C and 419 °C, are stored as a file. The enthalpy values of lead and zinc were 179 and 115 kJ/mole, respectively. The sample data file is then corrected using the calibration file. This procedure is covered in the Perkin Elmer instruction manual. To minimize thermal lag between the polymer sample and the DSC furnace, each sample holder was loaded with polymer samples weighing around 7.0 ± 0.5mg. Each sample was used only once and all the runs were carried out under a flow of nitrogen (20 ±5 ml/minute) to prevent thermal degradation. Experiments started with heating each sample from 30°C at a heating rate of 100 ± 0.1°C/min to a desired fusion temperature T_f (290°C). To ensure complete melting, the sample was kept at the respective T_f for a holding period of 5 minutes.

For the study of non isothermal crystallization, some samples were cooled at the desired cooling rate (ϕ) (5, 10, 15, and 20°C min^{-1}) to 30°C. The non isothermal crystallization exotherms were analyzed according to the models mentioned above. For the study of isothermal crystallization, the prepared samples were cooled to a desired crystallization

temperature (T_c). Identical temperatures for the polymers could not be maintained since PTT crystallized between 129 to 159 °C, PBT between 168 to 177°C and the blend between 170 to 183°C. Based in this temperatures, the (T_c) values chosen were 130, 138, 147, and 158 °C for PTT, 169,171,173 and 176°C for PBT polymer and 171, 173,176, and 182°C for the blend of PC/PTT/PBT (50:25:25 wt/wt %). The samples were kept at the isothermal temperatures to completely develop the isothermal crystallization peak. It was assumed that the crystallization was finished when the isothermal curve converged with the horizontal base line. The crystallization isotherms were recorded for further analysis.

3.3 Experimental approach for conducting experiments related to morphology and mechanical properties of neat polymers and blend

3.3.1 Scanning electron microscope (SEM) measurements

Morphology depends mainly on rheological and interfacial properties, the blending conditions and the volume ratio of the components. In this study, the phase morphology of the samples was investigated by a scanning electron microscope (JEOL JSM-410). Fractured surfaces of the blended samples were prepared, and gold coated and observed under 3500 ± 100 μm magnification.

3.3.2 X-ray measurements

The crystal structure study, was conducted using a wide angle x-ray diffractometer (WAXD)(SIEMENS, D-5000). The X-ray source was Cu k_α radiation, and the wavelength was $\lambda = 1.54A^o$. The 2θ scan ranged from 10° to 35°, and the scan rate was set at 0.02°/s with the x-ray generator operating at 40 kV and 30 mA.

Precision: Test results were obtained by this procedure are expected to differ in absolute value by less than 2.772 S, where 2.772 S is the 95% probability interval limit on the difference between two test results and S is the appropriate estimate of standard deviation.

3.3.3 Tensile measurements

The test methods were according to (ASTM D-638), Type I specimen standards. The properties were measured on Instron (Type 1112). Samples were strained at constant speed rates of 50 mm/minute. All tests were carried out at constant temperature of 23 ± 1°C and constant relative humidity of 35 ± 1%.

3.4 Experimental approach for conducting experiments related to rheology of neat polymers and blend

3.4.1 Sample preparation for rheological analysis

PC, PTT and PBT resins were dried in a vacuum oven at 110°C for 5 hours prior to use. PC/PTT/PBT (50:25:25 wt/wt %) pellets were placed in plastic zipper bags, mixed by vigorous shaking, and mechanically blended in a single-screw extruder at a screw speed of 100 rpm with extruder barrel temperature zones of 220, 250, 255, and 235 °C. The strands from the extruder were cooled in a water bath, pelletized and dried for 5 hours at 120°C. Samples of neat PC, PTT, PBT and blend in pellet shape were melt-pressed into circular disks of 3.0 mm in thickness and 25 mm in diameter. The sample disks were dried in a vacuum oven at 70°C for 5 hours prior to use. The sample discs were kept in

the desiccators to avoid any moisture. The samples were removed from the desiccators and loaded into the instrument furnace maintained at 260°C for rheological analysis.

3.4.2 Cone and plate rheometer measurements

Rheological measurements were carried out on a rheometer (Gemini 200 rheometer, Bohlin instrument Co., UK) equipped with a parallel plate geometry using 25 mm diameter plates. In the linear viscoelastic measurements, small amplitude oscillatory shear was applied, and the dynamic strain scan measurements and the dynamic frequency scan measurements were carried out. Before each measurement, the rheometer was heated up to 260 °C and the gap between the cone and plate was set at 1.55 mm, with accuracy of < 1μm. The maximum error in controlling the cone and plate temperatures is ±1 °C. For a steady rate sweep test, the shear viscosity of the materials was determined as a function of shear rate. In the case of a dynamic measurement, the strain values were chosen such that the experiments could be performed in the linear viscoelastic region. Torques measured are typically in the range 3.0 x 10^3 - 1.5 x 10^7 dyn cm, requiring a maximum deflection of the plate through an angle of 0.6 mrad, so that the correction for the reduction of the shear due to this small amount of plate rotation is negligible in comparison to the total shear introduced into the material and the total error is within ±1%.

Melt viscosity η (Pa s) as a function of shear rate, $\dot{\gamma}$ (1/s), and the dynamic properties, i.e., storage modulus G'(Pa), loss modulus G''(Pa), and phase angle tan (δ)= G''/G' as a function of frequency ω (rad/s) were measured. The shear rate range was varied from 0.10 to10 s^{-1} and similarly the frequency of oscillation was varied from 0.10 to 10.0 Hz.

3.5 Experimental approach for conducting experiments related to degradation of neat polymers and blend

3.5.1 Sample preparation for degradation studies.

PTT and PBT were weighed and dried at 110°C for 5 hours while PC was weighed and dried at 120°C for 5 hours. The three polymers were placed in plastic zipper bags, mixed by vigorous shaking then mechanically blended, in the weight ratio PC/PTT/PBT (50:25:25 wt/wt%), in a single-screw extruder at a screw speed of 50 rpm and extruder barrel temperature zones of 230, 265, 295 and 270°C from hopper to die. The strands from the extruder were cooled in a water bath, pelletized and dried for 5 hours at 120°C.

3.5.2 Thermogravimetric Analysis measurements

Thermogravimetric analysis was carried out with a TA instrument TA-SDT system, 2960. For a typical experiment 11 ±0.5 mg of PC, PTT, PBT and blend were weighed and dried at 110°C for 6 hours while PC was weighed and dried at 120°C for 6 hours Samples then were placed in alumina crucibles. An empty crucible was used as reference. Samples were heated from ambient temperature to 650°C in a 20 ±5 ml/minute flow of 99.9% pure N_2 and air based on the atmosphere chosen for the study. The temperature sensor is providing an indication of the specimen temperature to ± 0.1°C. Heating rates of 5, 10, 15 and 20°C/minute were used and continuous records of sample temperature, sample weight loss, its first and second derivative and heat flow were measured.

Chapter 4 RESULTS AND DISCUSSION

This chapter begins with the study of non isothermal crystallization kinetics of neat polymers and blend. The Avrami, Tobin and Malkin analysis were carried out to determine the crystallization kinetic parameters. The SEM analysis was used to determine the morphology of the polymers after blending PC/PTT/PBT in the weight ratio 50:25:25. X-ray analysis was carried out to check if the blend was crystalline in nature. The tensile properties were measured using a Instron (Type 1112) machine. The elongation at break, tensile strength break, yield point, elastic modulus and yield strength were also determined. The crystallization kinetic parameters were determined using Avrami, Tobin and Malkin analysis for the isothermal crystallization analysis. Rheological analysis was also carried out to check if trans-reaction occurred during the course of blending. The FTIR characterization of the blend and neat polymers were also carried out at room temperature to check the occurrence of trans-exchange reactions. Thermogravimetric analysis of the neat polymers and the blend was carried out to obtain the degradation kinetic parameters.

4.1 Non isothermal crystallization kinetics of neat polymers and blend

4.1.1 Non isothermal crystallization

The non isothermal crystallization exotherms of PTT, PBT and the blend PC/PTT/PBT (50:25:25 wt/wt %) recorded at four cooling rates, 5, 10, 15, and 20^{o}C min^{-1} respectively,

are presented in Figures 4.1 to 4.3. For PTT, Figure 4.1, it is noticed that the crystallization exotherm becomes wider and shifts to a lower temperature with increasing cooling rate. For PBT, Figure 4.2, it is noticed that with increasing cooling rate, the curves shift to lower temperatures. This behavior can be related to the amount of methylene groups in the polyester. With higher cooling rates, the peaks exhibited by the blend remain unchanged and no shift in peak temperatures is observed.

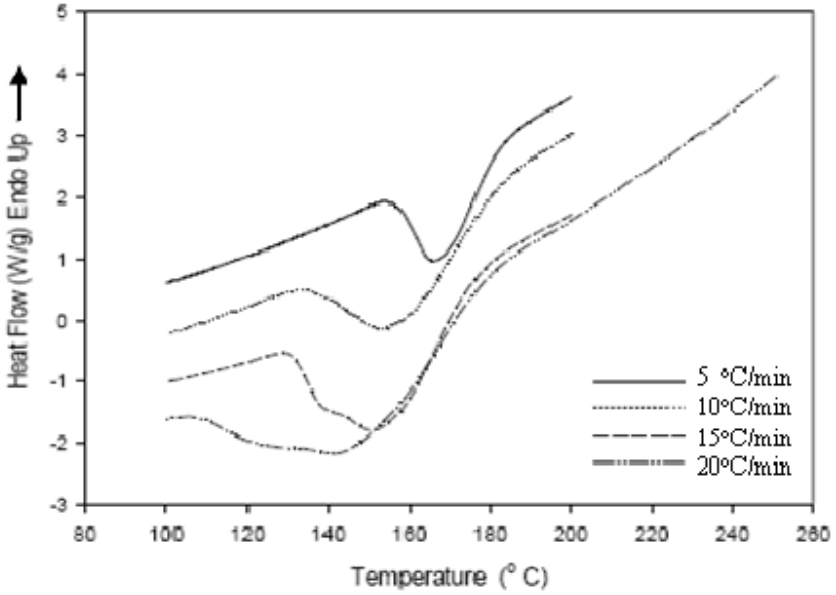

Figure 4.1: Non isothermal crystallization of PTT at four different cooling rates; 5, 10, 15 and 20 ^{o}C /min.

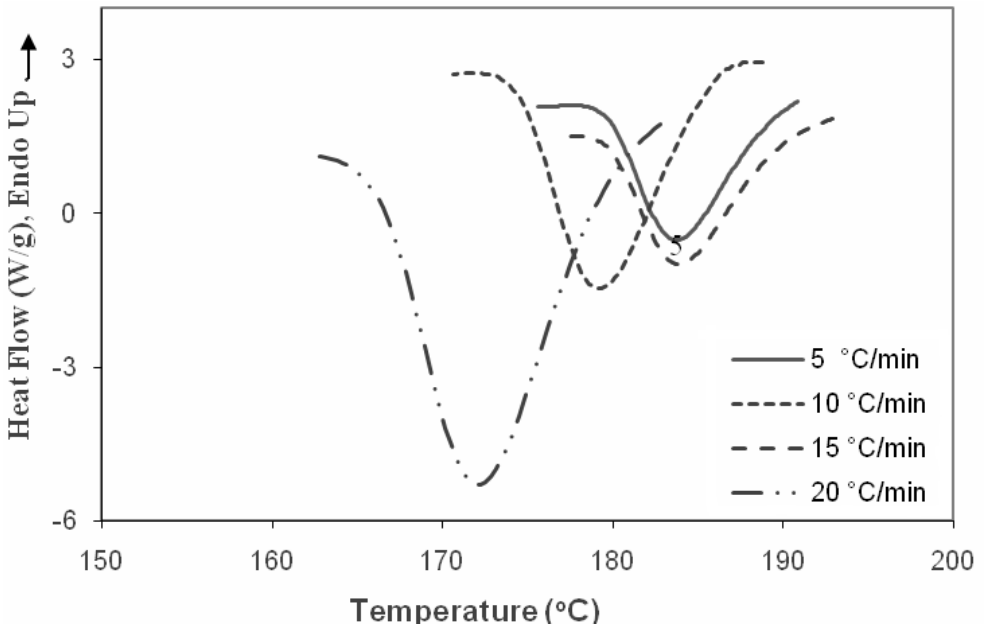

Figure 4.2: Non isothermal crystallization of PBT at four different cooling rates 5, 10, 15 and 20 ^{o}C /min.

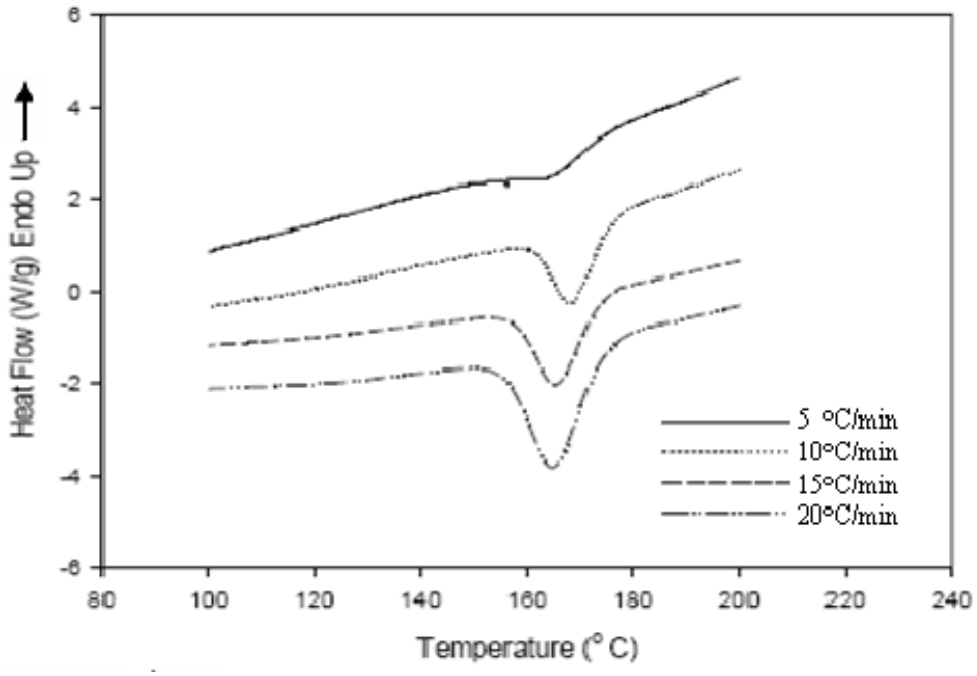

Figure 4.3: Non isothermal crystallization of blend at four different cooling rates; 5, 10, 15 and 20 ^{o}C /min.

To obtain quantitative kinetic information, the exotherms were converted into $\theta(T)$ values using equation (2.1). The temperature at 1% relative crystallinity ($T_{0.01}$), the temperature at the maximum crystallization rate or the peak temperature (T_p) and the temperature at 99% relative crystallinity ($T_{0.99}$), were obtained. $T_{0.01}$ and $T_{0.99}$ values represent the apparent onset and ending temperatures of the non isothermal crystallization process. These values are summarized in Table 4.1. $T_{0.01}$, T_p and $T_{0.99}$ values shift towards lower temperatures when the cooling rate increases. This observation is noted for the neat polymers but not for blend.

For non isothermal crystallization, the blend crystallization temperature does not shift much with the rate of cooling plausibly because the mobility of the molecules of PTT and PBT is restrained by the presence of PC which leads to long and varied relaxation times causing intermediate crystallization temperatures with increasing cooling rates.

This could possibly be due to transesterification reactions occurring between the neat polymers to form a new structure having thermal characteristics different compared to the parent polymers.

The onset ($T_{0.01}$ °C), peak (T_p °C) and endset ($T_{0.99}$ °C) for PTT, PBT and the blend given in Table 4.1 indicate that the majority of the later values of the blend lies between PTT and PBT for heating rates 10 °C /min and above. These observations indicate the contribution of PC as a nucleating agent in the crystallization process. In the blend, the polyesters form the continuous phase and PC form the dispersed phase [118]. At heating rate ≥ 10 °C /min, the dispersed phase might become more interconnected to form

interpenetrating networks. This complicated interpenetration of the three polymers which develops during phase separation may be causing hindrance to the growth of PTT and PBT lamellae. This can also be attributed to the melt miscibility effect between PBT and PC as well as the dilution effect to the crystallizable component PTT and PBT in the presence of PC. The miscibility of polyester and poly carbonate phases in the melt state leads to increase of molecular motions of the crystalline and non crystalline components in the blend leading to a decrease in the crystallization rate and level of crystallinity of PTT and PBT.

The data can be further analyzed by converting the temperature scale of the $\theta(T)$ function into time scale, using equation (2.2). The converted curves are illustrated in Figure 4.4. It is clear that the higher the cooling rate, the shorter the time required for the completion of the crystallization process possibly due to exchange reactions. The $T_{0.01}$ and $T_{0.99}$ values are qualitative measures of the onset and end of the non isothermal crystallization process. From these two values, the apparent total crystallization period (Δt) could be calculated (i.e., $\Delta t = t_{0.99} - t_{0.01}$), and the resulting values are summarized in Table 4.2. As seen in Table 4.2, with increasing cooling rate Δt values decrease. This indicates that the crystallization time decreases with increasing cooling rate. This suggests that non isothermal melt crystallization proceeds faster with increase in cooling rate. This behavior has been noted for PTT [68]. Another point observed is that Δt values for the blend lie between those of PTT and PBT. This could possibly be due to the presence of PC in the blend.

4.1.1.1 Avrami analysis

The data analysis based on Avrami macrokinetic equation was carried out through the direct fitting of the experimental θ (t) values to equation (2.3). Avrami kinetic parameters (i.e., k_A and n_A) were accordingly estimated. The average sum of errors (*ASE*) signifies the model's adherence to the experimental data. These parameters are summarized in Table 4.3. The n_A value of PTT ranged from 2.3 to 3.0 with an average value of 2.7. n_A for PBT ranged from about 4.4 to 6.8, average value being 5.6 while that of the blend ranged between 4.0 to 4.6 having the average value of 4.3. The value of n_A of the blend lies between that of PTT and PBT. The value of n is a general indication of dimensionality (e.g n = 1 for rod, n = 2 for disk and n = 3 for sphere). Ding and Spruiell [119] suggest that for n values greater than 4, primary nucleation could occur, accompanied by increasing nucleation rate. The crystallization rate constant, k_A, increased with increasing cooling rate. Another parameter that can be used to indicate the rate of reaction is the half-time of crystallization, $t_{1/2}$ which is defined as:

$$t_{1/2} = \left(\frac{Ln(2)}{k} \right)^{\frac{1}{n}} \tag{4.1}$$

Where k and n are the rate constant and order of crystallization. The values obtained using Avrami kinetics parameters are summarized in Table 4.3. These values are found to be increase with increasing cooling rate.

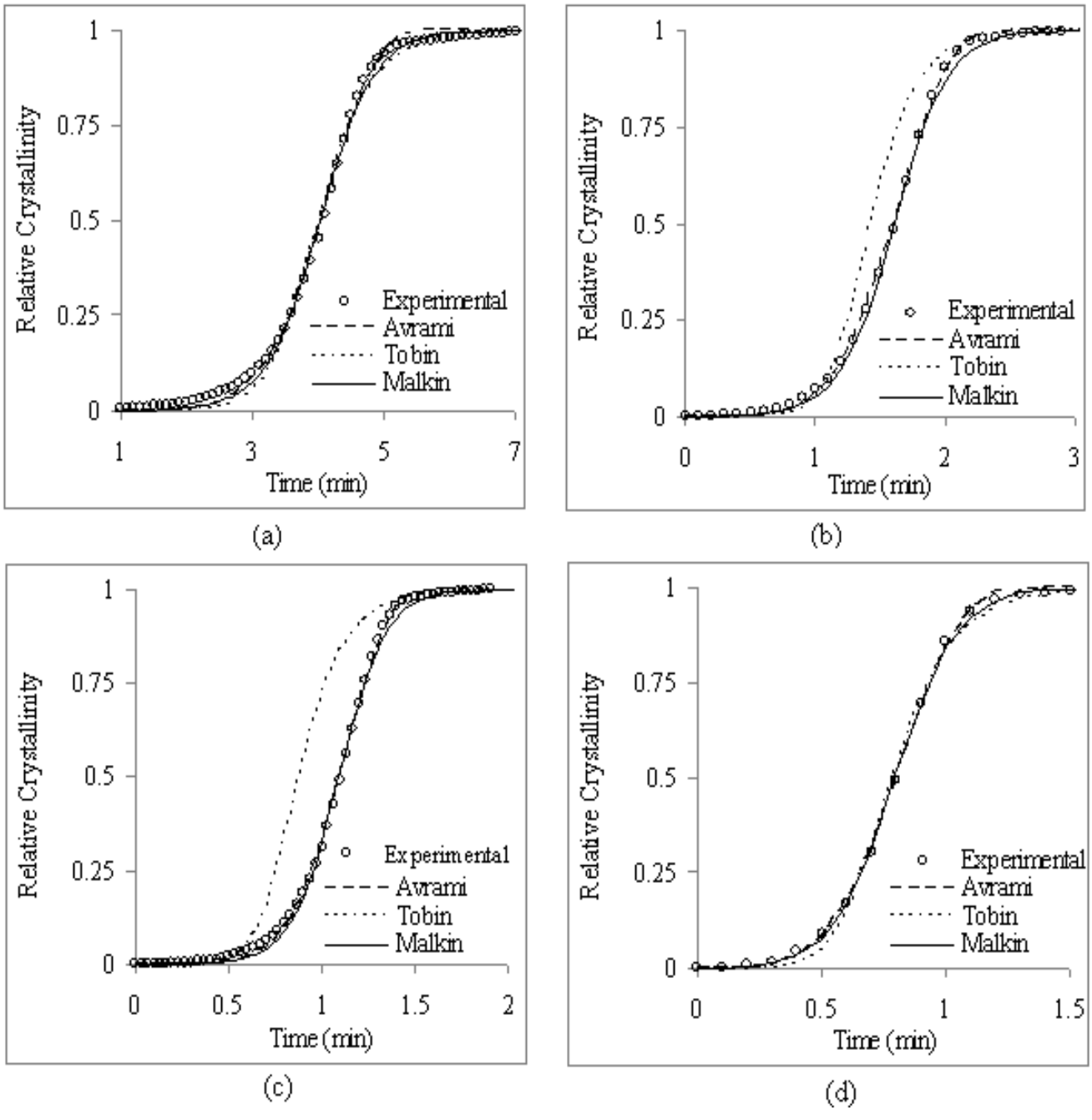

Figure 4.4: Comparison of the models fitting to the experimental data for PBT at different cooling rates, (a) 5 ^{o}C/min, (b) 10 ^{o}C/min, 15 ^{o}C/min, 20 ^{o}C/min.

Table 4.1: Characteristic data of non isothermal crystallization of PTT, PBT and the blend.

ϕ	PTT				PBT				Blend			
$^{o}C.min^{-1}$	5	10	15	20	5	10	15	20	5	10	15	20
$T_{0.01}(^{o}C)$	181.2	180	173.2	169.6	197.8	190.6	195.7	184.2	176.2	177.9	175.2	176.2
$T_{P}(^{o}C)$	167.6	157	152.7	147.7	183.9	183.9	179.3	172.2	164.3	168.3	165.5	164.9
$T_{0.99}(^{o}C)$	158.3	137	133.7	114	172.2	170.5	176.7	160.2	150.5	157.6	153.5	151.3

Table 4.2: Quantitative analysis of the relative crystallinity functions of time converted from non isothermal crystallization of PTT, PBT and the blend.

Heating Rate $^{o}C/min$	PBT			PTT			Blend		
	$t_{0.001}$	$t_{0.99}$	Δt	$t_{0.001}$	$t_{0.99}$	Δt	$t_{0.001}$	$t_{0.99}$	Δt
5	0.22	5.17	4.96	0.5	6.55	6.05	1.702	7.51	5.80
10	0.18	4.71	4.54	0.23	2.58	2.35	0.316	3.33	3.02
15	0.1	2.91	2.81	0.12	1.65	1.53	0.284	1.97	1.68
20	0.07	2.99	2.93	0.08	1.43	1.35	0.166	1.70	1.53

Table 4.3: Non isothermal crystallization kinetics for PTT, PBT and the blend based on Avrami analysis.

Heating Rate ^{o}C/min	PTT				PBT				Blend			
	$t_{0.5}^{-1}$	k_A	n_A	*ASE*	$t_{0.5}^{-1}$	k_A	n_A	*ASE*	$t_{0.5}^{-1}$	k_A	n_A	*ASE*
5	0.25	0.02	3.08	1.59E-04	0.25	0.002	6.81	1.81E-04	0.20	0.0004	4.65	1.79E-04
10	0.62	0.05	2.83	1.07E-04	0.38	0.05	5.35	6.51E-05	0.60	0.09	4.02	4.55E-04
15	0.91	0.18	2.69	1.58E-04	0.61	0.39	5.98	9.79E-05	0.83	0.33	4.11	5.70E-04
20	1.25	0.27	2.30	2.44E-02	0.66	1.87	4.45	8.17E-03	0.98	0.63	4.50	8.82E-03

4.1.1.2 Tobin analysis

The data analysis based on the Tobin macrokinetic equation was carried out by fitting of the experimental $\theta(t)$ data to equation (2.3). Tobin kinetic parameters (i.e., k_T and n_T), along with the *ASE* values, were obtained from the best fits, and the values of these parameters are summarized in Table 4.4. According to Table 4.4, n_T for PTT ranged from about 3.5 to 4.6 with the average value being 4.1, PBT ranged between 6.7 to 10, with an average value being 8.2, and for blend ranged from 6.0 to 6.9 with the average value of around 6.5. The n_T values of PTT are found to be lower than those of PBT and the blend. n_T values for the blend also lie between those of PBT and PTT. Tobin crystallization rate constant k_T is found to increase with increasing cooling rate.

4.1.1.3 Malkin analysis

Unlike the Avrami and Tobin models there is no direct analytical procedure to find the Malkin kinetic parameters. The Malkin kinetic parameters C_o and C_1 were found using the Avrami kinetic parameters (n_A and k_A). The Malkin kinetic parameters (i.e., C_o and C_1) were obtained using equations (2.5) and (2.6) and are summarized in Table 4.5. The *ASE* parameters were obtained using equation (2.7). C_o values for PBT were found to be in the range 711 to 18947. The C_o values for PTT ranged from 21 to 84 while those of the blend varied between 387 and 1069. Malkin crystallization rate constant C_1 is found to generally increase with increasing cooling rate.

Table 4.4: Non isothermal crystallization kinetics for PTT, PBT and the blend based on Tobin analysis.

Heating Rate °C/min	PTT				PBT				Blend			
	$t_{0.5}^{-1}$	k_T	n_T	*ASE*	$t_{0.5}^{-1}$	k_T	n_T	*ASE*	$t_{0.5}^{-1}$	k_T	n_T	*ASE*
5	0.85	0.34	4.62	1.49E-03	0.90	0.249	10.03	7.36E-04	0.84	0.21	6.98	2.01E-04
10	0.88	0.39	4.34	1.38E-03	0.99	0.688	8.50	1.36E-01	0.98	0.61	6.03	4.43E-05
15	0.98	0.63	4.15	1.43E-03	1.07	1.136	7.37	5.87E-04	1.03	0.87	6.83	1.95E-04
20	1.00	0.69	3.56	8.88E-02	1.09	1.27	6.72	5.13E-02	1.05	0.99	6.80	2.64E-04

Table 4.5: Non isothermal crystallization kinetics for PTT, PBT and the blend based on Malkin analysis.

Heating Rate ^{o}C/min	PTT			PBT			Blend		
	C_o	C_1	*ASE*	C_o	C_1	*ASE*	C_o	C_1	*ASE*
5	84.32	1.46	2.80E-04	18,947	2.44	2.18E-04	1,069	1.43	1.09E-04
10	46.90	1.48	1.81E-04	2,588	4.87	1.20E-04	387.78	3.65	2.10E-04
15	39.48	2.29	6.84E-05	6,312	8.01	1.62E-04	777.89	5.76	2.04E-05
20	21.77	2.11	3.67E-02	711.93	8.25	5.50E-03	725.69	6.59	4.90E-06

4.1.1.4 Comparison of modeling results

Avrami and Malkin models are found to exhibit the lowest ASE values. The kinetic parameters obtained using Malkin model is found to be high compared to that of Avrami and Tobin. This could possibly be due to the equations proposed by Malkin. The differences in kinetic parameters are not believed to be due to experimental error, as all the data points were counterchecked. PTT exhibits the highest crystallization rate constant, followed by the blend and then PBT. The presence of PC in the blend could possibly be the reason behind the low rate constant values of the blend. The increase in rate constant values with increasing cooling rate for all the models and systems shows the effects of cooling on crystallization. This suggests that polyesters crystallize faster at greater cooling rate.

4.1.2 Scanning electron microscope (SEM) measurements

Blend morphology depends mainly on rheological and interfacial properties, blending conditions and volume ratio of the components. In this study, the blend specimens and the neat samples were prepared by extrusion and injection molding. The morphology of the blends was investigated by Scanning Electron Microscopy (SEM). Figure 4.5 shows the fractured samples of the PC, PTT, PBT and the blend specimens at 10 μm. Uniform fracture surfaces are seen for PC PTT, and PBT samples. The blend shows surface cleavage, indicating immiscibility of its constituents. No holes are seen in the fractured surfaces of the injection molded specimens of the blend samples.

4.1.3 X-ray analysis

The crystal structure of PTT is observed at scattering angles (2θ) of 17.00 and 25.65. For PBT, the (2θ) is displayed at 13.95, 17.50, 24 and 24.00 and for PC, it appears at

17.55. The blend showed peaks at 17.00, 23.75, and 25.48, Figure 4.6. WAXD was carried out to validate the existence of unreacted soluble PC presented after blending the polyester and polycarbonate. Pure PC shows a reflection around 17 degree which corresponds to the amorphous phase. Compared with pure PC and the polyesters, the blend exhibits a sharp reflection at 17.00. These changes in WAXD spectra of the blend containing high percentage of unreacted PC leads to an increase in the crystallinity of PC in the blend.

Apart from the peak of the pure components, no new peaks were observed in the diffraction patterns of the blend sample, indicating that PTT and PBT crystallized separately. This is another indication of the immiscibility of the blend.

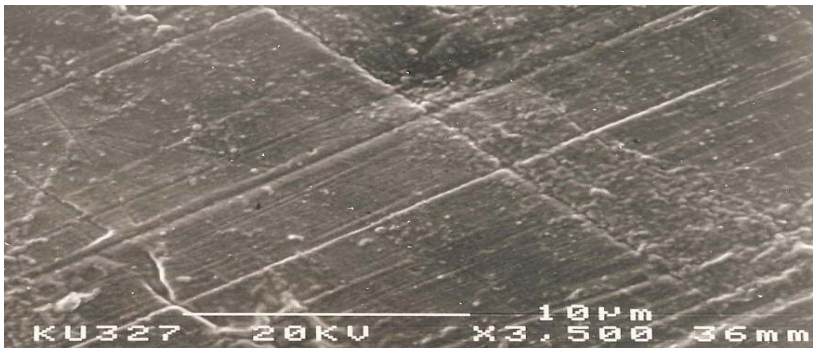

a

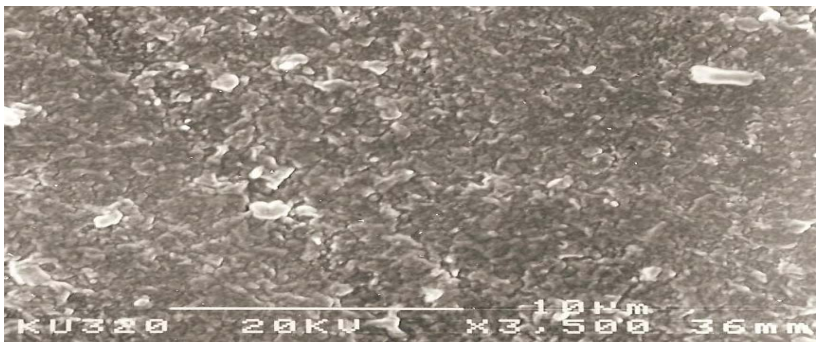

b

c

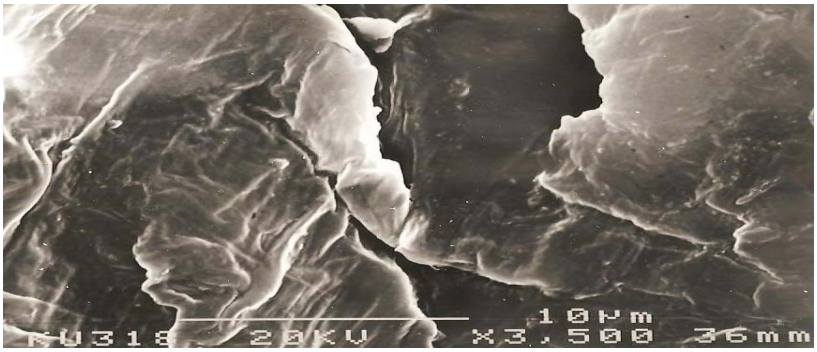

d

Fig 4.5: Scanning Electron microscope of the fractured surfaces of (a) PC, (b) PTT, (c) PBT and (d) the blend.

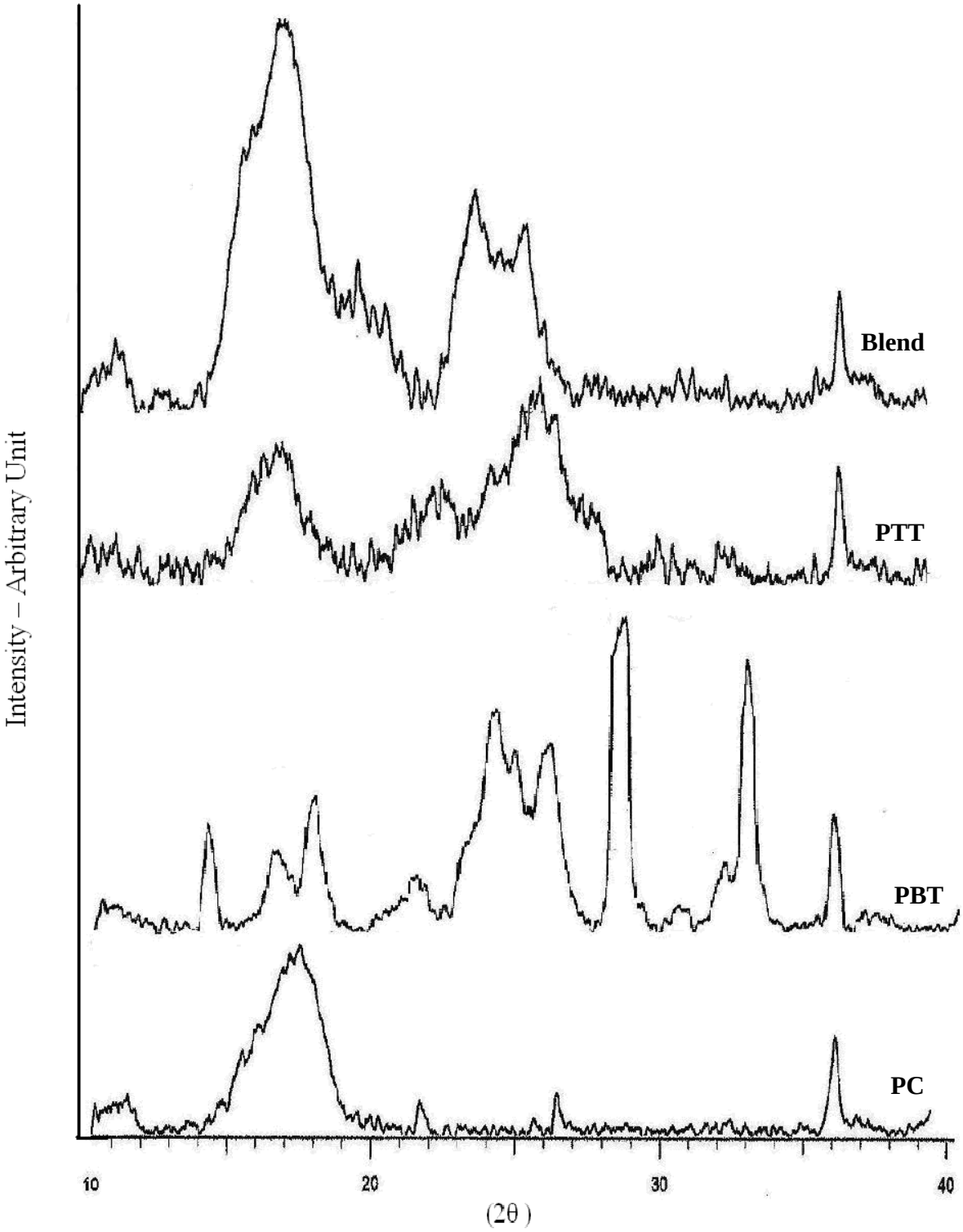

Figure 4.6: Wide-angle x-ray diffractograms for PTT, PBT, PC and the blend.

4.1.4 Tensile properties

Table 4.6 summarizes tensile properties of PC, PTT, PBT and blend measured using an Instron (Type 1112) machine. The ASTM standard used to measure the mechanical properties was ASTM D638-08. PC shows higher values of elongation at break (88.44 %), tensile strength (61.1Mpa) and elongation at yield (6.6%). The yield strength of the blend is higher than polyesters and polycarbonate. The elastic modulus of the blend is also higher than that of polyester and the polycarbonate.

Knowledge of the yield point is vital when designing a component since it generally represents an upper limit to the load that can be applied. It is also important for the control of many materials production techniques such as forging, rolling, or pressing.

Table 4.6: Mechanical properties of neat polymers and the blend.

Polymer	Elongation at Break (%)	Tensile Strength at Break (MPa)	Elongation at Yield (%)	Elastic Modulus (GPa)	Yield Strength (MPa)
PC	88.44 (± 0.9)	61.06 (± 0.3)	6.64 (± 0.2)	1.18 (± 0.3)	61.35 (± 0.6)
PTT	6.72 (± 0.2)	58.05 (± 0.2)	4.57 (± 0.4)	1.40 (± 0.1)	61.49 (± 0.2)
PBT	26.10 (± 0.3)	20.46 (± 0.2)	4.65 (± .02)	1.36 (± 0.1)	56.18 (± 0.3)
Blend	16.27 (± 0.5)	36.41 (± 0.3)	5.11 (± 0.1)	1.52 (± 0.2)	64.08 (± 0.4)

Ester interchange reactions may be useful in very limited amounts in determining the blend performance [11, 12]. Such reactions are not easily controlled and excessive reaction can result in a loss in mechanical properties. Interchange reactions normally reduce the ability of the blend to form PTT and PBT crystalline phase owing to copolymer formation in transesterification reactions. The yield strength of the blend is found to be the highest possibly because of the strong interfacial adhesion between the polyesters and PC domain. The PC-PTT-PBT interfacial adhesion plays a critical role in determining the tensile properties of the blend. This is because PC is a stress-rate sensitive material and undergoes brittle fracture when it is subjected to plane strain condition where PTT and PBT are strain –rate sensitive polyesters and tends to have higher rigidity and lower fracture toughness when deformation rate is high. Figure 4.7 shows the stress- strain curves of the neat polymers and the blend at 26 ^{o}C and 50 mm/min cross head speed. The tensile stress shows a definite upper yield point followed by load drop for the blend and the polymers. For PBT and PC a slight strain-hardening region is found before ultimate rupture. The blend has higher yield strength. PC has the highest elongation at break, tensile strength at break and wider cold drawing region, Figure 4.7.

The values of tensile strength at break for the blend is low compared to PC and PTT indicating that PC does not induce a proper reinforcement.

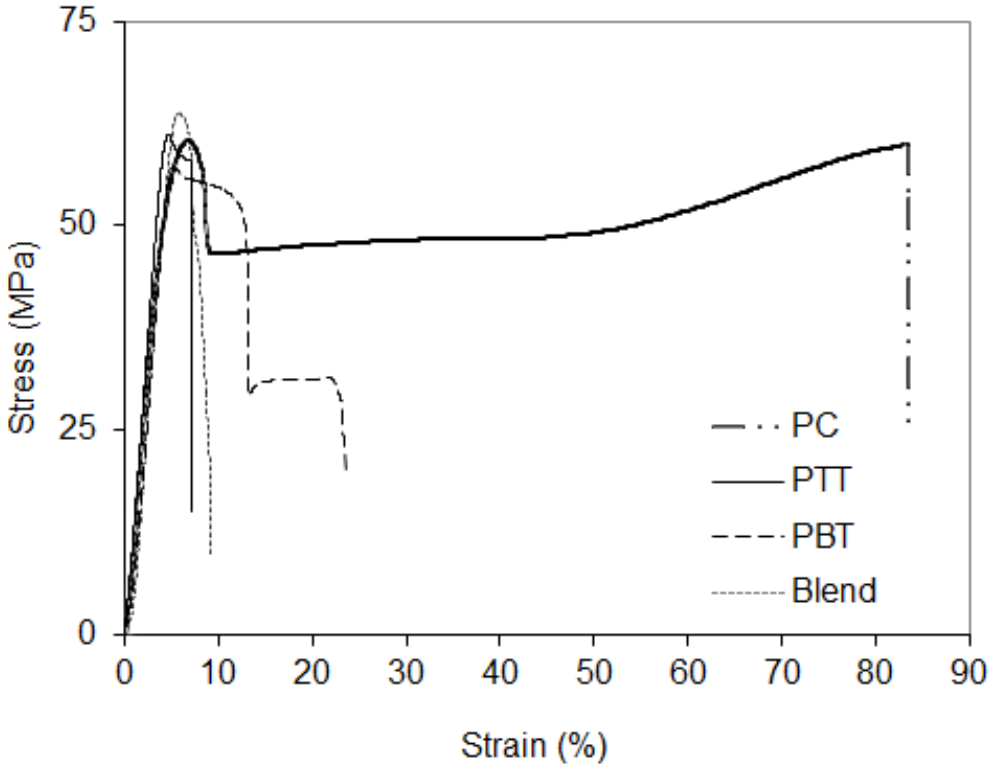

Figure 4.7: The stress and strain relation of PC, PTT, PBT and blend.

4.2 Isothermal crystallization kinetics of neat polymers and blend

4.2.1 Isothermal crystallization

Identical temperatures for the polymers could not be maintained since PTT crystallized between 129 and 159 °C, PBT between 168 and 177°C and the blend between 170 and 183°C. Based in these temperatures, the T_c values chosen were 130, 138, 147 and 158°C for PTT, 169,171,173 and 176°C for PBT and 171, 173, 176 and 182°C for the blend. Common crystallization temperatures for PTT and PBT could not be obtained because of large differences seen in the crystallization temperatures of each polymer. Similar behavior was noted for PTT and the blend. Common

crystallization temperatures were noted for PBT and the blend Table 4.7. The high percentage of PC (50wt %) is found to influence the crystallization temperature for the blend. Figure 4.8 illustrates the sigmoidal nature of the time-dependent relative crystallinity function, $\theta(t)$, of the blend crystallized at four different temperatures (i.e., 171, 173, 176 and 182°C, respectively).

Table 4.7: The Isothermal crystallization temperatures obtained using DSC.

PTT	PBT	Blend
130 °C	169 °C	171 °C
138 °C	171 °C	173 °C
147 °C	173 °C	176 °C
158 °C	176 °C	182 °C

The behavior noted by Xue *et al* [120] in PTT/PC blends was also detected in the tricomponent blend. They noted that the crystallization time of PC/PTT blends increased with increasing concentration of PC. Within the temperature range studied, the time to reach ultimate crystallinity (i.e. complete crystallization) increased with increasing crystallization temperature T_c. An important crystallization kinetic parameter which can be determined from the $\theta(t)$ data is the half-time of crystallization ($t_{0.5}$), equation 4.1. It is obvious that for the blend the crystallization half time increases with crystallization temperature. Similar trend has been noted for neat PBT, Figure 4.9. The analysis of half time of crystallization demonstrates that

the presence of PC in the blend leads to some kind of retardation of the PTT, PBT crystallization. This behavior could possibly be caused by the decreasing segmental mobility of the polyester olefinic chains in the presence of PC.

PC is a non crystalline amorphous thermoplastic polymer. It has good engineering properties over a temperature ranged (-140) to 200 ^{o}C. The crystallizable characteristics of PTT and PBT may improve some of the properties of PC. Referring to Table 4.8 the $t_{1/2}$ value of each polyester and the blend increased with temperature of crystallization. The polyesters are found to crystallize at a faster rate than the blends. In the blend, PC might be inhibiting the crystallization of the polyesters. The reduction in crystallization rate could be due to a physical characteristics relating to the growth of PC domains. Density results have shown that the presence of PC hinders the crystallization process of polyesters [121]. Thus, PC affects the crystallization kinetics of polyesters leading to the formation of more stable spherulites when it is present in sufficient quantities in the blend causing an effect on the isothermal crystallization properties of the blend.

This indicates that transesterification reaction plays an important role in controlling the thermal properties of PC/PTT/PBT blends. Another conclusion that can be drawn is that there is at least partial dissolution of the polyesters in the PC, the amorphous polymer. Another plausible conclusion is that the polyester component can dissolve to a higher degree in the PC rich phase than for the PC component to dissolve in the polyester rich phase exhibiting a higher T_g and T_c for the blend.

The analysis of half time of crystallization demonstrates that the presence of PC in the blend leads to some kind of retardation of the PTT, PBT crystallization. This behavior

could be possibly caused by the decreasing segmental mobility of the polyester olefinic chains in the presence of PC.

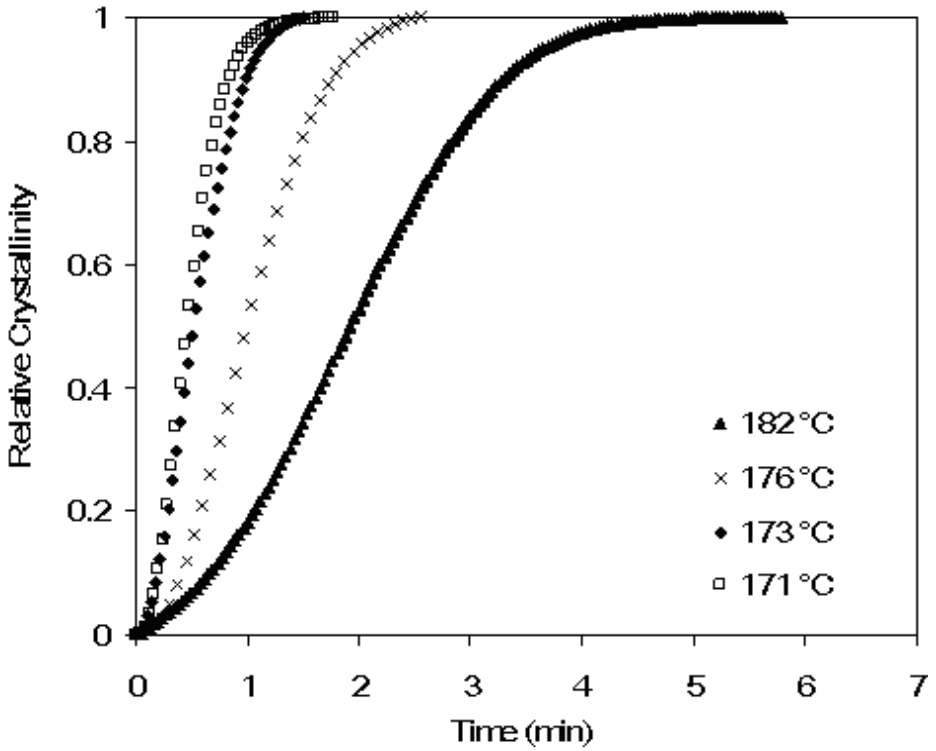

Figure 4.8: Relative crystallinity as a function of time for blend at 182 °C, 176 °C, 173 °C and 171°C.

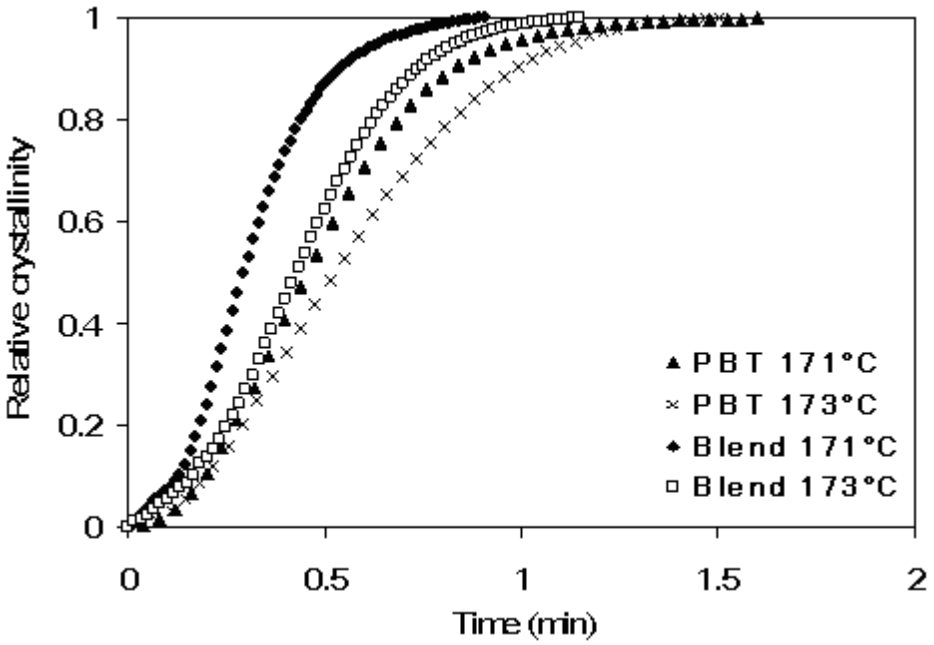

Figure 4.9: Relative crystallinity as a function of time for PBT and blend at 171°C and 173°C.

4.2.1.1 Avrami analysis

The analysis of kinetic data based on the Avrami model was done by fitting the $\theta(t)$ function obtained for each crystallization temperature to equation (2.2). The Avrami exponent, n_A, and the Avrami rate constant, k_A, obtained using solver program, are summarized in Table 4.8. The exponent n_A for the crystallization process was found to range from 1.58 to 2.32 for PTT, 1.59 to 2.23 for PBT, and 1.91 to 2.12 for blend, respectively. These values possibly correspond to a two dimensional growth with a combination of thermal and athermal nucleation [122]. The temperature dependence of the exponent n_a, within the nucleation-controlled region, should be such that n_a decreases with decreasing crystallization temperature. This may be explained based on the fact that the number of athermal nuclei increases as the temperature decreases [123, 124]. In other words, as the crystallization temperature decreases, the number of athermal nuclei that become stable at that temperature also increased, resulting in the nucleation mechanism becoming more instantaneous in time and causing the Avrami exponent, n_a, to decrease. Similar observation was noted also for the blend. The n_a average value of the blend is similar to PTT. It was also noted that the half life time of blend was higher than that of neat polymers. Similar observation was noted for PET/PC isothermal crystallization studies by Kong *et al*., [125]. The crystallization rate constant, $k_{A,}$ increased monotonically with decreasing crystallization temperatures, and this was in general agreement with the values of the reciprocal half-time of crystallization ($t_{0.5}^{-1}$), which are also summarized in Table 4.8.

Table 4.8: The overall crystallization kinetic data for PTT, PBT and the blend based on Avrami, Tobin, and Malkin models.

	T °C	$t_{1/2}$ (min)	$t_{1/2}^{-1}$ (min^{-1})	k_A	k_T	n_A	n_T	C_0	C_1	*ASE*		
										Avrami	*Tobin*	*Malkin*
PTT	130	0.37	2.70	5.73	2.78	2.13	3.36	17.42	7.90	5.58E-06	9.12E-04	4.76E-05
	138	0.48	2.08	3.26	2.12	2.16	3.33	18.92	6.16	3.68E-04	3.36E-04	5.87E-04
	147	0.55	1.82	1.77	1.88	1.58	2.47	4.76	3.39	6.36E-04	2.74E-03	4.02E-04
	158	1.20	0.83	0.44	0.85	2.32	3.66	25.52	2.73	6.09E-05	2.94E-04	6.39E-05
					Average	2.05	3.21					
PBT	169	0.10	10.00	29.95	10.53	1.59	2.60	5.00	19.41	3.35E-05	4.67E-04	7.33E-05
	171	0.29	3.45	8.69	3.47	2.08	3.32	16.18	9.65	1.70E-04	4.30E-04	1.55E-04
	173	0.42	2.38	4.30	2.43	2.12	3.37	16.73	6.85	3.99E-04	1.51E-03	1.85E-04
	176	0.68	1.47	1.63	1.51	2.23	3.45	21.05	2.23	3.75E-05	7.44E-04	1.07E-04
					Average	2.01	3.18					
Blend	171	0.46	2.17	3.46	2.24	2.08	3.31	15.92	6.18	4.19E-05	3.98E-04	1.00E-04
	173	0.52	1.92	2.34	1.96	1.91	3.00	10.79	4.76	1.57E-05	9.63E-04	1.18E-04
	176	1.00	1.00	0.69	1.03	2.12	3.31	17.15	2.91	3.90E-06	8.57E-04	8.56E-05
	182	1.89	0.53	0.180	0.54	2.08	3.30	15.36	1.49	1.48E-04	1.50E-03	8.47E-05
					Average	2.05	3.21					

4.2.1.2 Tobin Analysis

The analysis based on the Tobin model can be performed by fitting the $\theta(t)$ function obtained for each crystallization temperature to equation (2.3). Table 4.8 summarizes the Tobin kinetic parameters n_T and k_T, as well as the *ASE* parameter. The Tobin exponent, n_T, for crystallization was found to range from 2.47 to 3.66 for PTT, 2.60 to 3.45 for PBT, and 3.00 to 3.31 for blend. The n_T values of PBT are lower than that of PTT and the blend. The n_T value for the blend is higher than both PBT and PTT. The Tobin crystallization rate constant k_T is found to increase with increasing crystallization temperatures. Comparison between Avrami and Tobin models, reveal that, at an arbitrary crystallization temperature, the Avrami exponent, n_A, is lower in value than the Tobin exponent, n_T. By taking the average value of the difference between the two values, (n_A and n_T) we are able to conclude, (based on our experimental observation), that $n_T \approx n_A + 1.2$, which is in general accordance with previous observations [126].

4.2.1.3 Malkin Analysis

The analysis based on the Malkin model can be carried out by fitting the $\theta(t)$ function obtained for each crystallization temperature to equation (2.4). The kinetic parameters specific to the Malkin model, C_0 and C_1, as well as *ASE* parameter, are listed in Table 4.8. The C_0 parameter was found in the range of 4.76 to 25.52 for PTT, 5.00 to 21.05 for PBT and 10.79 to 15.92 for blend. Unlike the Avrami and the Tobin models, there is no direct analytical procedure for the determination of the Malkin kinetic parameters. The Malkin exponent C_0 is directly related to the Avrami exponent n_A. According to equation (2.5), it

should exhibit similar temperature dependence to that of Avrami exponent, n_A. According to the data presented in Table 4.8, the Malkin rate constant C_1 exhibited temperature dependence in a similar fashion as the crystallization rate constant of the Avrami and Tobin models. This is not surprising since the Malkin rate constant C_1 relates to the Avrami kinetic parameters (i.e. n_A and k_A) according to the equation (2.6) [28].

4.2.1.4 Comparison of modeling results

The quality of each macrokinetic equation in describing the experimental data $\theta(t)$ is quantitatively represented by not only the *ASE* parameter obtained for the best fit of the data, but also the quality of the prediction in comparison with the experimental data such as those shown in Figure 4.10. From the comparison of the model predictions of the experimental data and the comparison of the values of the *ASE* parameter summarized in Table 4.8, it is clear that the Avrami and Malkin models provide very good correlation of the experimental data, while the Tobin model was not satisfactory in describing the experimental data.

In the case where $t_{0.5}$ data can be measured accurately over the whole temperature range in which polymers can crystallize, the plot of the $t_{0.5}^{-1}$ versus ΔT (T_m-T_c) is expected to exhibit the typical bell-shaped curve, which is characterized by the nucleation-controlled character at "high" T_c or "low" ΔT values and the diffusion-controlled one at "low" T_c or "high" ΔT values [127, 128]. From the results shown in Figure 4.11, it is apparent that, within the T_c range studied, PBT and blend within the nucleation-controlled region while PTT does not show this behavior. This could be due to the longer butyl chains present in PBT.

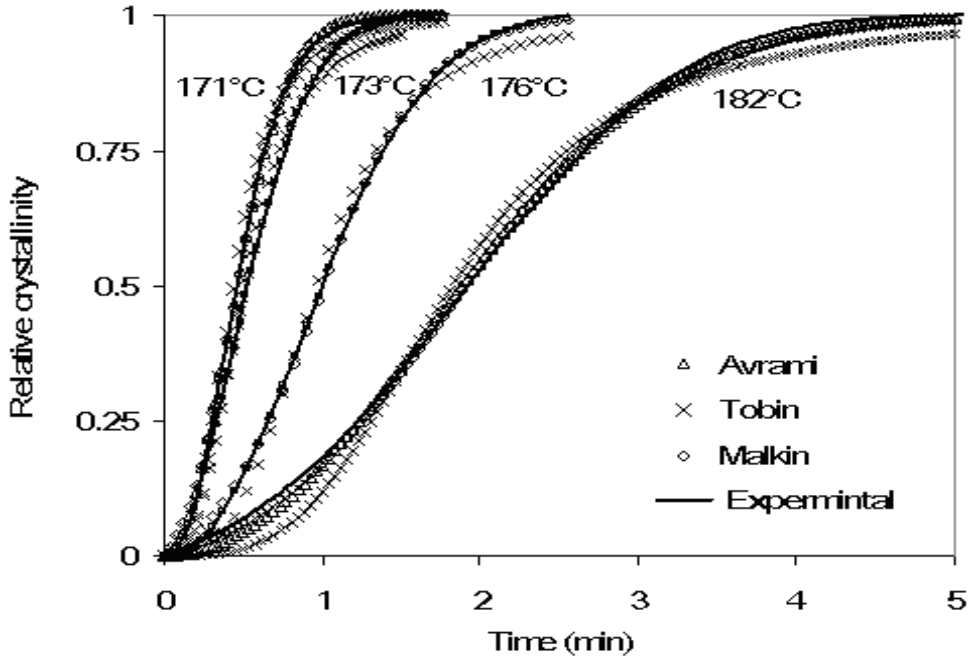

Figure 4.10: Relative crystallinity as a function of time for blend with the Avrami, Tobin and Malkin models at 171 ^{o}C, 173 ^{o}C, 176 ^{o}C and 182 ^{o}C.

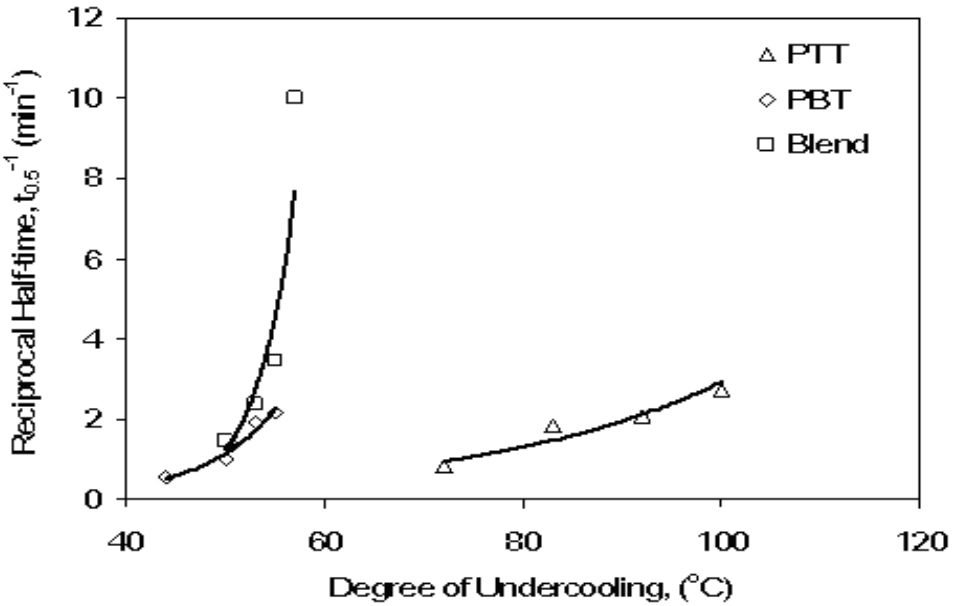

Figure 4.11: Reciprocal half-time of crystallization $t_{0.5}^{-1}$ as a function of degree of undercooling for PTT, PBT and blend.

4.3 Results and discussion of study of rheology of neat polymers and blend

4.3.1 Rheology

Viscosity is a property of fluids that indicates resistance to flow. Viscosity is defined as proportionality constant of the shear stress to the shear strain rate. Increasing the concentration of dispersed substance generally gives rise to increase in viscosity. Interfacial interaction caused by transesterification reaction of ternary blend plays an important rule in its rheological behavior. For the ternary blend investigated in the study, the processing time in an extruder and possible residual catalyst present in the commercial polyester could cause sufficient degree of transesterification. The variation of different rheological viscosities of neat polymers and the blend will be investigated in this research work. The rheological behavior of molten polymers is of importance as it is relates to their microstructure and governs their processing characteristics. Small amplitude oscillatory shear experiments are employed to measure to storage (G'), which are related to the elastic and viscous character of the material and the complex viscosity ($\eta*$) as function of angular frequency. Three different temperatures 255, 260 and 265 ^{o}C were used in the rheological studies of the neat polymers and the blend. No color change or degradation was noted in the blend or the neat polymers at the highest temperature, 265 ^{o}C, employed in this study. For the isothermal measurements, 260 ^{o}C was chosen as a safe operating temperature to prevent any possible degradation reactions.

Figures 4.12 and 4.13 both show the shear viscosity and shear stress versus the shear rate of the blend PC/PTT/PBT at three different temperatures. With the increase of shear rate, the shear viscosity decreases and the shear stress increases. At low shear rate region, Figure 4.13, the slope of the curve is higher than at the high shear rate. But at high shear rate (over 8 s^{-1}), the shear stress increases and shear viscosity decreases with increase of shear rate. This is typical for all the polymer melt exhibiting a shear thinning phenomenon. It is obvious from these plots that the polymer melts are pseudo plastic fluids, which correspond with power law model. The higher the temperature of the polymer melt, the lower the shear stress and shear viscosity at constant shear rate. The shear stress versus shear rate curve is commonly used to identify the existence of the melt fracture and the wall slip.

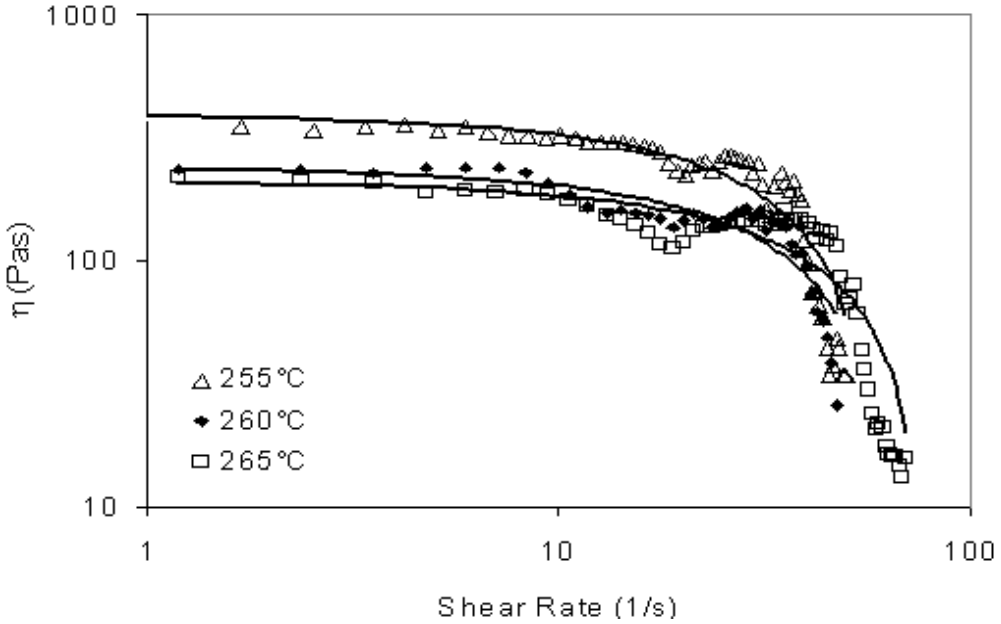

Figure 4.12: Log shear viscosity versus log shear rate of the blend measured at different temperatures.

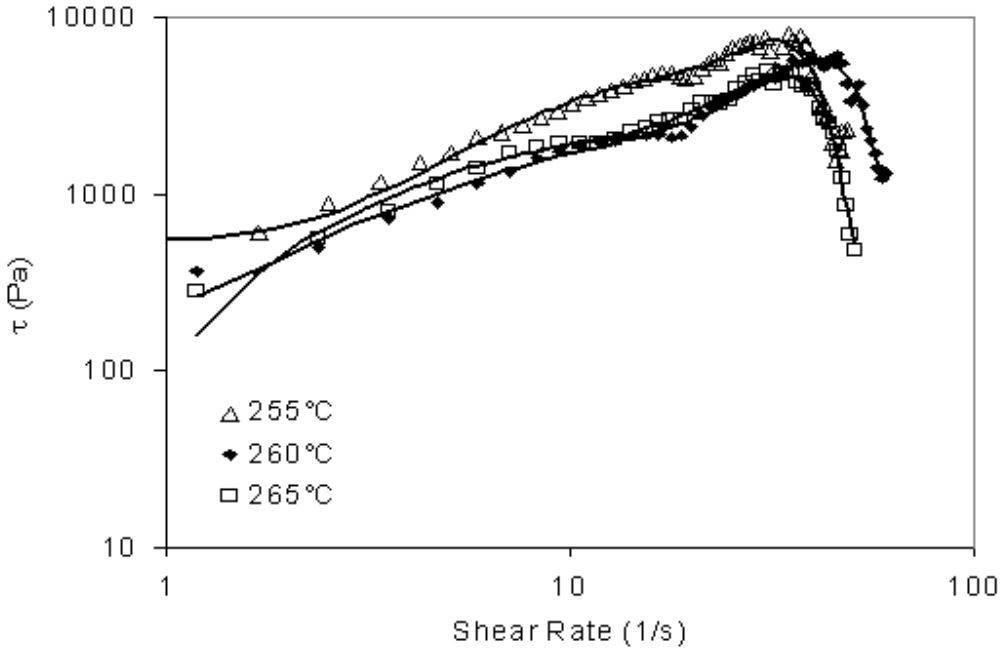

Figure 4.13: Log shear stress versus log shear rate of the blend measured at different temperatures.

Figure 4.13 shows the melt flow curves of PTT, PBT, PC and blend at 260°C a temperature considered to be approximately the temperatures of melt inside the cylinders in the extrusion process and injection molding process of this study. Melt flow curves are thought to be important in polymer processes because together with thermal properties, they determine both extrudability and moldability. The polyesters show almost comparable viscosities. The shear viscosity of blend is found to be greater than the polyesters but lower than that of polycarbonate. This could possibly be due to transesterification between polycarbonate and polyesters in the blend leading to olefinic carbonates. The curves given in Figure 4.14 show a mild shear thinning behavior at low shear rate. At high shear rates, the flow curves of all polymers and blend show a distinct shear thinning behavior. The viscosity of all the polymers show generally a gradual decreasing behavior. According to Onogi *et al.,* [129] in the plateau region, the flow does

not change the structure whereas at high shear rates, the flow orients the macromolecules in a single direction, thus changing the structure from polydomain to monodomain. The monodomain structure easily orients in the shear direction (very low viscosity). As far as transesterification is concerned, rheological properties of PC/PTT/PBT blend essentially depend on miscibility between PC and the polyesters, and morphology of the dispersed polyester phase. An enhancement in miscibility and a size reduction of polyester droplets during transesterification decrease the viscosity of PC/PTT/PBT blend compared to PC. The apparent effects of transesterification on rheological properties of PC/PTT/PBT blends depend on the 'struggle' among the three. Figure 4.15 describes the relation between complex viscosity (η^*) versus frequency (ω) for neat PC, PTT, PBT and the blend. The figure indicates that both neat polymers and the blend exhibit nearly a Newtonian behavior in the experimental frequency range studied. The complex viscosity (η^*) of the blend is found to be higher than that of the polyesters. This is presumably due to plausible transesterification reactions between PC and the polyesters. This could also be due to the formation of new polycarbonate-polyester molecular sequences which have relatively lower viscosities compared to that of polycarbonate. Storage modulus (G') and loss modulus (G") are linear viscoelastic material functions. The storage modulus is the elastic contribution of the material. It is a measure of energy storage. The loss modulus is the viscous contribution or a measure of energy dissipation. Melt rheological behavior of the neat and blend polymers were studied in order to get an idea of the microstructure in the melt state.

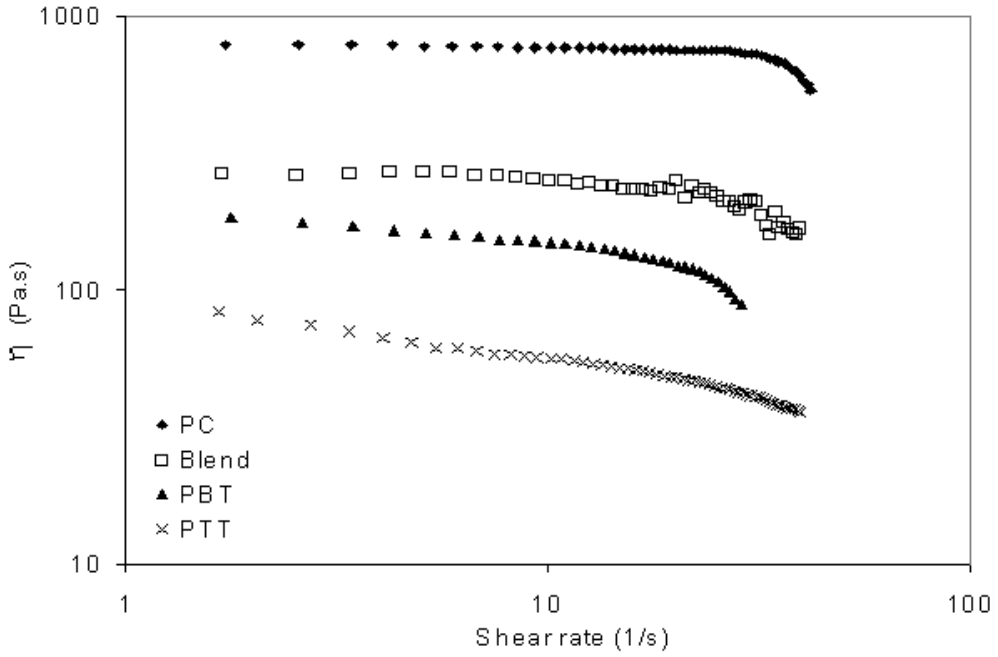

Figure 4.14: Log viscosity (η) versus log shear rate of PC, PTT, PBT, and blend at 260 ^{o}C.

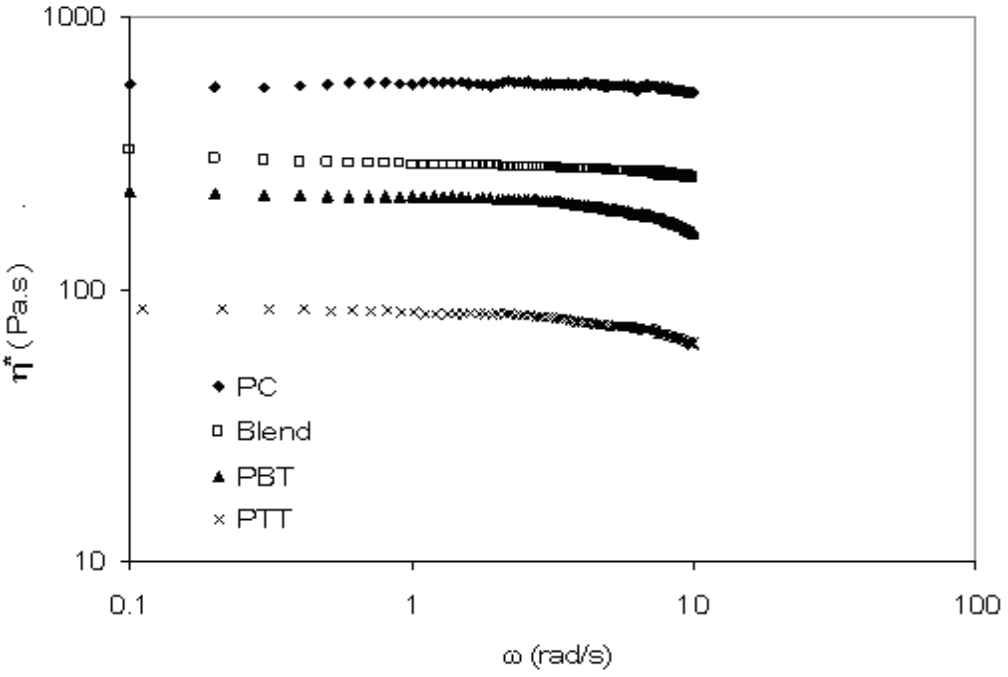

Figure 4.15: Log complex viscosity (η*) versus log (ω) for PC, PTT, PBT and blend at 260^{o}C.

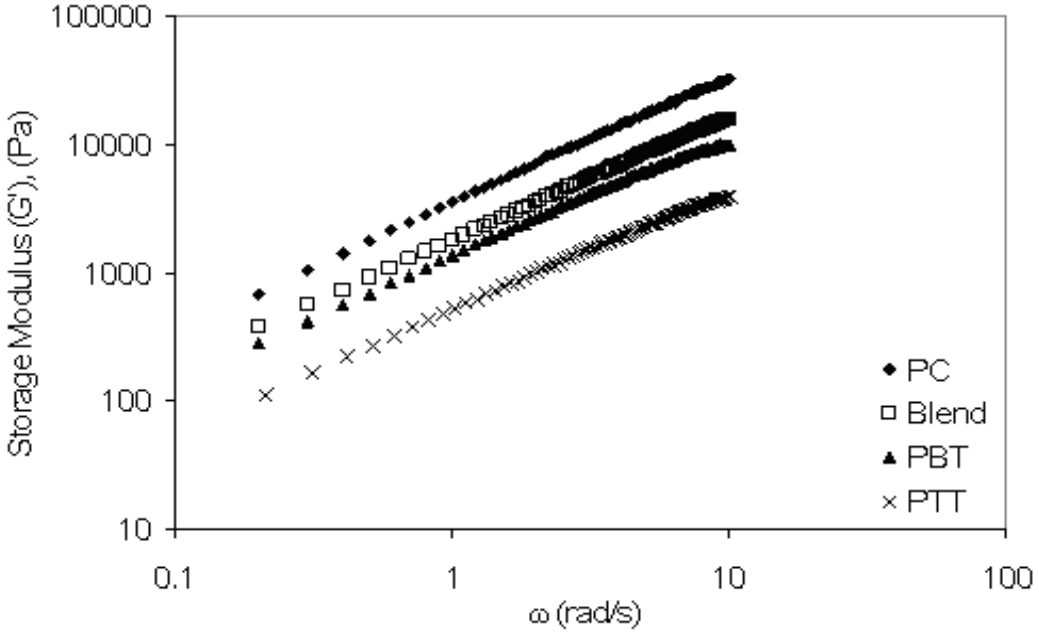

Figure 4.16: Log (G') versus log (ω) for PC, PTT, PBT and blend at 260°C.

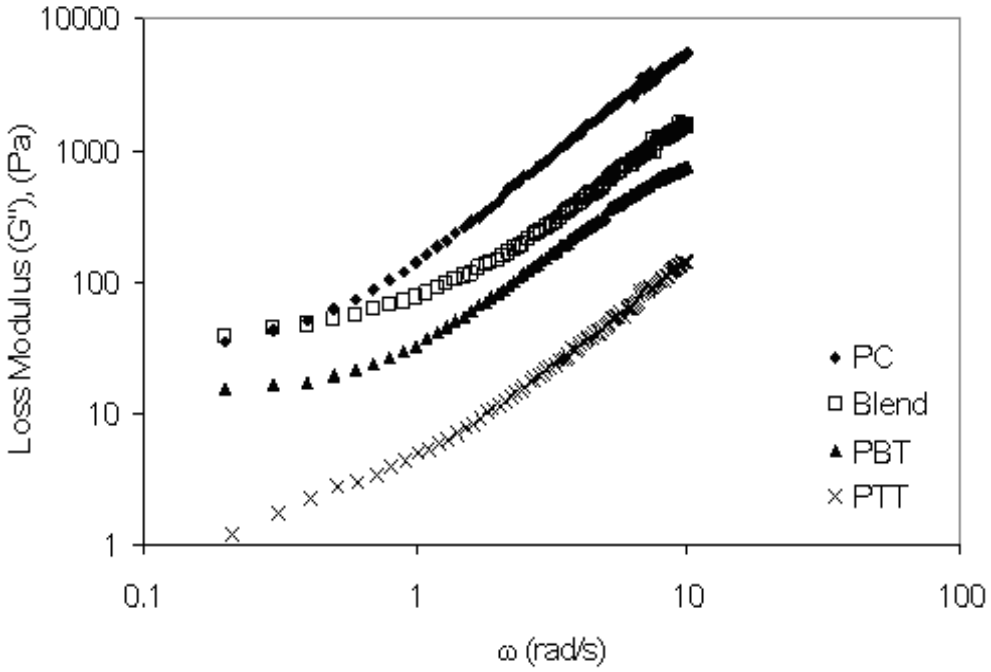

Figure 4.17: Log (G") versus log (ω) for PC, PTT, PBT and blend at 260°C.

Melt rheological behavior is also important from processing point of view. Storage modulus (G') and loss modulus (G") of the neat and blend polymers are shown in Figures 4.16 and 4.17. It is observed from these figures that G' and G" of the polycarbonate is higher compared to that of blend and polyesters. These figures also show that the blend has higher G' and G" compared to that of the polyesters. The increase in modulus of the blend is prominent at high frequency range. Thus, at higher frequencies, the rheological behavior of the blend is dominated by each of the individual components in the blend. The storage modulus and loss modulus of the blend increased with increasing frequencies. This is due to unraveling of the entanglements so that a large amount of relaxation occurs. It is observed from Figure 4.16 that the storage modulus of blend is higher than that of polyester moreover the slope of G' of the blend is almost similar to that of other polymers. This could be an indication of the formation of a complex chemical structure in the blend due to transesterification reaction. The slope of loss modulus of blend in Figure 4.17 is higher than that of the polyesters at higher frequencies. This indicates that the dispersed polyesters in blend significantly contribute to the rheological behavior of the blend especially at higher frequencies of the blend. Figures 4.16 and 4.17 also indicate that G' and G" in the lower and higher frequencies regions of the blend are larger compared to that of the polyesters. This indicates that polycarbonate in the blend behaves almost like a solid in the frequency range investigated. This solid like behavior of polycarbonate in the blend shows that a highly complex chemical structure comprising of PC, PTT and PBT is formed when the three components are melt mixed. This complex structure may consist of tran-exchanged products of PC, PTT and PBT with possible structure as shown Figure 4.18.

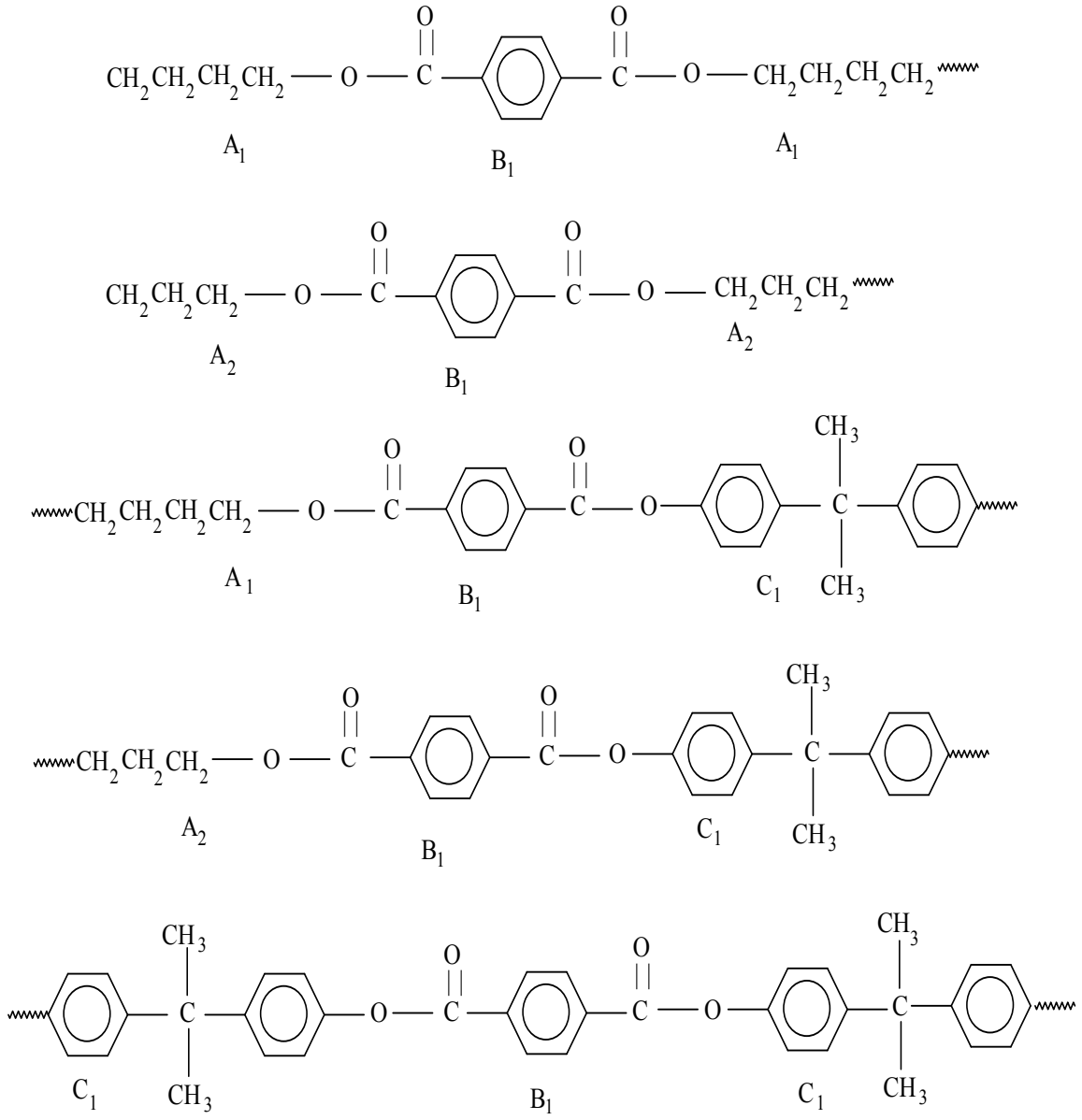

Figure 4.18: The probable structures present in PC/PTT/PBT blend after transesterification reaction, with terephthalate groups as central unit A_1, A_2, B_1, C_1 are tetramethylene, trimethylene terephthalate units.

Another general observation noted is that the enthalpy values of PTT, PBT and the blend obtained using a DSC at a typical rate of 20°C/minute are 53, 42 and 23 J/g respectively. The storage and loss modulus value for the blend are found to be lower than that of PC and higher than that of the polyesters. In the Figure 4.17, the loss modulus for blend is almost same or even slightly higher than that of PC at low frequency. This could plausibly be related to shape relaxation of the blend and also the amount of interfacial area (morphological characteristic) occupied by the blend on the melting. The increased sensitivity of the trans-exchange products formed in the blend at 260 °C leading to slightly higher G" values compared to PC at low frequencies could also be due to interfacial tension effect and this is found for many polymer blend systems [130]

Possibly transesterification reaction between PC and PBT could lead to random copolymers which are amorphous in nature. Therefore, crystallinity and enthalpy value of the blend is lower compared to polyesters. This also means that the blend could have attained a more amorphous character compared to the polyesters indirectly meaning that the crystallinity of blend is lower than that of polyesters.

Figure 4.19 gives G′ versus G″ plots for neat PC, PTT, PBT and blend. G' versus G" plots are sensitive to morphological state of polymer. To explore the effect of complex chemical structure on the viscoelastic properties of the blend, the curves of G' versus G" in the oscillatory shear measurement mode at constant strain of 0.0954 and a temperature of 260°C is plotted in Figure 4.19. The figure shows that all the polymers are dependant on the chemical nature of each material till 4000 Pa (G"), after this value of (G"), the chemical structure becomes independent of chemical nature of different

polymers, indirectly meaning that the complex nature of three different polymers in the blend remain independent of structure after 4000 Pa. The G' versus G" plot also reveal the different morphological state of blend compared to neat polymers. The plot also reflects that the blend is heterogeneous at 260 °C compared to the isotropic neat polymers.

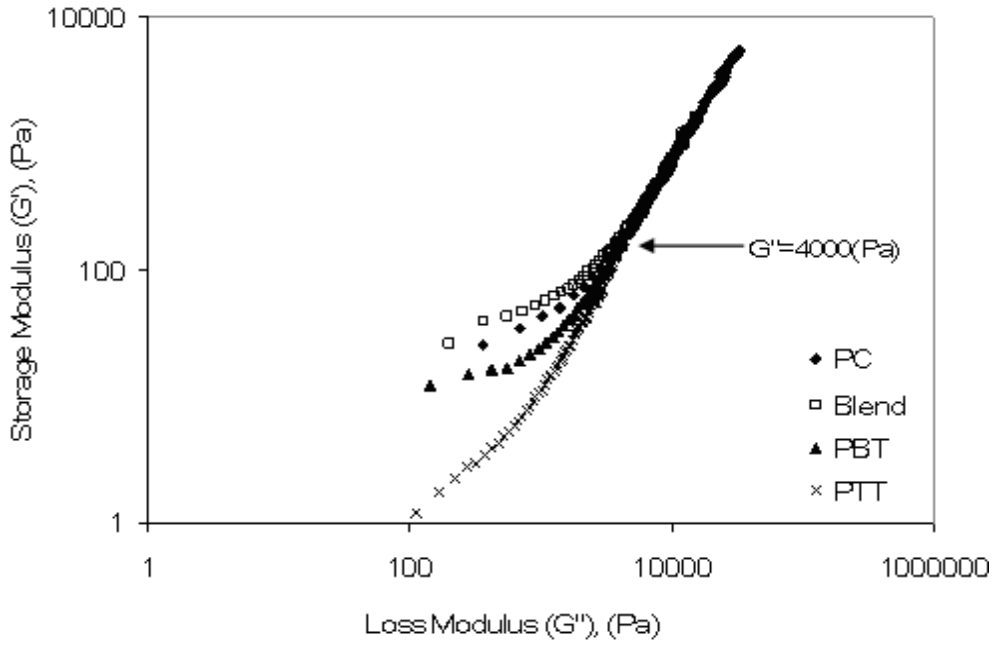

Figure 4.19: Plot of log (G") versus log (G") for PC, PTT, PBT and blend at constant strain and a temperature of 260°C.

From Figure 4.19, the viscoelastic dependence of molecular structure of the neat polymers and blend for flexible polymers is discernible till G" value of 4000Pa. Above G" value of 4000Pa, the dependence of molecular structure for all the materials is not discernible in this plot. As seen in Figure 4.19, the blend is seen to have the highest G' value till around G" equals to 4000Pa. The physically miscible blend comprising of three different polymers (heterogeneous state) and transesterifed, has elastic deformation

which is accompanied with high storage of energy with individual structure of the blend and slippage which involves less input of viscous energy till G" equals 4000Pa.

4.3.2 FTIR analysis

Infrared (IR) spectra were recorded on a Fourier Transform Infrared spectrometer (FTIR) (Perkin-Elmer 16PC) and scans were collected with a spectral resolution of 2 cm^{-1}. The solution of neat polymers and blend (2% w/v, in phenol/tetrachloroethane (1:6)) was cast onto potassium bromide (KBr) disk. Film thickness was adjusted such that the maximum absorbance of any band was less than 1.0 at which the Beer-Lambert law is valid. It was slowly dried for 24 hours in fume hood until most of the solvent evaporated and then dried at 50 °C for two days in a vacuum oven. Samples were then stored in a desiccator until it was used.

All subtractions were carried out using standard Ominic software. Selected IR bands were resolved using a peak fitting program (Galactic) to determine the area under the peaks, the precision of the wavenumbers are ± 0.1 cm^{-1}. The bands were assumed to be Lorentzian in shape with a linear baseline. Peak area of the isolated vibrational bands were measured using "peak area tool" of the "Omnic software". The FTIR peaks corresponding to PC, PTT, PBT and blend are indicated in Figures 4.20, 4.21, 4.22 and 4.23 respectively.

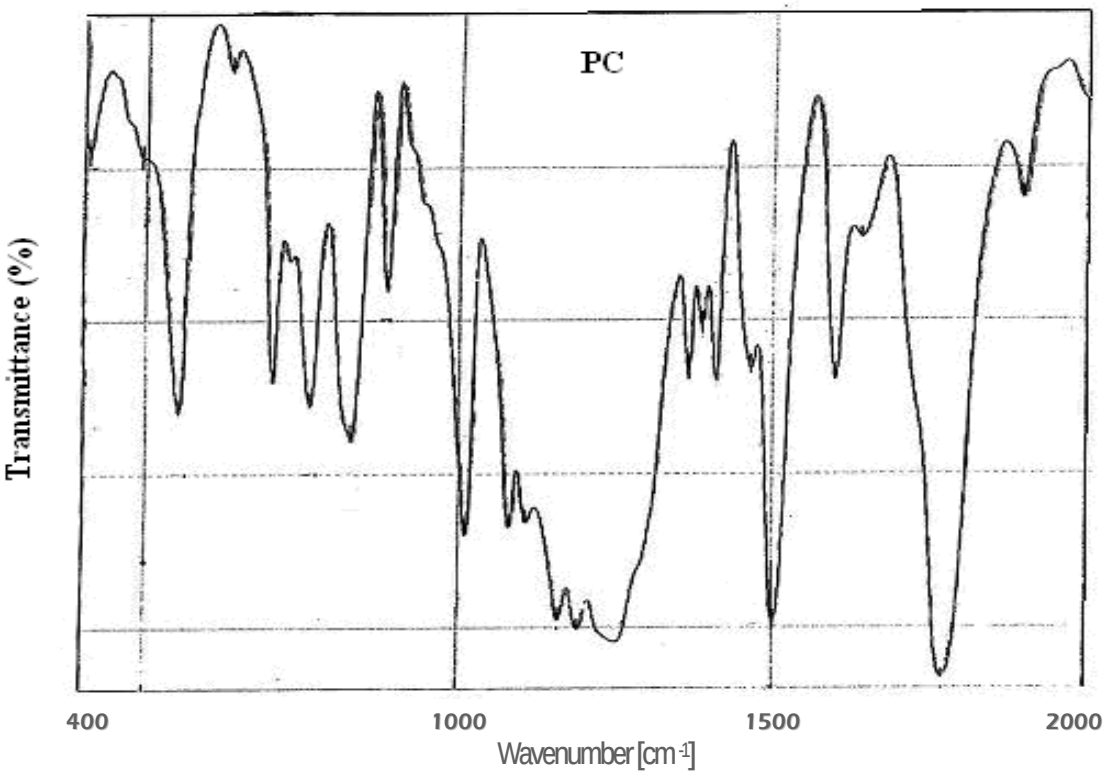

Figure 4.20: FTIR peaks corresponding to PC

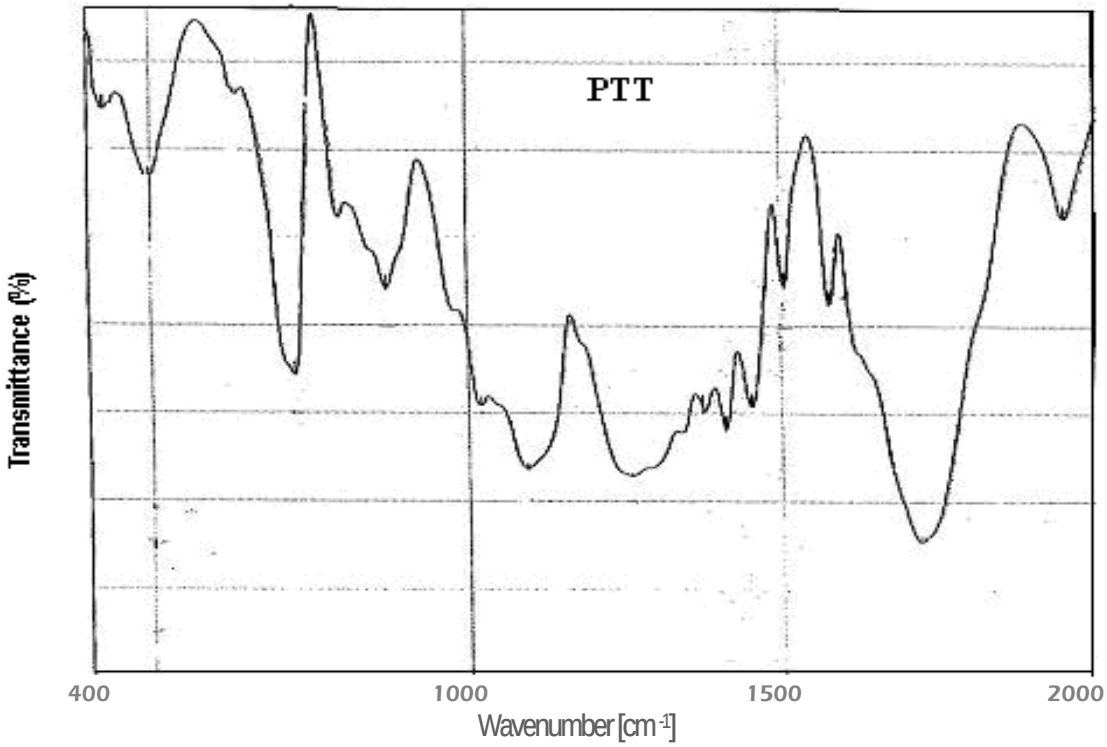

Figure 4.21: FTIR peaks corresponding to PTT

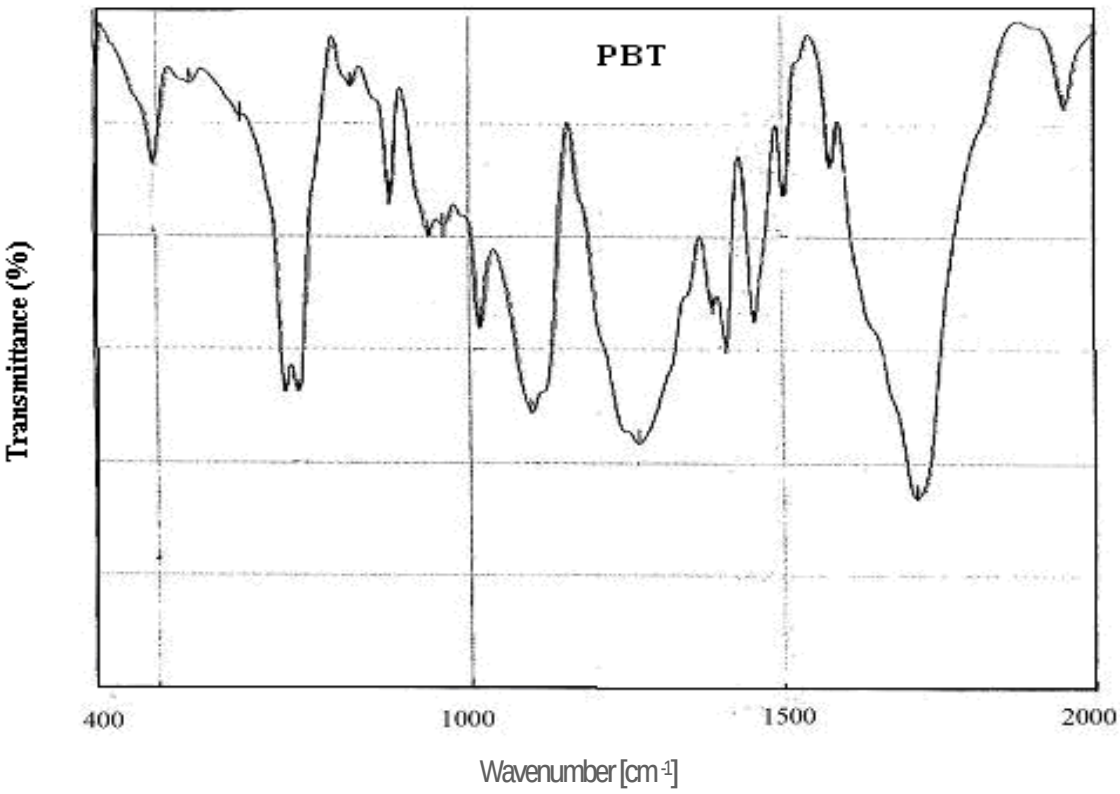

Figure 4.22: FTIR peaks corresponding to PBT

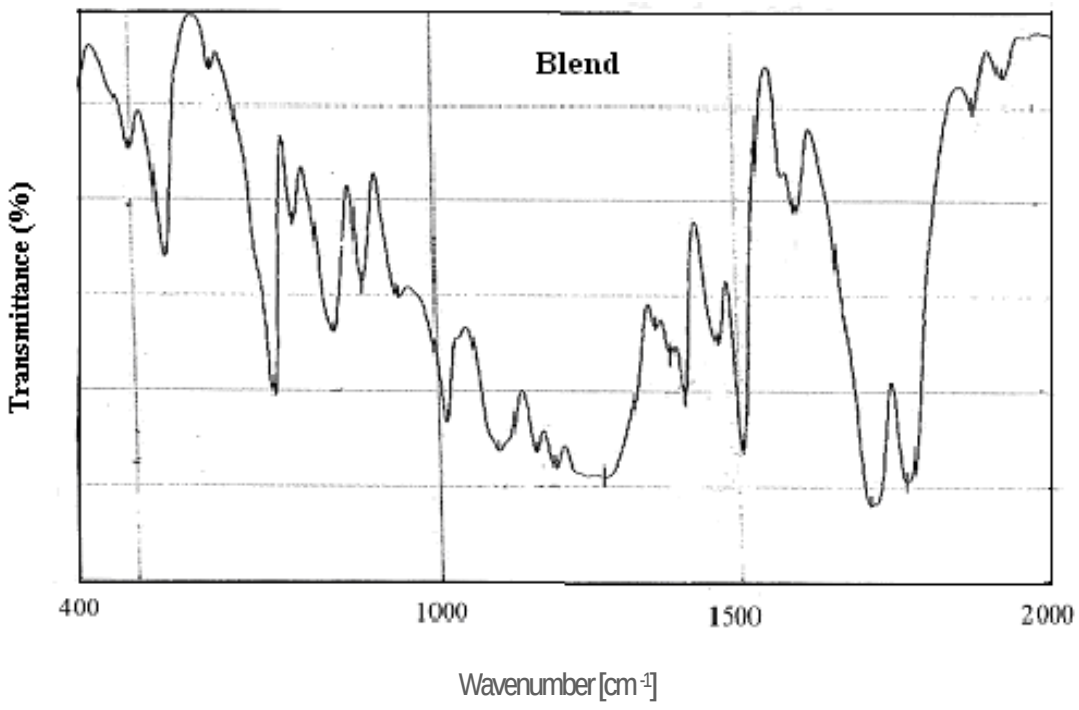

Figure 4.23: FTIR peaks corresponding to blend (PC, PTT, PBT).

FTIR spectroscopy has been used to analyze ester interchange reaction in PC/PTT/PBT blends. Transesterification is reported to occur in blends containing antimony catalyst and is facilitated and accelerated by the presence of titanium catalyst [102, 131]. Transesterification is dependent upon the temperature and mixing time. Higher temperature and longer mixing time increase the extent of ester interchange [102, 131, 132]. The 633cm^{-1}, Table 4.9, band is used as a reference peak, since it is due to the bending motion of the phenyl ring and all homopolymers contain phenyl ring. It is observed that the percentage transmission for the neat polymer is observed between 94 to 98 while for the blend, the percentage transmission decreased to 93. The aromatic C-H out of plane vibration for para disubstituted aromatic polycarbonate occurs around 827 cm^{-1} and in the blend around 830 cm^{-1}. These blends correspond to the aromatic carbon-hydrogen out of plane vibration, which implies that para disubstituted aromatic compounds are formed in the blend. This complex aromatic nature becomes more pronounced for the blend as depicted by the percentage transmission decreasing from 86 (polycarbonate) to 69 (blend). The peak at 1191cm^{-1} corresponds to isopropylidene vibration of polycarbonate [133]. Polyesters (PTT and PBT) do not show absorption in this range. In the blend, a strong absorption is seen corresponding to this molecular unit, at 1192 cm^{-1}. The percentage transmission of polycarbonate which is around 79 decreases to 51 in the blend indicating that the blend has acquired this structural group due to exchange reaction. C-H band stretching occurs at 1159 cm^{-1} in PC and aromatic ether stretching occurs at 1160cm^{-1}. The absorbance occurring at 1409 cm^{-1} in polycarbonate, polyester and the blend corresponds to CH_2 bending and wagging vibrations. Absorbance of band at 1506, 1503 and 1504 cm^{-1} are attributed to aromatic ring vibration in polyester and polycarbonate. This effect is noticed at 1506cm^{-1} in the

blend. These bands can be used to investigate structural changes if occurring due to exchange reaction in the polyesters. The reduction in percentage transmission to 53 for the blend from 80 and 91 in PC and polyester confirms that the blend acquires a mixed character of PC and the polyesters. In PTT and PBT, wavenumber occurring at 725 cm^{-1} corresponds to coupled vibration of carbonyl out of plane ring deformation of phenyl group.

An occurrence of exchange reaction between PC/PTT/PBT (50:25:25 wt/wt %) mixture was established using solubility test. The wavelength of IR spectroscopy from 1700 to 1800 cm^{-1} was studied for PC/PTT/PBT (50:25:25 wt/wt %) mixture. PC sequences characterized by their C=O stretching absorbance at 1775 cm^{-1} progressively appear in soluble fraction while PTTC and PBTC blocks with their C=O band at 1720 cm-1 are identified in the insoluble part. C=O stretching vibrations are found to occur at 1720 cm^{-1} and 1714 cm^{-1} in PTT and PBT and for the blend it occurs around 1718 cm^{-1}. The absorbance at 1777cm-1 results from the C=O stretching of aliphatic aromatic carbonate and the structure could be as follows:

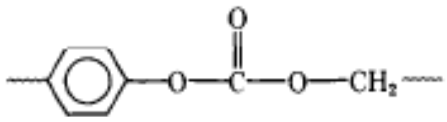

From this study on solubility and IR absorption exchange reaction, it is found that exchange reaction takes place between PC, PTT and PBT. The possible products due to exchange reactions are shown in Figure 4.18

Table 4.9: IR absorption for PC, PTT, PBT and the blend at room temperature.

Band Assignment	PC (cm^{-1})*	%T**	PTT (cm^{-1})*	%T**	PBT (cm^{-1})*	%T**	Blend (cm^{-1})*	%T**
bending motion of phenyl ring	633	95	633	98	633	94	633	93
coupled vibration of carbonyl out of plane deformation of phenyl group	-	-	725	88	725	83	725	55
aromatic C-H out of plane vibration	827	86	-	-	-	-	830	69
Isopropylidene vibration	1191	79	-	-	-	-	1192	51
C-H stretching	1159	80	-	-	-	-	1160	54
ν_s C-O-C in-plane ring deformation	-	-	1259	85	1268	81	1271	47
aromatic ring vibration of C-C group	1504	80	1506	91	1503	91	1506	53
C-C band stretching in benzene ring stretching	1600	88	-	-	-	-	1609	79
C=O stretching vibration	-	-	1720	83	1719	78	1718	43
C=O stretching absorption	1775	78	-	-	-	-	1777	53

*wavenumber
**%T is percentage transmission

4.4 Results and discussion of study of degradation of neat polymers and blend

4.4.1 DSC analysis

PTT and PBT had a T_m of 257 and 223 °C, respectively, while T_g for both was observed around 71 °C. PC depicted a T_g of 160 °C. The blend showed a T_m of 226°C and two diffuse T_g's around 84 and 116°C, indicating the low compatibility of the blend.

4.4.2 Thermogravimetric analysis

The thermal degradation kinetics of PC, PTT, PBT and the blend were characterized by modeling mass loss during heating. The TG curves of the blend run at different heating rates from room temperature to 700°C in air atmosphere are presented in Figure 4.24. It is noted that the curves shift to higher temperatures as the heating rate increases from 5 to 20°C/min.

By analyzing the TG and DTG curves of PC, PTT, PBT and the blend, it is possible to notice the competing processes of destruction that accompany the pyrolysis of a polymeric material.

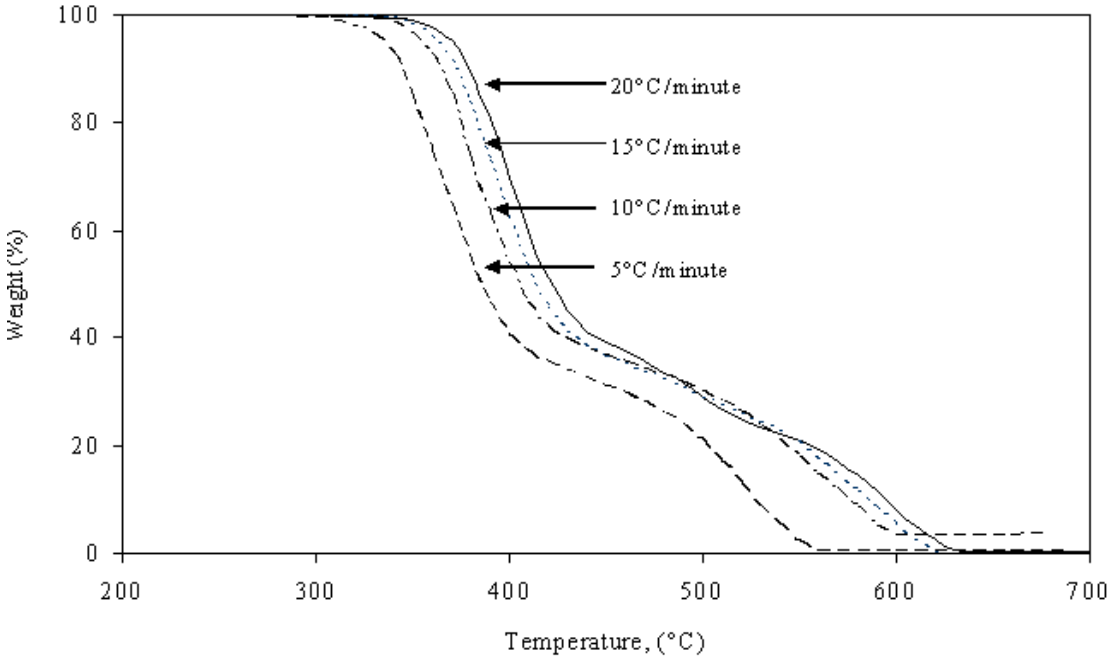

Figure 4.24: TG curves of blend (PC, PTT, PBT) at different heating rates in air atmosphere

The predominance of the destruction process leads to full disintegration of the initial material to monomers (depolymerization process) and simple compounds and to a carbon frame representing the carbonized product (raw carbon) [99]. Generally, the TG curves show that the blend and neat polymers, degrade in two stages and nearly crumble between 600-650°C (char yield around 2.4%). This reveals that all the polymer mass turns into gaseous product at 600-700°C. The decomposition pathway of a polyester composed of glycol and diacid are described in literature as a three stage process. The first stage is elimination of terephthalic acid. The second stage, around 350°C, is possibly caused by the release of styrene and a complex mixture of other materials, while the third stage above, 500°C, relates to the loss of high boiling

tars and oxidation of the char formed [134]. This observation is relevant to the degradation mechanism for PTT and PBT used in our study.

This work will be focused on the first stage of the thermal degradation for the polycarbonate and polyesters. The first stage of degradation of PC, determined from the TG curve, extends over the temperature range 430 to 550°C, while for PTT it is observed to start at 330°C and end at 430°C. For PBT, the first stage of degradation was found to fall in the range 310 – 440°C. For the blend, the first stage of degradation began at 330°C and ended at 440°C. DTG curve for the blend PC/PTT/PBT shows one shoulder, characteristic of an overlap of different degradation process [120]. The first stage of sharp loss in mass for the polyesters is mostly attributed to degradation of the aromatic components. During the break down of polymers, nucleophilic terminal hydroxyl groups are replaced with less reactive groups like alkyl group [120].

The degradation temperatures of the blend and the neat polymers in nitrogen and air at different conversions are shown in Table 4.10. It can be seen that the degradation temperatures of the neat end-capped polyesters and polycarbonate in nitrogen are higher than those in air. This indicates that oxygen has a noticeable effect on the decomposition of polymers due to oxidation reactions occurring in the system.

Table 4.10: Thermal degradation characteristics for neat PC, PTT, PBT and the blend in air and N_2 atmosphere.

Polymer	Heating Rate ^oC/min	$T_{\alpha=10\%}$ (^oC)		$T_{\alpha=30\%}$ (^oC)		$T_{\alpha=50\%}$ (^oC)		T_{max}	
		Air	N_2	Air	N_2	Air	N_2	Air	N_2
PC	5	405	449	438	478	454	496	441	492
	10	430	469	460	495	481	513	480	512
	15	444	477	479	504	491	520	497	519
	20	460	489	499	514	516	528	515	527
PTT	5	351	356	369	372	379	382	383	384
	10	366	370	383	386	393	394	393	396
	15	374	379	390	393	401	403	402	408
	20	383	383	399	399	408	408	410	412
PBT	5	343	358	364	371	375	380	379	381
	10	357	371	377	384	389	393	390	396
	15	366	378	386	392	397	401	399	403
	20	371	385	392	399	403	407	404	410
Blend	5	344	351	364	370	385	397	357	362
	10	364	366	382	388	404	417	379	377
	15	372	373	392	396	414	421	389	390
	20	379	382	400	402	421	426	392	398

From the TG curves, it can be seen that PC, PTT and PBT show relatively good thermal stability, since no significant weight loss (only 1.2%) occurs until the temperature reaches 305°C. Early weight loss was observed in poly(propylene terephthalate) (PPT) with low number-average molecular weights, ranging between 13,000 and 23,000 g/mol, where the first decomposition step corresponded to small weight loss (2-4%) of PTT. The weight loss was attributed to the volatilization of small molecules, residual catalysts, and 1,3-propanediol and carbon dioxide that evolved from chain ends [135]. Thus, the temperature at maximum weight-loss rate at this stage increases significantly with molecular weight while the weight loss decreases steadily.

The TG and DTG curves of all polymers at 10°C/min in air and nitrogen are shown in Figures 4.25 and 4.26. Temperatures of maximum degradation T_{max} increase in the following sequence: PC > PTT > PBT > blend. As seen in Figures 4.25 and 4.26, degradation occurs at slightly higher temperatures in nitrogen than in air. The peak temperatures, T_{max}, extracted from the DTG curves are listed in Table 4.10. From the table it can be seen that the peak temperatures of the pure polymers are higher than those of the blend. The DTG curves of PC have a shoulder in the range 470 to 500 °C, however PTT and PBT do not show this behavior. This implies that the degradation of PC and polyesters follow different mechanisms. Chain unzipping mainly contributes to the degradation of PC till the first T_{max}. In both air and nitrogen, the DTG curves of the blend exhibit shoulders around 390 and 410°C.

Referring to Table 4.10, as the heating rate increases, T_{max} increases and as the conversion increases, the degradation temperature is also found to increase, in both air

and nitrogen. In general, the peak temperature for the degradation of PC is found to be the highest.

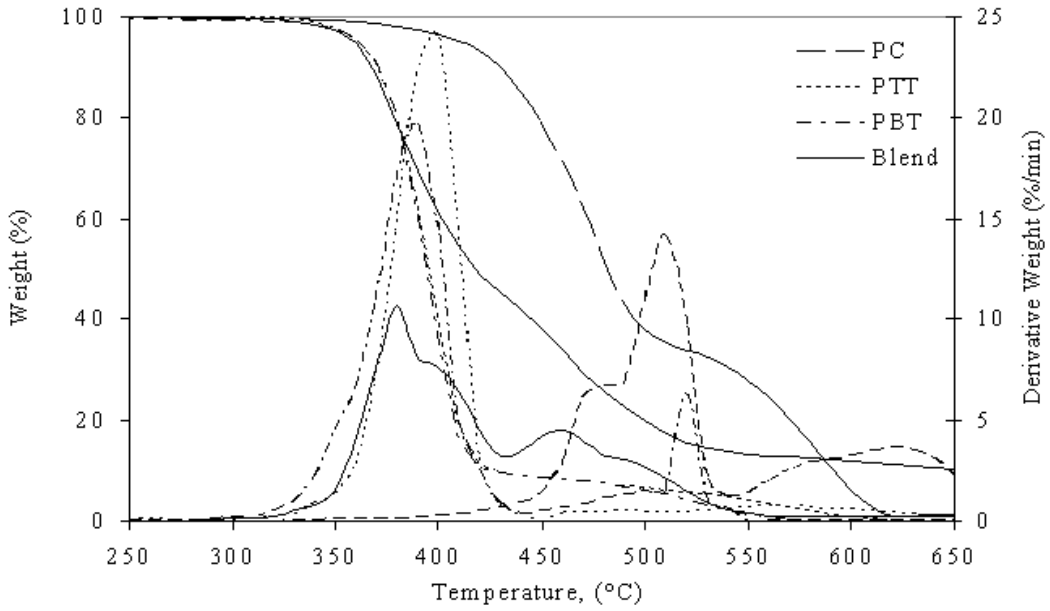

Figure 4.25: TG and DTG curves of PC, PTT, PBT and blend at 10°C/minute in air atmosphere.

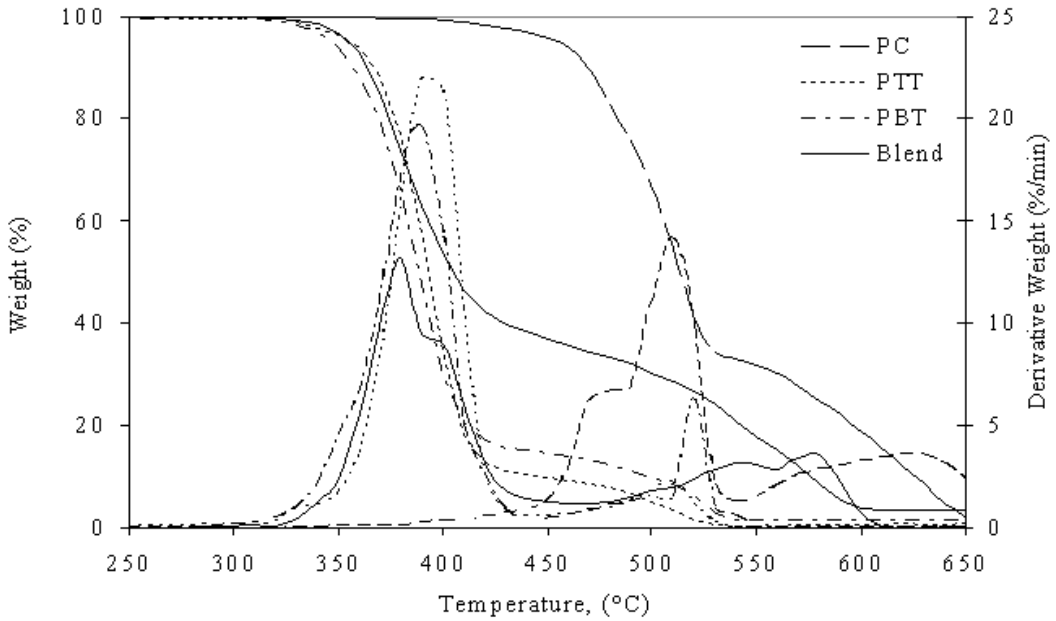

Figure 4.26: TG and DTG curves of PC, PTT, PBT and blend at 10°C/minute in nitrogen atmosphere.

For PTT and PBT, the maximum temperature for degradation appears at around 400°C. The volatile matter evolved at T_{max} is around 58% for both in nitrogen and around 42% and 52%, respectively, in air. This is indicated in Figures 4.25 and 4.26. T_{max} values are comparable to decomposition temperatures reported for aromatic polyesters of terephthalic (PET, PBT, PPT) and naphthalic acid like poly (ethylene naphthalate) (PEN)[29].

Even if the shape of the mass loss curves does not change and exhibits the same starting temperature of decomposition, Figure 4.27 shows that the maximum temperature of degradation obtained for polyesters is shifted to higher values as the heating rate increases. A similar observation is noted for PC and the blend, with PC degrading at higher temperatures, as shown in Figure 4.28.

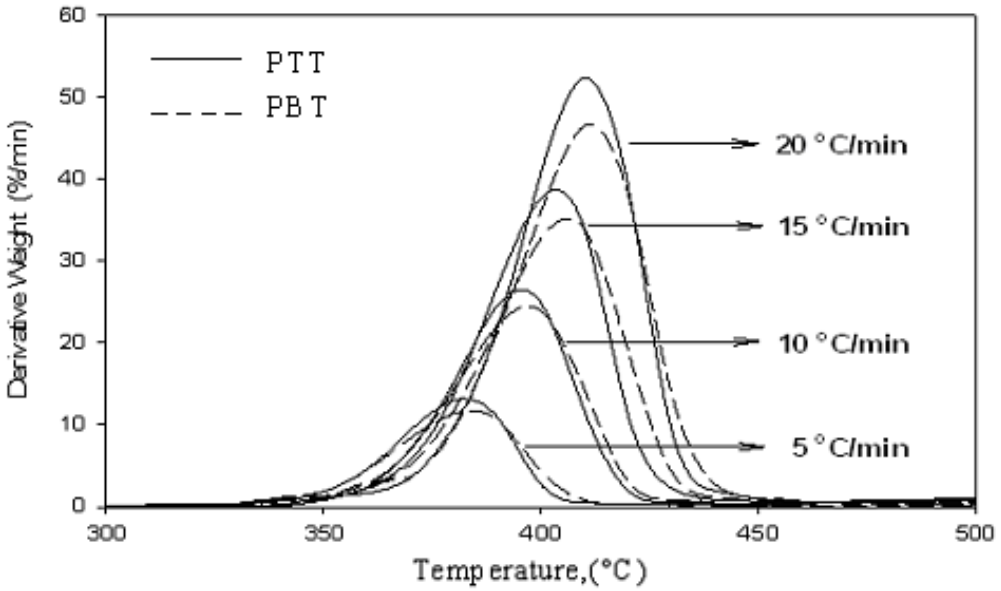

Figure 4.27: DTG curves of PTT and PBT at different heating rates in N_2 atmosphere.

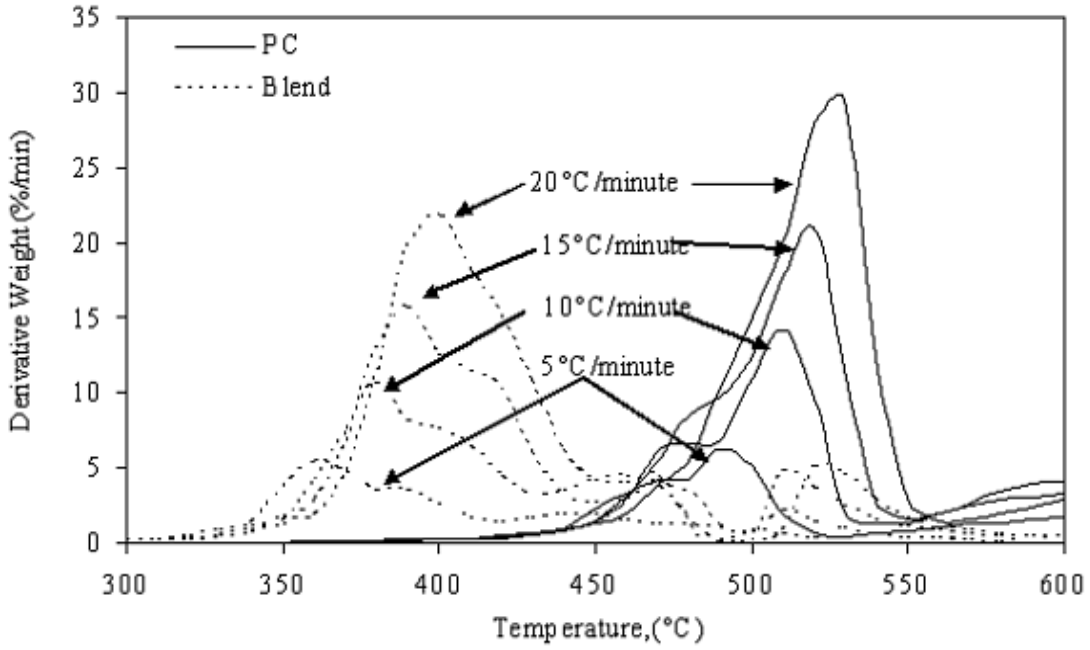

Figure 4.28: DTG curves of PC and blend at different heating rates in N_2 atmosphere

Second Derivative Thermogravimetric (DDTG) curves (indicated in Figures 4.29 and 4.30) were used to identify overlapping peaks, determine peak maxima and detect small endothermic deflections. The DDTG curves for the blend at different heating rates lie between 315 and 460°C for thermal degradation in air, and between 325 and 450°C for thermal degradation in nitrogen. Peaks appearing before 460°C have only been considered since they correspond to the first stage of degradation.

The activation energy of degradation was estimated using Kissinger method [78]. As reported previously [78], it is assumed that the instantaneous value of peak temperature is directly proportional to the degradation process rate and that this process obeys a first-order rate equation. The peak temperatures T_{max} at a given heating rate were reproducible to about $\pm$1%.

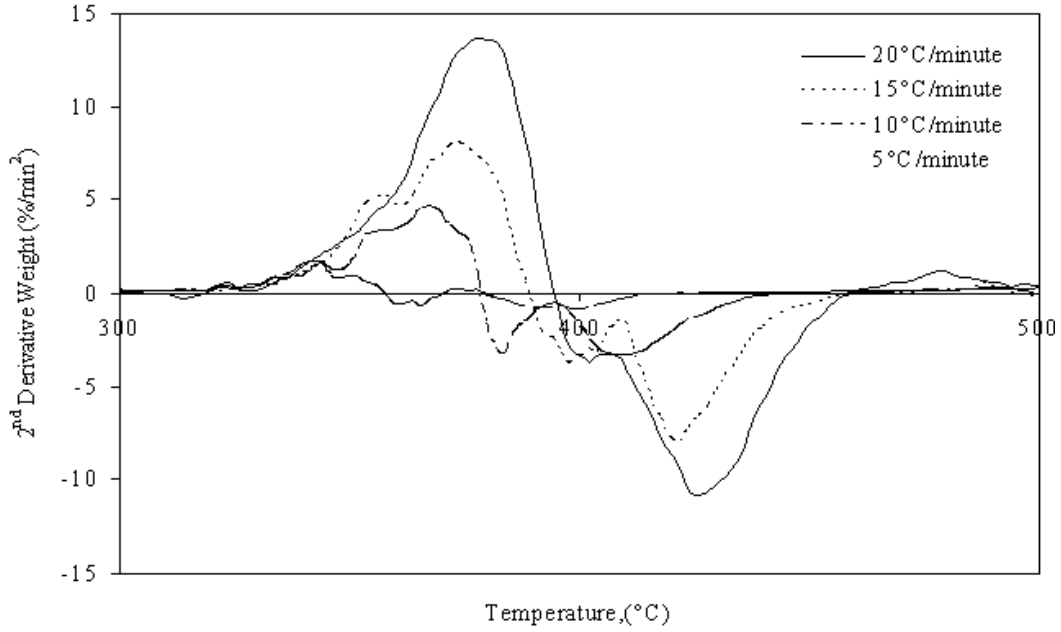

Figure 4.29: DDTG curves of blend at different heating rates in air atmosphere

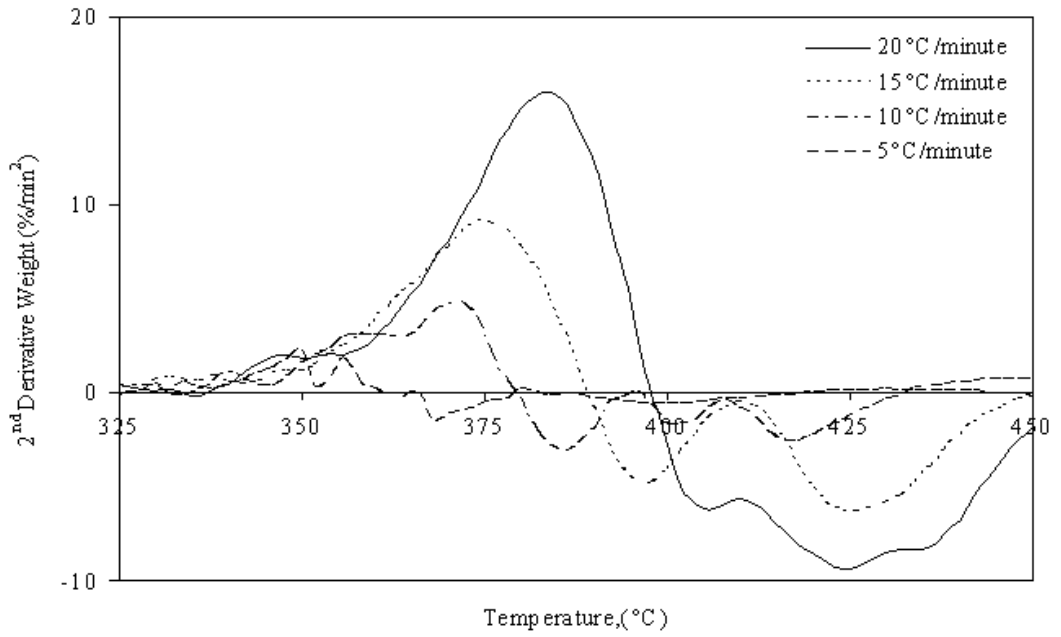

Figure 4.30: DDTG curves of blend at different heating rates in N_2 atmosphere

The plots for Kissinger method are presented in Figures 4.31 and 4.32. The values of *E* and *A* obtained are presented in Table 4.11. Though Kissinger method fittings resulted in

r^2 values greater than 0.98, the model remains questionable due to the large difference between *E* values obtained for degradation in air and nitrogen for PTT. PBT comprises of an extra methylene group compared to PTT. Comparison of the *E* values of PTT and PBT in air raises doubt on the validity of the model for evaluating degradation parameters.

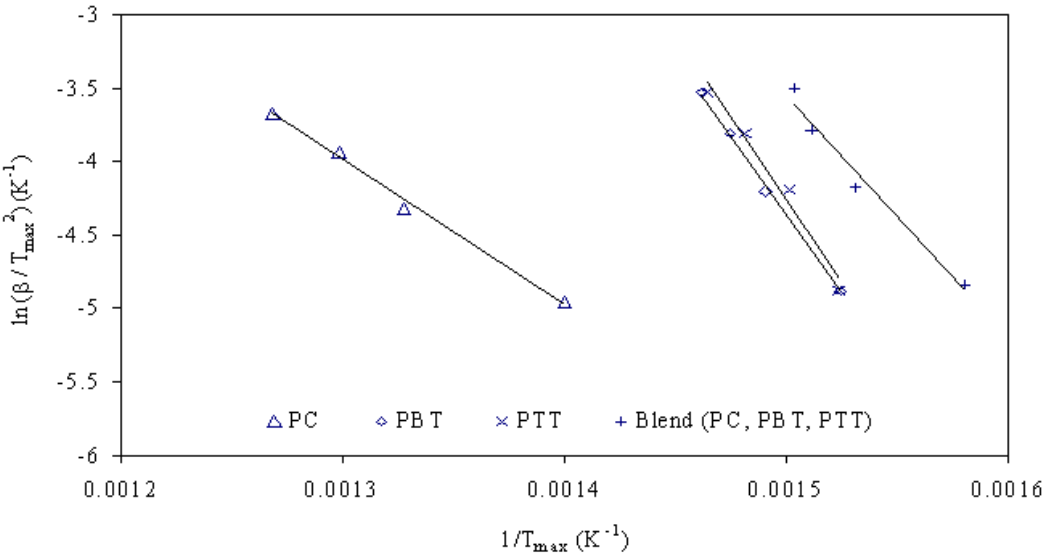

Figure 4.31: Application of Kissinger method to the degradation of PC, PTT, PBT and the blend in air atmosphere.

Another observation noted is that activation energy *E* of some polymers in air is higher than that in nitrogen. This contradicts the chemical reaction hypothesis in which oxygen reacts with the polymer in air atmosphere, leading to accelerated degradation. Figures 4.29 and 4.30 represent a sample of the curves used in estimating the reaction order *n* following Kissinger method. Small shoulders seen on the endothermic and exothermic peaks are attributed to electronic noise. This behavior may be related to heat transfer problems between sample and instrument. The *n* values of polyesters in air are greater than those in nitrogen, as shown in Table 4.11.

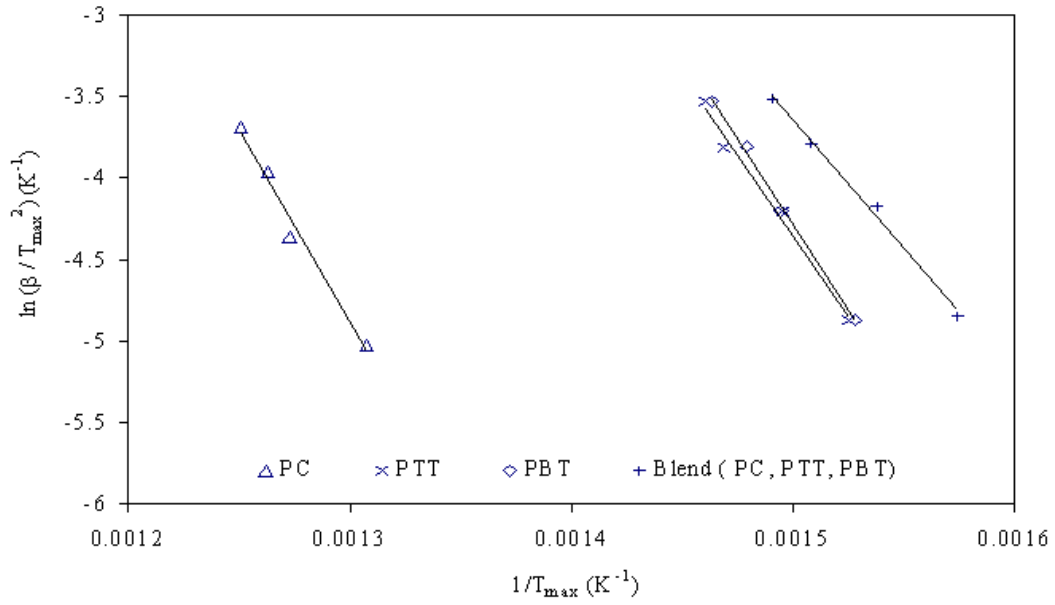

Figure 4.32: Application of Kissinger method to the degradation of PC, PTT, PBT and the blend in N_2 atmosphere.

This plausibly signifies that the degradation mechanism in air is more complex. In general, the kinetic parameters indicated in Table 4.11 reveal that the properties of the neat polymers are better compared to the blend, arising from differences in degradation mechanisms. Ozawa method was employed in determining the activation energy at different conversion values by plotting $\log \beta$ versus *1/T,* as shown in Figures 4.33 and 4.34. The order of degradation *n* determined from Kissinger method was used in this method. Ozawa plots show straight lines with high correlation coefficient, thus indicating the applicability of Ozawa method to the first stage of the degradation process of the blend and its components.

Table 4.11: Kinetic Constants of neat PC, PTT, PBT and the blend calculated using Kissinger model under air atmosphere.

Polymer	Heating Rate ^{o}C/min	n		E (kJ/mol)		ln(A) (min^{-1})		r^2	
		Air	N_2	Air	N_2	Air	N_2	Air	N_2
PC	5 10 15 20	1.14	1.64	188.55	165.23	32.83	28.47	0.979	0.988
PTT	5 10 15 20	2.06	1.89	81.89	196.16	32.91	28.95	0.994	0.981
PBT	5 10 15 20	2.43	1.75	177.57	175.74	31.14	30.53	0.998	0.996
Blend	5 10 15 20	1.58	2.89	137.48	130.59	23.85	18.32	0.97	0.993

Ozawa plots show straight lines with high correlation coefficient, thus indicating the applicability of Ozawa method to the first stage of the degradation process of the blend and its components. The results extracted from this model are summarized in Table 4.12. The degradation temperature profiles of the polymers at 50% conversion are observed as follows: PC>blend>PTT>PBT. The high percentage of PC in the blend might have influenced the increase in degradation temperature of the blend compared to that of the polyesters. The *E* and *A* values in nitrogen are greater than those in air. The highest *E* value observed (around 184 kJ/mol) is for PC in nitrogen.

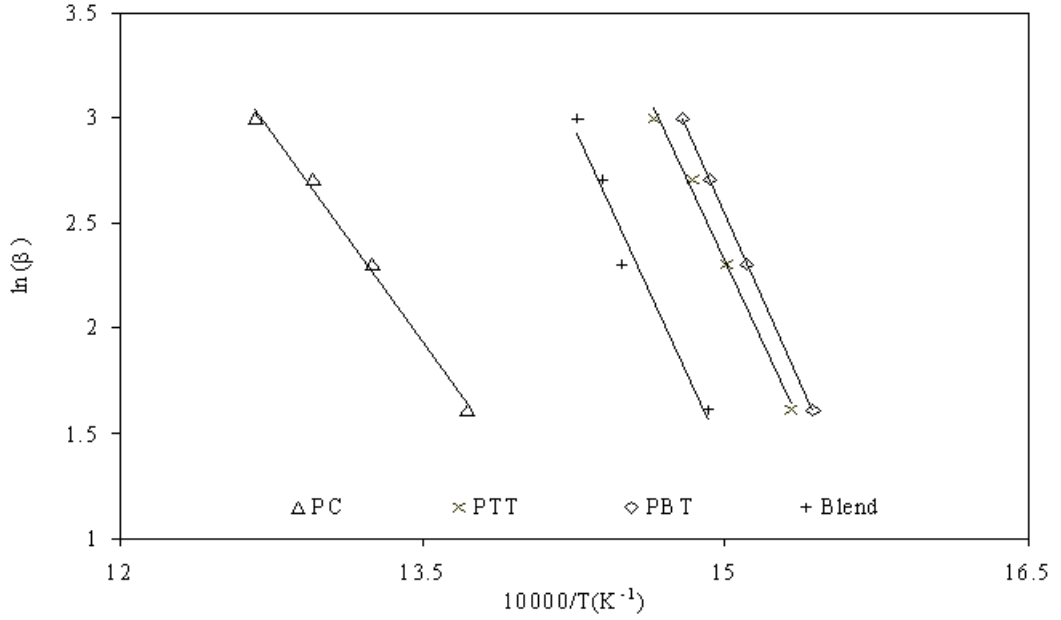

Figure 4. 33: Ozawa plot of ln (β) as function of inverse temperature (1/T) at α =50% for PC, PTT, PBT neat polymers and the blend in air atmosphere.

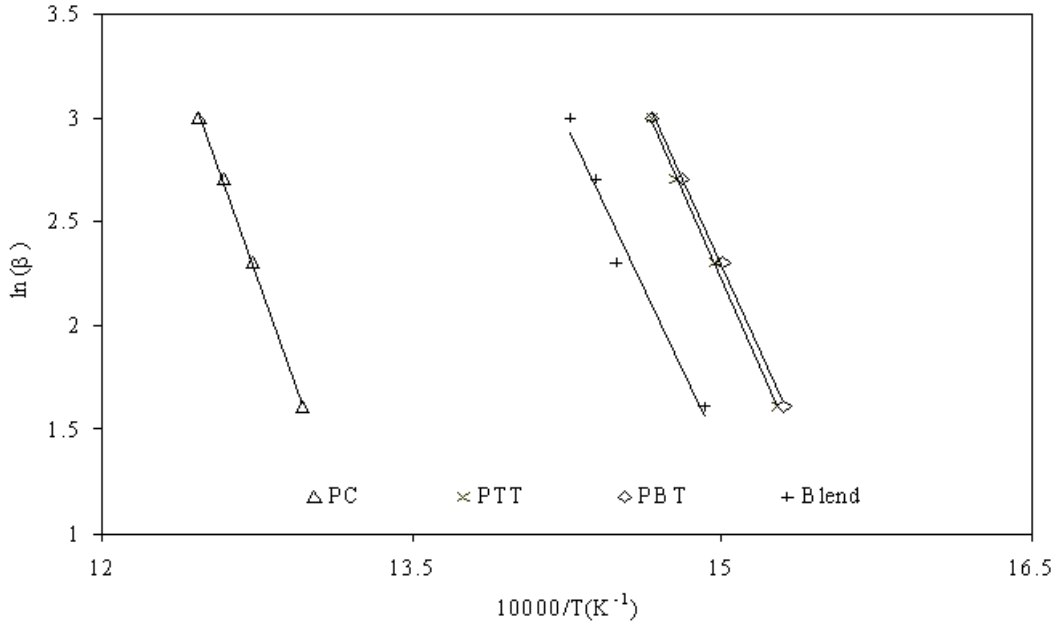

Figure 4.34: Ozawa plot of ln (β) as function of inverse temperature (1/T) at α =50% for PC, PTT, PBT neat polymers and the blend in N_2 atmosphere.

Based on Ozawa's analysis for the degradation in air of the polymers studied, the change in the values of E with respect to α is minimal till $\alpha = 30\%$ as represented in Figure 4.35. The dependence of E on α is then shifted to a monotonous increase. As for the polyesters, E displays an increasing trend over the range studied. This observation supports the assumption that PC and the blend experience multiple degradation mechanisms, while the degradation of PTT and PBT follow one mechanism. The case is a bit different when degradation takes place as presented in Figure 4.36, in nitrogen. The blend shows an average constant value of E. PBT displays two distinct regions, the first extends to α equal to 30% and E is characterized with a slightly increasing trend, and the second shows constant E value. Both PC and PTT have two regions with increasing trends of E, each with a different intensity.

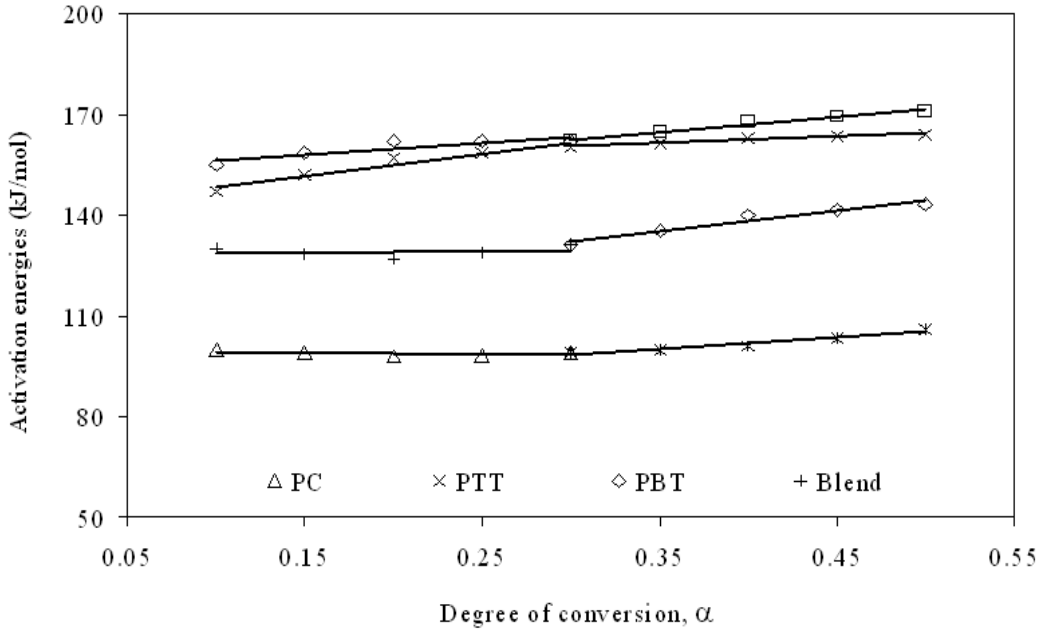

Figure 4.35: Dependence of Ozawa's activation energy as function of conversion for thermal degradation in air atmosphere.

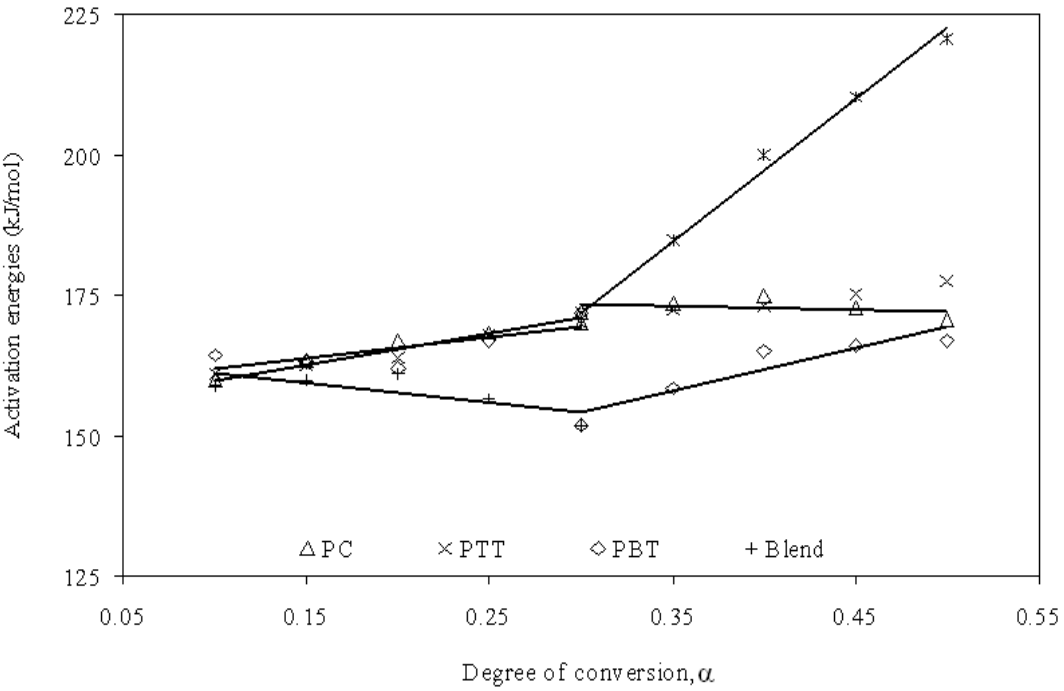

Figure 4.36: Dependence of activation energy on the different conversion values for neat polymers and blend in N_2 atmosphere.

Plots of $\ln(d\alpha/dt)$ versus *1/T* according to Friedman method are presented in Figure 4.37 and 4.38. The activation energies and pre-exponential factors are indicated in Table 4.13. The *E* and *A* values for the neat polymers and the blend are greater in nitrogen compared to those in air. The value of *n* is obtained by plotting ln *(1-*α) versus *1/T*. The highest value of *n* (about 5.5) is observed for the degradation of the blend in nitrogen. No definite trend in *E* or ln *A* values was observed. It is also obvious that as *E* increases, the value of ln *A* also increases. The kinetic parameters calculated using Friedman method are slightly higher than those obtained using Ozawa. The *E* values for all polymers are lower in air than in nitrogen. The *E* values for PBT are greater than those of PTT, in both air and nitrogen. PBT degradation in nitrogen is found to have the highest *E* value of 327 kJ/mol. The r^2 values obtained are all above 0.99, indicating the validity of the model to analyze the polymers studied.

Table 4.12: Kinetic parameters of thermal degradation for PC, PTT, PBT and the blend calculated using Ozawa model in air and N_2 atmospheres.

	Fractional Conversion α	Ξ (kJ/mol)	ln(A) (min^{-1})	r^2	E (kJ/mol)	ln (A) (min^{-1})	r^2	E (kJ/mol)	ln (A) (min^{-1})	r^2	E (kJ/mol)	ln (A) (min^{-1})	r^2
	PC				PTT			PBT			Blend		
Air	0.1	100	18.71	0.997	147	29.59	0.998	155	31.48	1.000	130	26.76	0.987
	0.2	98	18.58	0.975	157	31.87	0.998	162	32.87	0.999	127	26.6	0.994
	0.3	99	18.94	0.985	160	32.65	0.998	162	33.19	0.999	131	27.33	0.998
	0.4	101	19.47	0.991	163	33.27	0.998	168	34.42	1.000	140	28.69	0.998
	0.5	106	20.4	0.994	164	33.58	0.993	171	34.85	0.999	143	29.16	0.996
	Mean	101	19.22	0.989	158	32.19	0.997	164	33.36	0.999	134	27.71	0.995
N_2	0.1	160	27.83	0.998	161	32.24	0.997	164	32.94	0.998	159	32.14	0.994
	0.2	167	28.79	0.993	164	33.19	0.999	162	32.91	0.999	161	32.84	0.989
	0.3	170	29.33	0.99	172	34.82	0.997	172	34.80	0.998	152	26.35	0.988
	0.4	200	33.95	0.997	173	35.12	0.999	175	35.49	0.996	165	28.47	0.979
	0.5	221	37.11	0.998	178	36.02	0.999	171	30.25	0.998	167	28.51	0.967
	Mean	184	31.4	0.995	170	34.28	0.998	169	33.28	0.998	161	29.66	0.983

The values of the thermal degradation activation energies, E, are summarized in Table 4.13. In general E values tend to increase with an increase in the $–CH_2-$ group content for polyesters. A high value of E reflects better thermal stability of polymeric sample as is shown in Table 4.13. For the degradation reaction order, n, an order of zero has been known for rapid degradation and an increase in this degradation parameter reflects a slow degradation process. In Table 4.13 the blend shows the highest average n value, indicating very slow degradation.

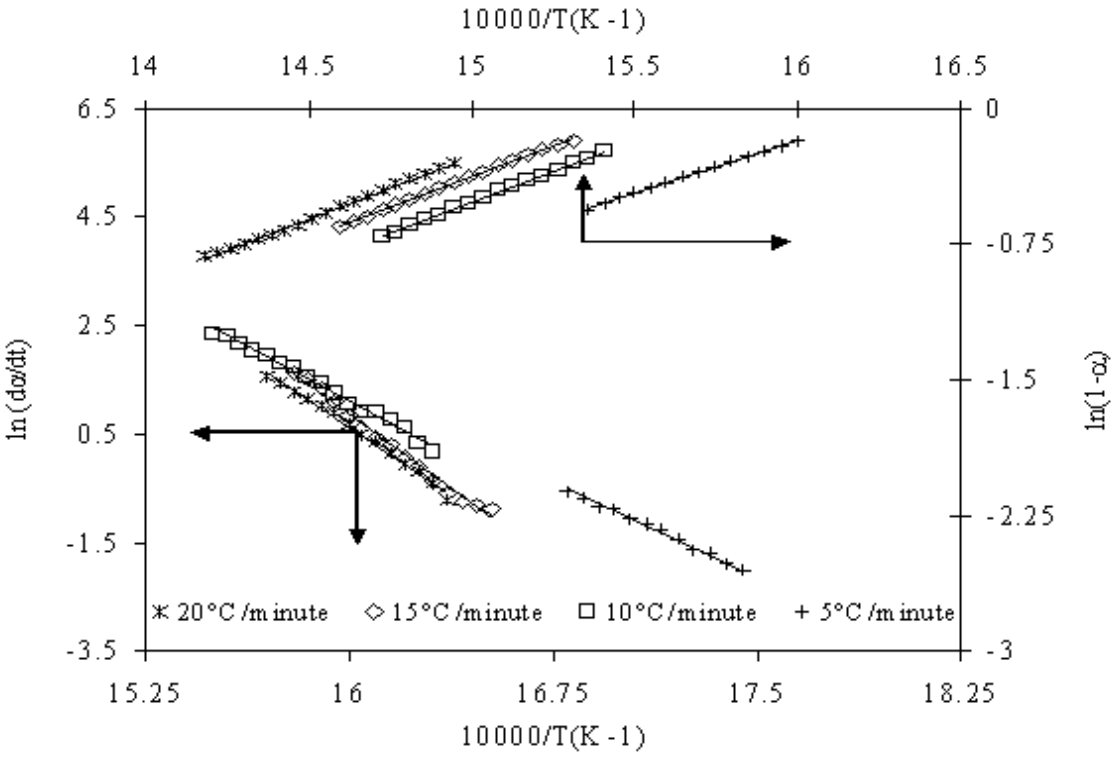

Figure 4.37: Friedman plots of ln(dα/dt) and ln(1-α) as a function of 1/T for the blend at different heating rates in air atmosphere.

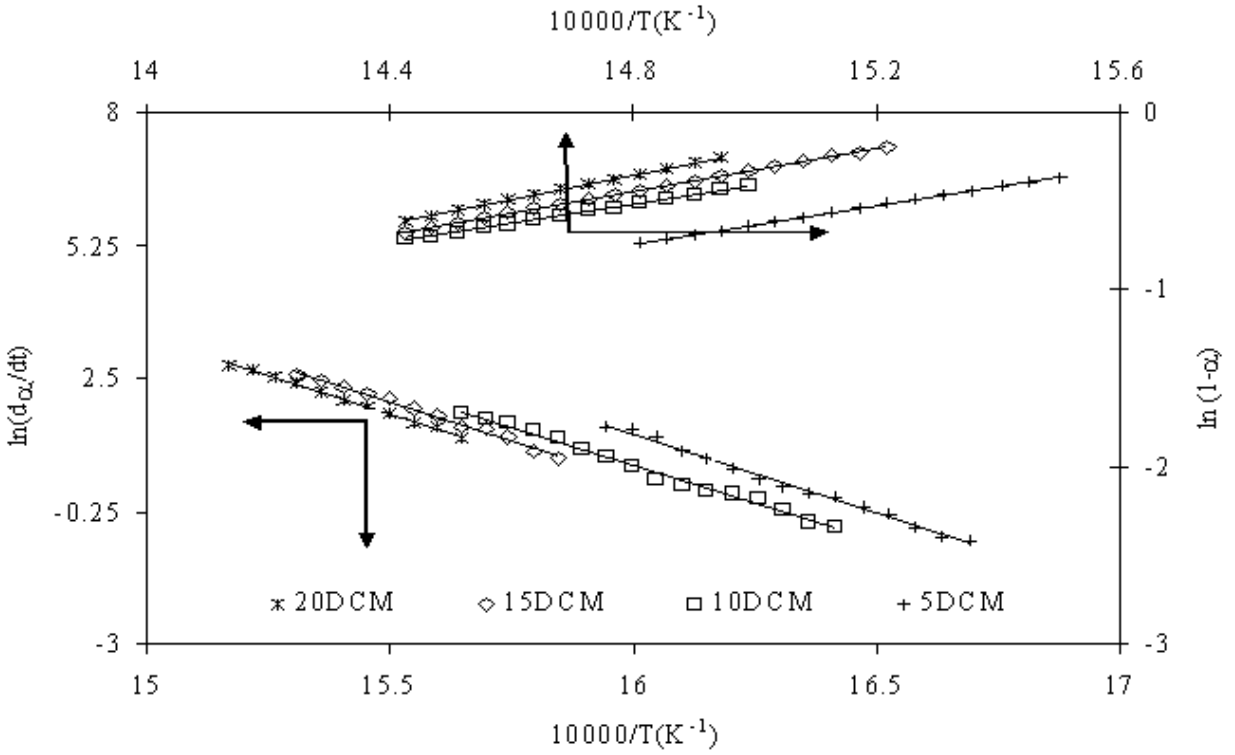

Figure 4.38: Friedman plots of ln(dα/dt) and ln(1-α) vs.1/T for estimation of E and n of the blend at different heating rate in N_2 atmosphere.

Figures 4.39 and 4.40 present plots in accordance with the Chang model, in which *n* is assumed to be one. The corresponding degradation kinetic parameters are reported in Table 4.14. It was found that for the polyesters, the kinetic parameters tend to increase with the increase in heating rate. *A* values in nitrogen are higher than those in air. The high *E* values observed for degradation of PBT in nitrogen are almost similar to those given by the Friedman model. The r^2 values are greater than 0.99. ln *A* for the blend shows the highest value of 47, indicating that the chemical mechanism of degradation is highly complex. Furthermore, it is been known that the variation in kinetic parameters should reflect the change in thermal degradation mechanism i.e., the thermal degradation transferring from diffusion-controlled kinetics to the degradation-controlled kinetics, or vice versa [136].

Table 4.13: Characteristic temperatures and kinetic parameters of the first thermal degradation stage for PC, PTT, PBT and blend in air and N_2 atmosphere using Friedman model.

Polymer	Heating Rate (°C/min)	Air				N_2			
		E (kJ/mol)	n	ln(A) (min^{-1})	r^2	E (kJ/mol)	n	ln(A) (min^{-1})	r^2
PC	5	107	2.459	19.41	0.997	167	2.843	28.02	0.99
	10	168	3.218	30.24	0.995	170	3.232	24.44	0.993
	15	111	2.144	19.92	0.998	321	2.507	53.87	0.991
	20	129	2.148	22.98	0.995	176	1.294	29.58	0.994
	Average	129	2.492	23.14	0.996	208	2.469	33.98	0.992
PTT	5	184	0.973	36.24	0.994	257	1.156	50.42	0.997
	10	193	0.864	37.97	0.99	286	1.105	55.49	0.998
	15	241	1.072	47.03	0.997	278	1.154	53.70	0.998
	20	282	1.321	54.44	0.996	304	1.268	58.34	0.995
	Average	225	1.058	43.92	0.994	281	1.171	54.49	0.997
PBT	5	253	1.617	50.63	0.996	255	0.987	59.92	0.991
	10	237	1.559	47.37	0.9997	400	2.198	64.22	0.99
	15	260	1.676	51.41	0.993	330	1.304	63.06	0.998
	20	265	1.873	52.27	0.993	321	1.235	61.45	0.993
	Average	254	1.681	50.42	0.995	327	1.431	62.16	0.993
Blend	5	188	3.864	37.52	0.993	275	6.173	54.59	0.993
	10	225	3.920	44.54	0.9925	262	5.823	51.38	0.9927
	15	275	4.956	56.69	0.99	271	5.394	53.02	0.99
	20	270	4.635	53.29	0.994	266	4.701	51.66	0.997
	Average	239	4.344	48.01	0.992	269	5.523	52.66	0.993

For the polyesters, at lower heating rate, the physical diffusion of degradation intermediate products does not apparently influence the kinetics of the degradation process, so the kinetic parameter values tend to be low. Therefore, for polyesters at a low heating rate, thermal degradation would proceed under the diffusion-controlled mechanism. Accordingly, higher kinetic parameters were observed with increasing heating rate [137]. This is observed in Table 4.14.

Among the above four analytical models, Friedman model was found to give the highest degradation activation energy E and the highest degradation reaction order parameter n. The activation energy and pre-exponential factor values given by Friedman and Chang are almost identical. These values obtained by Friedman and Chang do not match with those of Kissinger and Ozawa. This behavior has also been reported earlier [137]. This suggests that the kinetic parameters would vary more or less with the experimental temperature, even though we assumed they would not change with temperature in each proposed model [138].

Here it could be seen that Chang model actually tends to display good linear relationship in a wide temperature range. However, in this study, the thermal scanning range to achieve good linear relationship was indeed found to be wide enough for accurate determination of degradation kinetic parameters according to the Friedman, Kissinger and Ozawa methods.

In general, the values of E in air are found to be lower than those obtained in nitrogen, with PC having the lowest value of E in air. E obtained in nitrogen for both polyesters are found to be comparable. As the value of E increases, the value of ln A is also found to increase. Based on Friedman method, it seems clear that more reproducible results are obtained for the complete temperature interval for all heating rates. Activation energies decrease dramatically with the increase in heating rate from 5 to 15°C/min. This drop is probably caused by the thermal lag in the instrument as well as in the sample thermal conductivity.

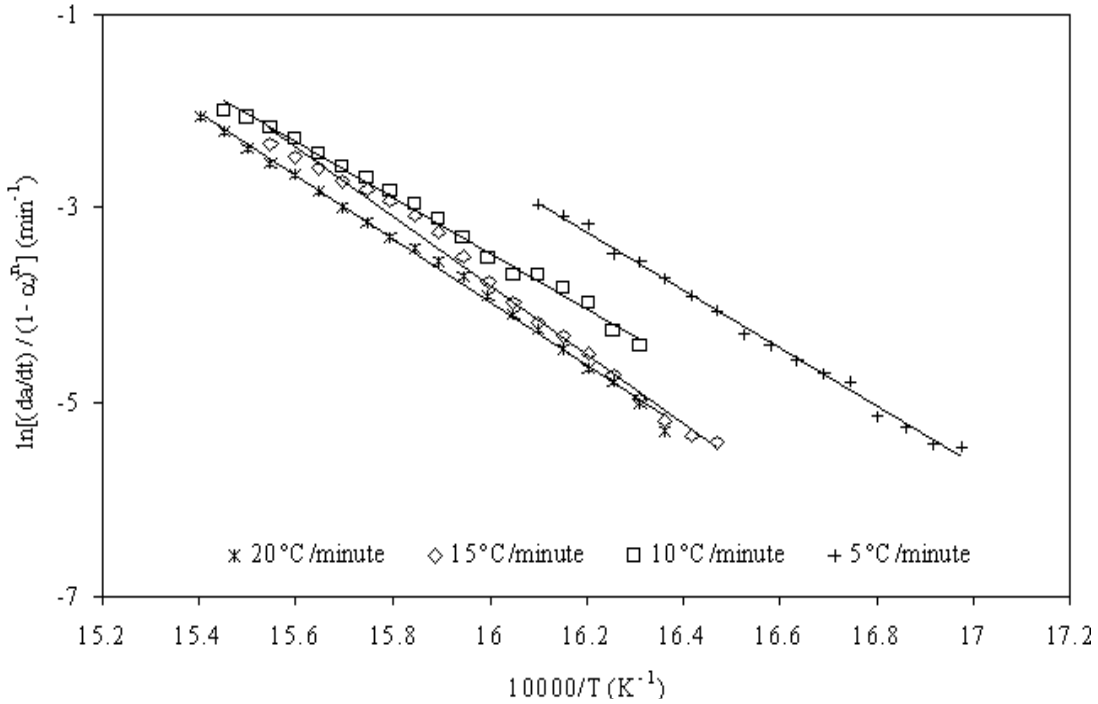

Figure 4.39: Chang plot of $\ln[(d\alpha/dt)/(1-\alpha)^n]$ vs.1/T for estimation of E of the blend at different heating rates in air atmosphere.

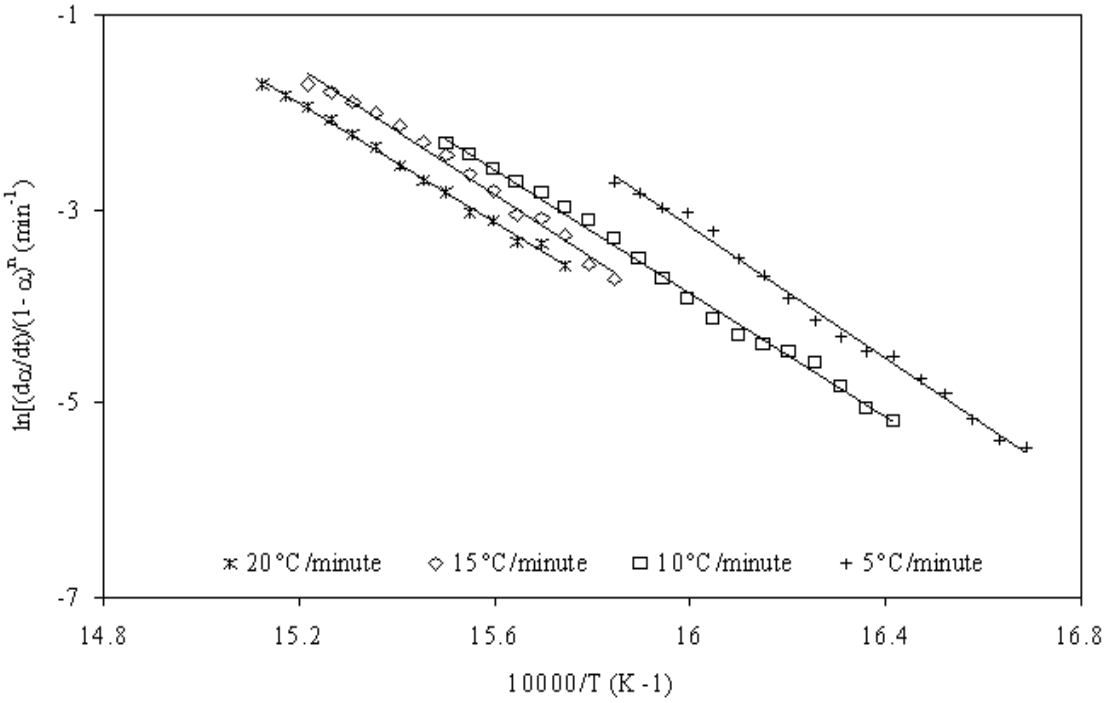

Figure 4.40: Chang plot of $\ln[(d\alpha/dt)/(1-\alpha)^n]$ vs.1/T for estimation of E of the blend at different heating rates in N_2 atmosphere.

Table 4.14: Characteristic temperatures and kinetic parameters of the first thermal degradation stage for PTT, PBT, PC and blend in air and N_2 atmosphere using Chang model.

Polymer	Heating Rate (°C/min)	Air			N_2		
		E (kJ/mol)	ln(A)	r^2	E (kJ/mol)	ln(A)	r^2
PTT	5	183	28.31	0.99	191	28.1	0.99
	10	175	30.42	0.99	259	36.98	0.996
	15	149	22.08	0.996	154	22.13	0.984
	20	159	33.35	0.997	193	28.93	0.997
	Average	166	28.54	0.993	199	29.03	0.992
PBT	5	262	46.92	0.998	281	50.47	0.998
	10	271	48.35	0.998	299	53.38	0.998
	15	284	50.46	0.999	309	54.89	0.997
	20	291	51.37	0.999	302	53.32	0.998
	Average	277	49.28	0.998	298	53.01	0.997
PC	5	196	34.79	0.990	316	57.11	0.993
	10	205	36.44	0.995	310	55.34	0.993
	15	230	40.87	0.999	328	60.07	0.999
	20	233	41.29	0.996	343	60.92	0.997
	Average	216	38.35	0.995	324	58.36	0.995
Blend	5	250	45.45	0.995	281	50.96	0.994
	10	237	42.23	0.994	265	47.22	0.995
	15	297	53.33	0.992	273	48.34	0.989
	20	270	47.99	0.997	255	44.71	0.996
	Average	264	47.25	0.995	269	47.80	0.994

*For Chang model, n is assumed to be 1.

Transesterification reactions between polycarbonate and polyester can possibly decrease the degradation temperature of the blend compared to the virgin materials (example PC). In these reactions the length of crystallizable segments in the copolyester as well as the chances for it to crystallize decrease. The newly transesterified blend in such cases may tend to have a more amorphous character. Ester interchange reactions occurring between polycarbonate/polyester blends are well known to start in the range of 250-300°C [135], eventually causing the formation of copolymers having mechanical and thermal properties not necessarily coincident with those of the neat polymers. The dynamic technique of TGA can provide a useful impression of the mechanisms of thermal degradation. As seen in Figures 4.24 and 4.25, the blend and neat polyesters begin to degrade at a lower temperature compared to PC. The blend is found to exhibit an intermediate behavior between PTT and PBT until 30 percent conversion. This is a qualitative evidence of some exchange reactions occurring between the polyester and polycarbonate.

Another quantitative approach adopted to check whether transesterification played a role in lowering the degradation temperature of the blend, was by determining the amount of char remaining after heating blends containing various percentage of PC. PC was found to form an insoluble char upon degradation under air and nitrogen [139]. Two additional blends with the compositions PC25/PTT37.5/PBT37.5, and PC75/PTT12.5/PBT12.5, weight/weight percent were developed using a single screw extruder under similar conditions discussed in the experimental section for PC50/PTT25/PBT25 composition. This additional work was only carried out to establish a relationship between exchange reactions occurring between polyester and polycarbonate and amount of char left on blend decomposition. Figure 4.41 shows the mass fraction of the blend at 550°C. If no interchange reactions were to occur between PC and the

polyesters, a linear relationship would be expected; however the experimental observations assume a slightly curved shape. This indirectly proves that, addition of polyesters interferes with polycarbonate char formation. Also an examination of Figure 4.24 and 4.25 indicates that the presence of polyesters in the blend causes early decomposition of polycarbonate in the blend. These observations reveal that some chemical reactions occur between PC and the polyesters. Similar observations have been made for other blend systems and have been attributed to free radical-initiated exchange processes [140].

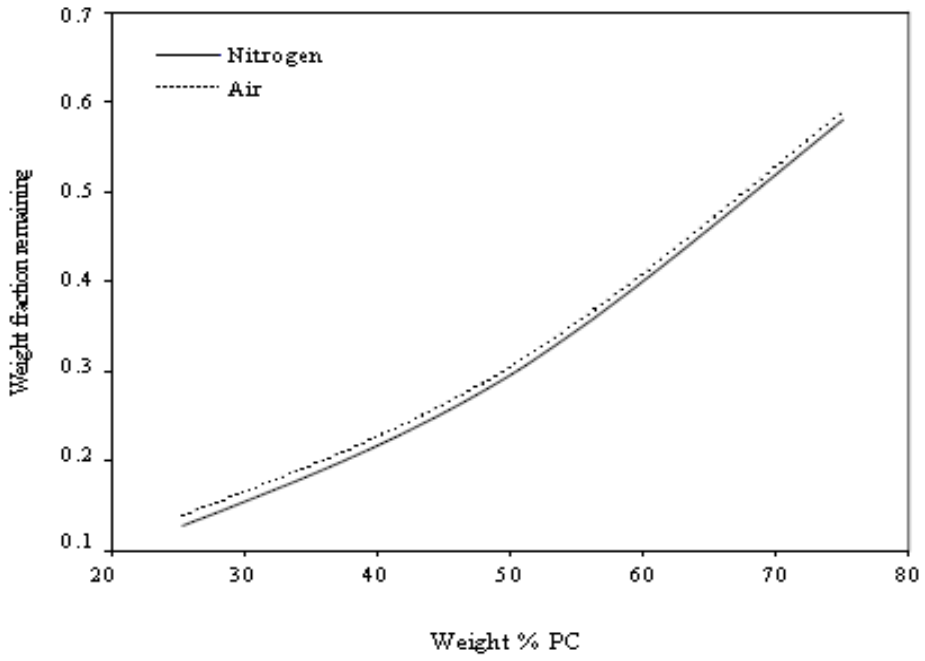

Figure 4.41: Char fraction remaining at 550^{o}C for blend in air and N_2.

The results obtained from the kinetic analysis of the TG data for PTT degraded in air and nitrogen atmosphere according to mechanisms $A_{n,}$ R_n and D_1 to D_4, refer Table 4.15, are shown in Figures 4.42 and 4.43. If $(T/T_{0.5})$ in equation is considered close to unity, a plot of $[(d\alpha/dt)/(d\alpha/dt)_{0.5}]$

against α gives a series of master curves, Figures 4.42 and 4.43, depend neither on the kinetic parameters nor the heating rate but only on the reaction mechanism [141].

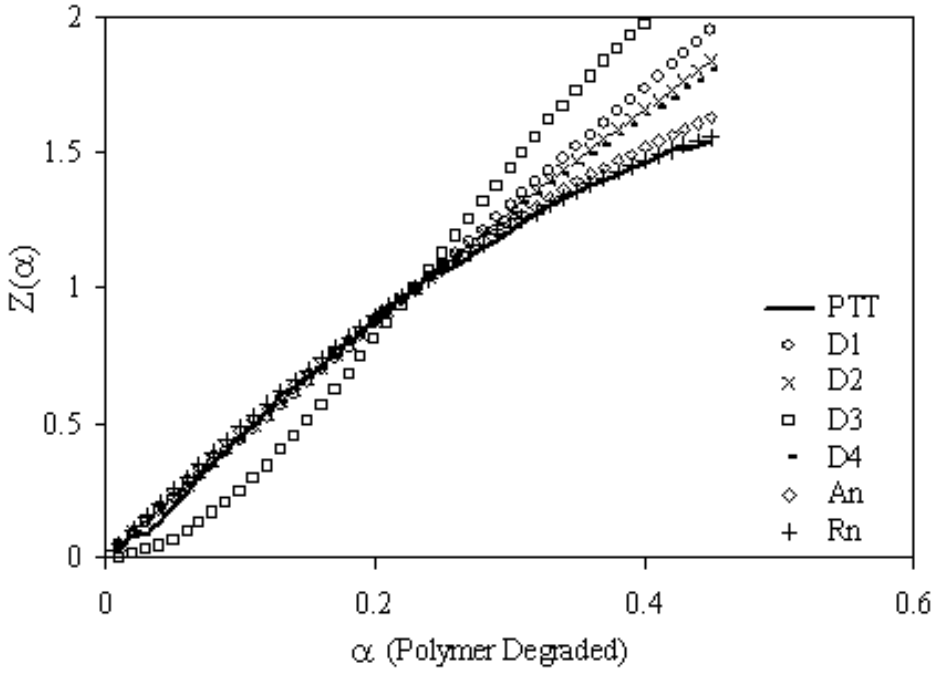

Figure 4.42: Determination of reaction mechanism by applying different curves to neat PTT at 10°C/min in air atmosphere.

In the present work the functions for f(α) and g(α) used to develop the master curves for the phase boundary controlled mechanism for PTT, PBT, PC and the blend are $(1-\alpha)^n$ and $\frac{1-(1-\alpha)^{1-n}}{1-n}$ respectively where, n is the order of the degradation mechanism. Solver, an optimization tool in Excel was used to optimize the experimental and theoretically generated values to determine the value of n. It is seen that the experimental data, Figures 4.42 and 4.43, do not fit well the kinetic models D_1 to D_4, and A_n.

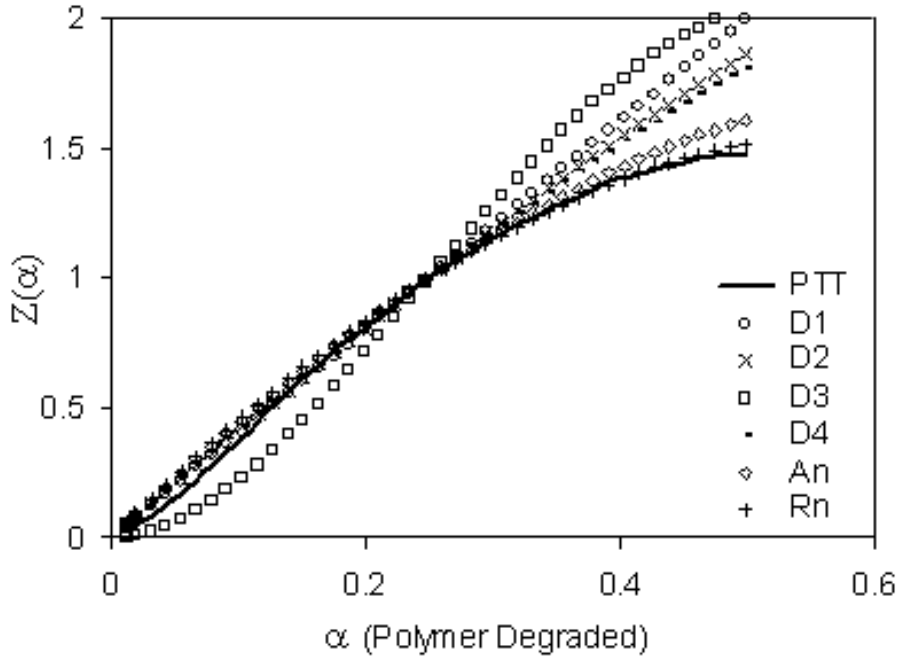

Figure 4.43: Determination of reaction mechanism by applying different curves to neat PTT at 20°C/min in air atmosphere.

The correlation coefficient (r^2) values obtained for the later models are < 0.9.

Figures 4.42 and 4.43 indicates that the R_n (phase boundary controlled) mechanism gives a good match between the experimental data points and the theoretically predicted values. The best values ($r^2 > 0.99$) of n in air and nitrogen for PTT and PBT is 2.0 while, that for PC both in air and nitrogen is 1.5. For the tricomponent blend the best value ($r^2 > 0.99$) of n was found to be 2.5.

Figure 4.44 confirms that the solid state degradation of the neat polymers and blend is typical of that of a phase boundary controlled process. In this mechanism, surface nucleation is rapid and is controlled by movement of the resulting interface towards the center [142].

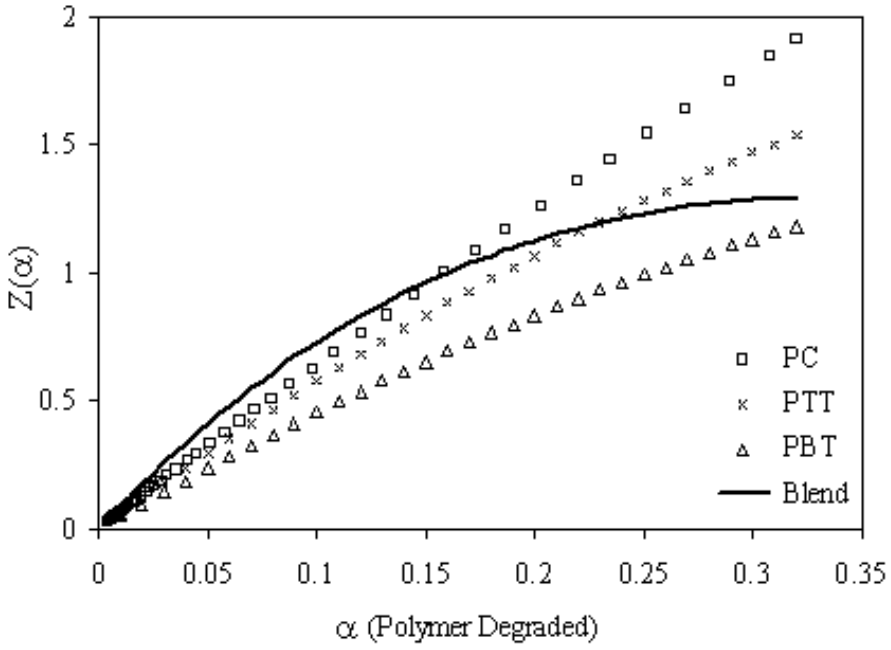

Figure 4.44: Fitting of phase boundary model to the conversion values of the neat polymers and blend at 15 °C/min.

Table 4.15: Algebraic expressions for the functions f(α) and g(α) for the most frequently used mechanisms of solid state processes.

Model	f(α)	g(α)	Solid state process
A_n	$n(1-\alpha)[-\ln(1-\alpha)]^{1-1/n}$	$[-\ln(1-\alpha)]^{1/n}$	General nucleation and growth equation.
R_n	$(1-\alpha)^n$	$\frac{1-(1-\alpha)^{1-n}}{1-n}$	General phase boundary controlled reaction.
D_1	$1/2\alpha$	α^2	Different diffusion controlled process
D_2	$\frac{1}{-\ln(1-\alpha)}$	$(1-\alpha)\ln(1-\alpha)+\alpha$	
D_3	$\frac{3(1-\alpha)^{2/3}}{2[1-(1-\alpha)]^{1/3}}$	$[1-(1-\alpha)^{1/3}]^2$	
D_4	$\frac{3}{2[(1-\alpha)]^{-1/3}-1]}$	$(1-2\alpha/3)-(1-\alpha)^{2/3}$	

Chapter 5 Conclusion

5.1 General conclusion on the study of non isothermal and isothermal crystallization kinetics, mechanical properties and morphology characterization, rheology and non isothermal degradation of neat polymers and blend.

The non isothermal crystallization exotherms of PTT and PBT showed that $T_{0.01}$, T_P and $T_{0.99}$ shifted towards lower temperature with the increase in cooling rates, while the blend displayed no such trend. A further analysis of the non isothermal crystallization behavior revealed that (Δt) decreased with increasing cooling rate.

Avrami, Malkin and Tobin models were used to characterize the non isothermal crystallization kinetics. Two kinetic parameters, rate constant and rate order were determined from each model. The kinetic parameters for the blend were found to lie between those of PTT and PBT. This could be due to the presence of PC in the blend. PC is an amorphous polymer and therefore may hinder the crystallization process in the blend. The SEM analysis of the blend reveals its immiscible nature. X-ray analysis showed the presence of peaks related to PTT and PBT, confirming again the immiscible nature of this system.

The isothermal crystallization kinetics of PTT, PBT, and their blend with PC, PC/PTT/PBT (50:25:25 wt/wt %) have been studied. Three different macrokinetic models namely the Avrami, Tobin, and Malkin models were applied. The crystallization kinetic parameters specific to each model were obtained from the best fits of the experimental data. The crystallization rate parameters $t_{0.5}^{-1}$, k_A, k_T, and C_1 were found to be sensitive to changes in the crystallization

temperature. Within the crystallization temperature range studied, the values of these parameters for polyesters were found to increase with decreasing temperature, suggesting that these polymers crystallize faster at low temperatures than at high temperatures. It was also shown that kinetic parameters (i.e. $t_{0.5}^{-1}$, k_A, k_T, and C_1) have a finite, definable relationship with the crystallization temperature T_c. Based on the ASE values, models of Avrami and Malkin followed by Tobin were good fit to the isothermal crystallization data, of the polyesters and the tricomponent blend.

The polymer melts displayed pseudoplastic behavior. The higher the temperature of the polymer melt, the lower was the shear viscosity at a constant shear rate. The shear viscosity of the blend is found to be lower than that of polycarbonate and greater than that of polyesters. This could possibly be due to transesterification reaction in the blend between polyesters and polycarbonate.

Steady shear viscosities for pure components and the blend showed slight decrease with increasing shear rate within the shear rate studies. The viscosity of the blend was found to lie in between that of PC and the polyesters. A possible enhancement in miscibility between PC and polyesters and a reduction in the size of the blend molecular constituents during transesterification could possibly lead to decrease in the viscosity of the blend.

Blend of PC and the polyester were concluded to be miscible and dynamic measurements in the molten state were dominated by PC behavior. It seems reasonable that for a component to dominate the rheological properties, especially, if the PC component is exactly half the weight ratio of the total mixture, a level of molecular miscibility is necessary. Complex viscosities of PC, polyesters and the blend displayed nearly Newtonian plateau at low frequencies with blend having a higher complex viscosity compared to neat PC.

This behavior of the blend could be possibly due to transesterification reaction occurring between PC and polyesters.

Bands in the infrared spectra of PC, PTT and PBT have been assigned to different modes of vibrations of the para-disubstituted benzene ring and this has been found common for all three neat polymers and the blend. The differences between the spectra occur on the basis of the degree of planarity of the terephthalate residue in the polyester and phenyl carbonate group in the PC. The difference has been noted due to the rotation of the carbonyl group about the carbonyl–phenylene group.

The storage and loss modulus value of the blend is found to be lower than that of polycarbonate and higher than that of polyesters, possibly due to attainment of more amorphous nature due to transesterification reaction between polyesters and polycarbonate.

Thermal degradation kinetics study for the blend of PC/PTT/PBT (50:25:25 wt/wt %) leads to the following conclusions:

1. TG curves shift to higher temperatures as the heating rate increases. Slower heating rates give more time for the degradation reaction to occur and thus serve as a promoting factor.
2. Degradation temperatures for PC are higher than those of the polyesters and the blend indicating its higher thermal stability.
3. Degradation temperatures for all polymers are higher in nitrogen than in air. This emphasizes the facilitating role oxygen plays in the degradation process.
4. The first stage of degradation of PC and the blend is more complex compared to the polyesters, as revealed by the DTG curves.
5. Among those investigated, Friedman and Chang models are probably most suitable for determining the kinetic parameters of degradation of the polymers studied. Chang method

assumes constant order (n =1) over the range of conversion. This means that *E* varies mostly only with heating rate.

6. These two models better represent the thermal degradation of the polymers studied in this work.
7. No definite trends in activation energy or pre-exponential factor values were observed with any of the models examined. Literature does not give reasons for absence of trends. This observation is worth investigating.

References

1. SU, C. C; Shin, C. K. *J. Colloid Polym. Sci.* (2005), 283, 1278.
2. Tjong, S. C.; Meng, Y. Z. *J. Appl. Polym. Sci.* (1999), 74, 1827.
3. Le, X. F.; Hay, J. N. *Polymer* (2001), 42, 9423.
4. Di Lorenzo, M. L.; Silvestre, C. *J. Prog. Polym. Sci.* 24 (1999), 917.
5. Zhu, Z.; Dakwa, P.; Tapadia, P.; Whitehouse, R. S.; Wang, S. *Macromolecules* (2003), 36, 4891.
6. Carrot, C.; Guillet, J.; Boutahar, K. *J. Rheo. Acta* (1993), 32, 566
7. Badr-Eddine, E.; Nicole, H. *Polymer* (2001), 42, 5661
8. DePorter, J. K.; Baird D. G.; Wilkes G. L. *J. Macro Sci. Part C*: *Rev in Macro Chem and Phys*. (1993), 33, 1.
9. Devaux, J.; Godard. P.; Mercier, J. P. *J. Polym. Sci. Polym. Phys. Edn*. (1982), 20, 1895.
10. Berti, C.; Bonora, V.; Pilati, F. *Macromole .Chem* (1992), 193,1665.
11. Devaux, J.; Godard. P.; Mercier, J. P. *J. Polym. Sci. Polym. Phys. Edn*. (1982), 20, 1901.
12. Devaux, J.; Godard. P; Mercier. J. P. *J. Polym. Sci. Polym. Phys. Edn*. (1982), 20, 1875.
13. Hetem, M. J. J. Internal Report, General Electric Plastics Europe.
14. Guijuan, L.; Kunyan, W.; Xueli, X.; Baojie, Y.; Shugang, L.; Yanmo. C. *J. Macro Sci, Part B* (2006), 45, 485.
15. Xue, M. L.; Yu, Y. L.; Sheng. J.; Chuah, H. H. *J. Macro Sci, Part B*, (2005), 44, 531
16. Keith, H. D.; Padden, F. J. *J Appl Phys* (1946), 35, 1270.
17. Keith, H. D.; Padden, F. J. *J Appl Phys* (1946), 35, 1283.
18. Verma, R.; Marand. H.; Hiaso, B. *Macromol* (1996), 29, 7767.

19. Kolmogoroff, N.; Akad, I. *USSR Ser Math* (1937), 1, 355.

20. Johnson, W. A.; Mehl, K. F. *Trans Am Inst Mining Met Eng* (1939), 135, 416.

21. Avrami, M. *J. Chem. Phys.* (1939), 7, 1103.

22. Avrami, M. *J. Chem. Phys.* (1939), 8, 212.

23. Avrami, M. *J. Chem. Phys.* (1939), 9, 177.

24. Evans, U. R. *Trans. Faraday Soc.* (1945), 41, 365.

25. Tobin, M. C. *J. Polym. Sci. Polym. Phys.* (1974), 12, 399.

26. Tobin, M. C. *J. Polym. Sci. Polym. Phys.* (1976), 14, 2253.

27. Tobin, M. C. *J. Polym. Sci. Polym. Phys.* (1977), 15, 2269.

28. Malkin, A. Y.; Beghishev, V. P.; Keapin, I. A.; Bolgov, S. A. *J. Polym. Eng. Sci*. (1984), 24,1396.

29. Ravindranath K.; Jog, J. P. *J. Appl. Polym. Sci.* (1993), 49, 1395.

30. Cruz-Pinto, J. C.; Martins, J. A.; Oliveira, M. *J. Colloid Polym. Sci.* (1994), 272, 1.

31. Wunderlich, B. *Macro. Phys.* (1976), 2, 132.

32. Supaphol, P.; Dangseeyun, N.; Srimoaon, P.; Nithitanakul, M. (2003) *Thermochim. Acta*, (2003), 406, 207.

33. Song, Wu. G.; Zheng, Y. H.; Zhang, Q.; Du, M.; Zhang, P. J. *J Appl Polym Sci* (2003), 88, 2160.

34. Nesarikar, A. R. *Macromolecules* (1995), 28, 7202.

35. Kapnistos, M.; Hinrichs, A.; Vlassopoulos, D.; Anastasiadis, S. H.; Stammer, A.; Wolf, B. A. *Macromolecules* 1996, 29, 7155.

36. Zheng, Q.; Du, M.; Yang, B. B.; Gang, W. *Polymer* (2001), 42, 5743.

37. Han, C. D.; Baek, D. M.; Kim, J. K.; Ogawa, T.; Sakamoto, N.; Hashimoto, T.

Macromolecules (1995), 28, 5043.

38. Varama D. S; Dhar, V.K .; Die Angew Macromol Chem 1989,169, 29.
39. Wu, D.; Zhou, C.; Hong, Z.; Mao, D.; Bian, Z. *Euro. Polym. J*. (2005), 41, 2199.
40. Xu, J.; Xu, X.; Zheng, Q.; Feng, L.; Chen, W. *Euro. Polym. J*. (2002), 38, 365.
41. Hong, S.M.; Kim, B. C. *J. polym. Eng. Sci*. (1994), 34, 1605.
42. Jackson**,** W. J.; Kuhfuss, H. F. *J. Polym. Sci. Polym. Chem .Ed.* (1996) 34, 3031.
43. Hamb, F. L. *J. Polym Sci.* (1997) 10, 3217.
44. Berti, C.; Bonora,V.; Pilati, F.; Fiorini, M. *Macromol Chem* (1992) 193, 1679.
45. Wilkinson, A. N.; Tattum, S. B; Ryan, A. *Polymer* (1997) 38, 1923.
46. Anton, M.; Eva, K.; Marcela, H.; Andrej, R.; Arun, P. A. *J. Appl. Polym. Sci*. (2006), 102, 4222.
47. Remiro, P. M.; Nazabal, J. *Eur Polym J*. (1992) 28, 243
48. ASTM D638 - 08 Standard Test Method for Tensile Properties of Plastics; Determination and report procedures; ASTM International: West Conshohocken, Pa, 2008.
49. Kim, S. J.; Kim, D. K.; Shin, B. S.; Cho, W. J.; Ha, C. S. *J. Polym. Eng. Sci*.(2003), 43, 1298.
50. Chiu, F.C.; Ting, M.H. *Polym Test*. 2007, 26, 338.
51. Marchese, P., Celli, A., Fiorini, M. *Macro Chem and Phys* (2002) 203, 695.
52. Reinsch, V.E.; Rebenfeld, L. *J. Appl. Polym. Sci*. (1996) 59,1913.
53. Denchev, Z.; Sarkissova, M.; Radusch, H, J.; Luepke, T.; Fakirov, S. *Macro Chem and Phys* (1998) 199, 215.
54. Zheng, W.; Wan, Z.; Qi, Z.; Wang, F. *Polym Int* (1994), 34,301.
55. Godard, P.; Dekoninck, J.M.; Devlesaver, V.; Devaux, J. *J. Appl. Polym. Sci.: Part A:*

Polym Chem (1986), 24, 3315.

56. Porter, R. S.; Wang, L. H. *Polymer* (1992), 33, 2019.
57. Murff, S. R.; Barlow, J. W.; Paul, D. R. *J. Appl. Polym. Sci.* (1984), 29, 3231.
58. Matthew J. H. High-performance polymer/layered silicate nanocomposites. PhD Thesis, Pennsylvania State University, PA, 2007.
59. Bo, Y. Z.; Min-Min, P.; Ming-Bo, Y. *Polym. Adv. Tech.*(2007), 18, 439.
60. Henrichs, P. M; Tribone, P. M.; Massa, D. J.; Hewitt, J. M. *Macromolecules,*(1988), 21, 1282.
61. Zhou, Z. L.; Eisenberg, A. *J. Polym. Sci., Polym. Phys. Edn*. (1983), 21, 595.
62. Aubin, M.; Pnid, R. E.'homme, *Macrmolecules* (1980), 13, 3655.
63. Wang, L. H.; Lu, M.; Yang, X.; Porter R.S. J. *Macromol. Sci. Phys*. (1990), 1329, 171.
64. Kugler, J.; Gilmer, J.W.; Wiswe, D.; Zachmann, H.G.; Hahm, K.; Fischer, E.W. *Macomol*ecules (1987), 20, 1116.
65. Mc Alea, K. P.; Schultz, J. M.; Gardner, K. H.; Wignall G. O. *Polymer* (1986), 27, 1581.
66. Deveaux, J.; Godard, P.; J.P. Mercier. J. P. *J. polym. Eng. Sci*. (1982), 22, 229.
67. Yuvari, A.; Asadinezhad, A.; Jafari , S. H.; Khonakdar, H. A.; Bohme, F.; Hassler, R. *Euro. Polym. J*. (2005), 41, 2880.
68. Supaphol, P.; Dangseeyun, N.; Srimoaon, P. *Polym. Test*. (2004), 23, 175.
69. Woo, E. M.; Hsiao Y.; Kuo *J. Polym. Sci.* (2003), 41, 2394.
70. Mc Neill, I. C.; Leiper, H. A. *Polym. Degrad. Stab*. (1985), 12, 373.
71. Shwu-Jer C.; Yi-Shiuan. W.; *J. Anal. Appl. Pyrolysis*. (2009), 86, 22.
72. Ma, S.; Hill, J.O.; Heng, S. *J. Thermal. Anal*. (1989), 35, 977.
73. Satava, V. *Thermal analysis, Proc. ICTA. H.G. Wiedeman (Ed.)* Birkhauser Verlag.

(1972), 2, 273.

74. Criado, J. M.; Gonzalez, F.; Morales, J. *Anal. Quim*. (1974), 70, 787.

75. Criado, J. M.; Gonzalez, F.; Morales, J. *Thermochim. Acta*. (1975), 12, 337.

76. Sharp, J. H.; Wenthworth, A. *Anal. Chem*. (1969), 41, 2060.

77. Clarke, T. A.; Evans, E. L.; Robbins, K. G.; Thomas, J. M. *Chem. Comm*. (1969), 266.

78. Kissinger, H. E. *Anal. Chem.* (1957), 29, 1702.

79. Ozawa, T. *Bull Chem. Soc. Jpn.* (1965), 38, 1881.

80. Friedman, H. L. *J. Polym. Sci. C* (1964), 6, 183.

81. Chang, W. L. *J. Appl. Polym. Sci.* (1994), 53, 1759.

82. Criado, J. M.; Morales. *J. Thermochim. Acta* (1976), 16, 382.

83. Ortega, A. Ph. D thesis, University of Seville, (1983).

84. Criado, J.M.; Ortega A. *J. non-cryst. solids* (1986), 87, 302.

85. Sivalingam, G.; Karthik, R.; Giridhar, G. M. *J. Anal Appl Pyrolysis* (2003), 70, 631.

86. Kim, J. H.; Lee, S. Y.; Park, J. H.; Lyoo, W. S.; Noh, S. K. *J Appl Polym Sci* (2000), 77, 693.

87. Kim, J. H.; Ha, W. S. *J Korean Fiber Soc*. (1994), 31, 788.

88. Kim, J. H.; Ha, W. S. *J Korean Fiber Soc* (1994), 31, 803.

89. Gochanour, C. R.; Weinberg, M. *J Rheol* (1986), 30, 101.

90. Kalika, D. S.; Giles D. W.; Denn, M. M. *J Rheol* (1990), 34, 139.

91. Lin, Y. G.; Winter, H. H. *Macromolecules* (1988), 21, 2439.

92. Escala, A.; Stein, R. S. *Adv. Chem. Series* (1979), 176, 455.

93. Avramova, N. *Polymer* (1995), 36, 801.

94. Shonaike, G. O. *Eur Polym J* (1992), 28, 777.

95. Huang, J. M.; Chang, F. C. *J Appl Polym Sci* (2002), 84, 850.

96. Godard, P. ; Dekominck, J. M.; Devlesaner, V. ; Devaux, J. *J. Polym. Sci. Polym. Chem. Ed*.(1986), 24, 3301.

97. Van Krevelon, D. W. *Polymer* (1975), 16, 615.

98. Murff, S. R.; Barlow J. W.; Paul, D. R. *J. Appl. Polym. Sci.* (1984), 29, 3231.

99. Kimura, M.; Porter, R. S.; Salee, G. *J. Polym. Sci. Polym. Phys. Ed*. (1983), 21, 367.

100. Kimura, K.; Salee G.; Porter, R.S. *J. Appl. Polym. Sci*. (1984), 29, 1629.

101. Robeson, L. M. *J. Appl. Polym. Sci*. (1985), 30, 4081.

102. Pilati, F.; Marianucci, E.; Berti, C. *J. Appl. Polym. Sci.* (1985) , 30, 1267.

103. Davis, A.; Golden, J. H. *J. Gas. Chromatogr.* (1967), 5, 81.

104. Davis, A.; Golden, J. H. *J. Macromol. Chem.* (1967), 110, 180.

105. Davis, A.; Golden, J. H. *J. Macromol. Sci. Rev. Macromol Chem.* (1968), C3, 49.

106. McNeill, C.; Rincon, A. *Polym. Degrad. Stab*. (1993), 39, 13.

107. McNeill, C.; Rincon, A. *Polym. Degrad. Stab*. (1991), 31, 163.

108. Jakeways, R.; Ward, I. M.; Wilding, M. A.; Desborough, I. J.; Pass, M. G. *J. Polym. Sci. Part B: Polym. Phys.* (1975), 13, 799.

109. Ward, I. M.; Wilding, M. A.; Brody, H. *J. Polym. Sci. Part. B: Polym. Phys.* (1976), 14, 263.

110. Poulin-Dandurand, S.; Pe´rez, S.; Revol, J. F.; Briss, F. *Polymer* (1979), 20,419.

111. Desborough, I. J.; Hall, I. H.; Neisser, J. Z. *Polymer* (1979), 20, 545.

112. Ho, R. M.; Ke, K. Z.; Chen, M. *Macromolecules* (2000), 33, 7529.

113. Wang, B.; Li, C. Y.; Hanzlicek, J.; Cheng, S. Z. D.; Geil, P. H.; Grebowicz, J.; Ho, R. M. *Polymer* (2001), 42, 7171.

114. Chuah, H. H. *Polymer. Eng. Sci*. (2001), 41, 308.

115. Huang, J. M.; Chang, W. C. *J. Polym. Sci. Part B: Polym. Phys*. (2000), 38, 934.

116. Hong, P. D.; Chung, W. T.; Hsu, C. F. *Polymer* (2002), 43, 3335.

117. Chuah, H. In Modern Polyesters; Scheirs, J: Long, T.,Eds., Wiley; NewYork, 2003; Chapter 11.

118. Hobbs, S.Y; Dekkers, M. E; Watkins, V. H.; *J. Mater. Sci* (1988), 23, 1219.

119. Ding, Z.; Spruiell, J. E.; *J Polym Sci Part B: Polym Phys* (1997), 25, 1077.

120. Xue, T. J.; Wikie, C. A.; *Polym. Degrad. Stab*. (1997), 56, 109.

121. Encyclopedia of Chemical Technology. H. F. Mark, Ed, Wiley-Interscience, New York, 1982, Vol 18.

122. Pyda, M.; Boller, A.; Grebowicz, J.; Chuah, H.; Lebedev, B.V.; Wunderlich, B. *J. Polym. Sci. Polym. Phys. Ed.* (1998), 36, 2499.

123. Pillin, I.; Pimbert, S.; Feller, J. F.; Levesque, G. *Polym Eng Sci* (2001), 41, 178.

124. Pyda, M.; Wunderlich, B. *J. Polym. Sci. Polym. Phys. Ed.* (2000), 38, 622.

125. Kong, Y.; Hay, J. N. Polymer 34 (2002) 1805.

126. Supaphol, P.; Spruiell, J. E. *J. Macromol. Sci. Phys.* (2000), 39, 257.

127. Hoffman, J. D.; Davis, G.T.; Lauritzen J. I., Jr., in: N.B. Hannay (Ed.), Treatise on Solid State Chemistry, Vol. 3, Plenum Press, New York, 1976 (Chapter 7).

128. Hoffman, J. D.; Miller, R. L. *Polymer* (1997), 38, 3151.

129. Onogi, S.; Asada, T. In *Rheology*; Astarita, G., Marrucci, G., Nicolais, G., Eds.; Plenum: New York, 1980; p 127.

130. Palierne, J. F. *Rheol Acta* (1990), 29, 204.

131. Huang, Z. H.; Wang, L.H. *Macromol. Chem., Rapid Commun* (1985), 7, 255.

132. Makarewicz, P. J.; Wilkes, G. L. *J. Apply. Polym Sci.* (1979), 23, 1619.

133. Puglisi, C.; Sturiale, L.; Montaudo, G. *Macromolecules* (1999), 32, 2194.

134. Atkinson, P. A.; Maines, P. J.; Skinner, G. A. *Thermochim Acta* (2000), 29, 360.

135. Britto, D.; Campana- Filho, S.P . *Polym. Degrad. Stab*. (2004), 84, 353.

136. Li, X. G.; Huang, M. R. *Polym. Degrad. Stab.* (1999), 64, 81.

137. Li, X. G.; Huang, M. R.; Guan, G. H.; Sun. T. *Polym. Int.* (1998), 46, 289.

138. Wang, X. S.; Li, X.G.;Yan, D.Y. *Polym. Degrad. Stab.* (2000), 69, 366.

139. Davis, A.; Gordon, J. H. *Macromol. Chem*. (1964), 78, 16.

140. Rechards, D. H.; Salter, D. A. *Polymer* (1967), 8, 129.

141. Criado, J. M. *Thermochim. Acta* (1978), 24, 186.

142. Jacobs, P. W. M.; Tompkins, F. C. *in W. E. garner (Ed.), Chemistry of the solid state*, Academic Press New York, 184 (1955).

Appendix A: Papers arising from this work

Adam Al-Mulla, Johnson Mathew, Lafi Al-Omairi and Sati Bhattacharya, "*Thermal Decomposition Kinetics Of Tricomponent Polyester/Polycarbonate systems*", *Polymer Engineering and Science, (Accepted)*, May, 2010

Al-Mulla, A; Mathew, J.; Al-Omairi, L.; Bhattacharya, S. N.*" Non isothermal Crystallization Kinetics of Polycarbonate/ Poly (Trimethylene Terephthalate)/ Poly (Butylene terephthalate)*", *J. Polym Eng. Sci.* (Submitted).

Al-Mulla, A; Mathew, J.; Al-Omairi, L.; Bhattacharya, S. N.*" Iisothermal Crystallization Kinetics of Tricomponent Blends of Polycarbonate, Poly (Trimethylene Terephthalate) and Poly (Butylene Terephthalate)*", *J. Polym Eng. Sci.* (Submitted).